International Telecommunication Union

ITU-R
Radiocommunication Sector of ITU

Report ITU-R P.2345-0
(08/2015)

Defining propagation model for Recommendation ITU-R P.528-3

P Series

Radiowave propagation

1865-2015

Foreword

The role of the Radiocommunication Sector is to ensure the rational, equitable, efficient and economical use of the radio-frequency spectrum by all radiocommunication services, including satellite services, and carry out studies without limit of frequency range on the basis of which Recommendations are adopted.

The regulatory and policy functions of the Radiocommunication Sector are performed by World and Regional Radiocommunication Conferences and Radiocommunication Assemblies supported by Study Groups.

Policy on Intellectual Property Right (IPR)

ITU-R policy on IPR is described in the Common Patent Policy for ITU-T/ITU-R/ISO/IEC referenced in Annex 1 of Resolution ITU-R 1. Forms to be used for the submission of patent statements and licensing declarations by patent holders are available from http://www.itu.int/ITU-R/go/patents/en where the Guidelines for Implementation of the Common Patent Policy for ITU-T/ITU-R/ISO/IEC and the ITU-R patent information database can also be found.

<div style="border:1px solid">

Series of ITU-R Reports

(Also available online at http://www.itu.int/publ/R-REP/en)

Series	Title
BO	Satellite delivery
BR	Recording for production, archival and play-out; film for television
BS	Broadcasting service (sound)
BT	Broadcasting service (television)
F	Fixed service
M	Mobile, radiodetermination, amateur and related satellite services
P	**Radiowave propagation**
RA	Radio astronomy
RS	Remote sensing systems
S	Fixed-satellite service
SA	Space applications and meteorology
SF	Frequency sharing and coordination between fixed-satellite and fixed service systems
SM	Spectrum management

</div>

Note: This ITU-R Report was approved in English by the Study Group under the procedure detailed in Resolution ITU-R 1.

© ITU 2015

REPORT ITU-R P.2345-0

Defining propagation model for Recommendation ITU-R P.528-3

(2015)

Scope

This Report will be used as background material for Recommendation ITU-R P.528-3.

This Report describes the IF77 propagation model for predicting basic transmission loss in the frequency range 125-20 000 MHz for aeronautical and satellite services. The IF77 model is the basis for the curves in Recommendation ITU-R P.528-3.

The IF77 model calculates the median basic transmission loss and then adds variabilities from precipitation, gaseous absorption, scintillation, long term fading, multipath, and time percentages.

1   Introduction

In the present time of frequency spectrum scarcity, sharing frequency bands has become ubiquitous in all aspects of wireless usage. The key to sharing frequency bands is performing good frequency sharing studies and the key to performing good frequency sharing studies is to use the appropriate propagation method.

While aeronautical and satellite links have many similar characteristics to terrestrial communication links, there are some additional characteristics of the aeronautical/satellite wireless channel not covered in propagation prediction methods for terrestrial systems. The IF77 propagation model has been used successfully for several years for propagation prediction of aeronautical and satellite links.

The organization of this Report is as follows. Section 2 covers the method description and includes calculations for the major outputs of the method. Horizon geometry is defined in section 3. Sections 4, 5 and 6 cover the diffraction region, the line-of-sight (LoS) region and the scatter region respectively. The diffraction region appears first since parameters described in that section define region boundaries. The rest of the sections cover terrain attenuation (section 8), free space loss (section 9), atmospheric absorption (section 10) and variability (section 11). This material is based on three reports [1], [2], [3] produced by the Institute for Telecommunication Sciences, ITS.

2   Method description

IF77 calculates propagation parameters for ground-ground, ground-air, ground-satellite, air-air and air-satellite links. Calculations of these links also cover air-ground, satellite-ground, air-air (where the higher antenna is the transmitting antenna) and satellite-air by reciprocity. This method always defines the lower antenna as the transmitting antenna designated as antenna 1 and all the parameters associated with antenna 1 have a designation of 1.The higher antenna with its associated parameters have the designation 2. Several parameters have multiple designations separated by a comma (i.e. $h_{1,2}$ or $G_{ET.R}$). This applies to multiple parameters (h_1 and h_2 or G_{ET} and G_{ER}). Equations with this type of parameter represent multiple equations, one for each number designation.

This method is a propagation prediction method for aeronautical and satellite links. There are restrictions on this model. It covers the frequency range of 0.1 to 20 GHz for antenna heights greater than 0.5 m. The radio horizon of the higher antenna, antenna 2, has a lower elevation than the higher antenna. It is, also, either common with the horizon of the lower antenna or is a smooth earth horizon with the same elevation as the effective reflective plane of the lower antenna.

Attenuation verses distance calculated for this model for three regions, LoS, diffraction, and scattering includes transition regions where the parameters are blended together. This method includes allowances for:

•   average ray bending;

•   horizon effects;

•   long-term power fading;

•   antenna pattern (elevation only) at each terminal;

•   surface reflection multipath;

•   tropospheric multipath;

•   atmospheric absorption;

•   ionospheric scintillation;

•   rain attenuation;

•   sea state;

•   a divergence factor;

•   very high antennas;

•   antenna tracking options.

IF77 addresses all these elements to provide a tool for frequency planning and sharing studies. The IF77 propagation model uses a combination of theoretical and empirical techniques to calculate the transmission loss of a defined system. The outputs of this method include transmission loss, power availability, power density and a desired-to-undesired ratio.

This section will present the equations to calculate the various outputs. The processes to calculate the parameters in these equations follow in the later sections.

2.1   Transmission loss

Transmission loss is the ratio of power radiated to power available at the receiving antenna. This loss does not include circuit losses of the receiving system other than the radiation resistance of the receiving antenna. The calculation for transmission loss, $L(q)$, not exceeded during a fraction of time q is:

$$L(q) = L_b(0.5) + L_{gp} - G_{ET} - G_{ER} - Y_\Sigma(q) \quad \text{dB} \tag{1}$$

L_b (0.5) is the median basic transmission loss and L_{gp} is the path antenna gain loss. L_{gp} is zero for this method which is valid when (*a*) the transmitting and receiving antennas have the same polarization which is true by definition in this method and (*b*) the maximum antenna gain is less than 50 dB. The values G_{ET} and G_{ER} are the free space antenna gains for the transmitting and receiving antennas respectively and $Y_\Sigma(q)$ is the total variability of the channel. The median basic transmission loss calculation is:

$$L_b(0.5) = L_{br} + A_Y + A_a \quad \text{dB} \tag{2}$$

The value L_{br} is a reference level for the basic transmission loss and A_a is loss due to atmospheric absorption. A_Y is a conditional adjustment factor to prevent available signal powers from exceeding expected free space by an unrealistic amount. This condition can occur when the variability, $Y(q)$ is large and the median basic transmission loss is near the free space level.

The reference for basic transmission loss, L_{br}, comes from the free space basic transmission loss, L_{bf}, the terrain attenuation, A_T, and a variability adjustment term, V_e (0.5).

$$L_{br} = L_{bf} + A_T - V_e(0.5) \quad \text{dB} \tag{3}$$

The free space antenna gains, $G_{ET,R}$, are calculated from:

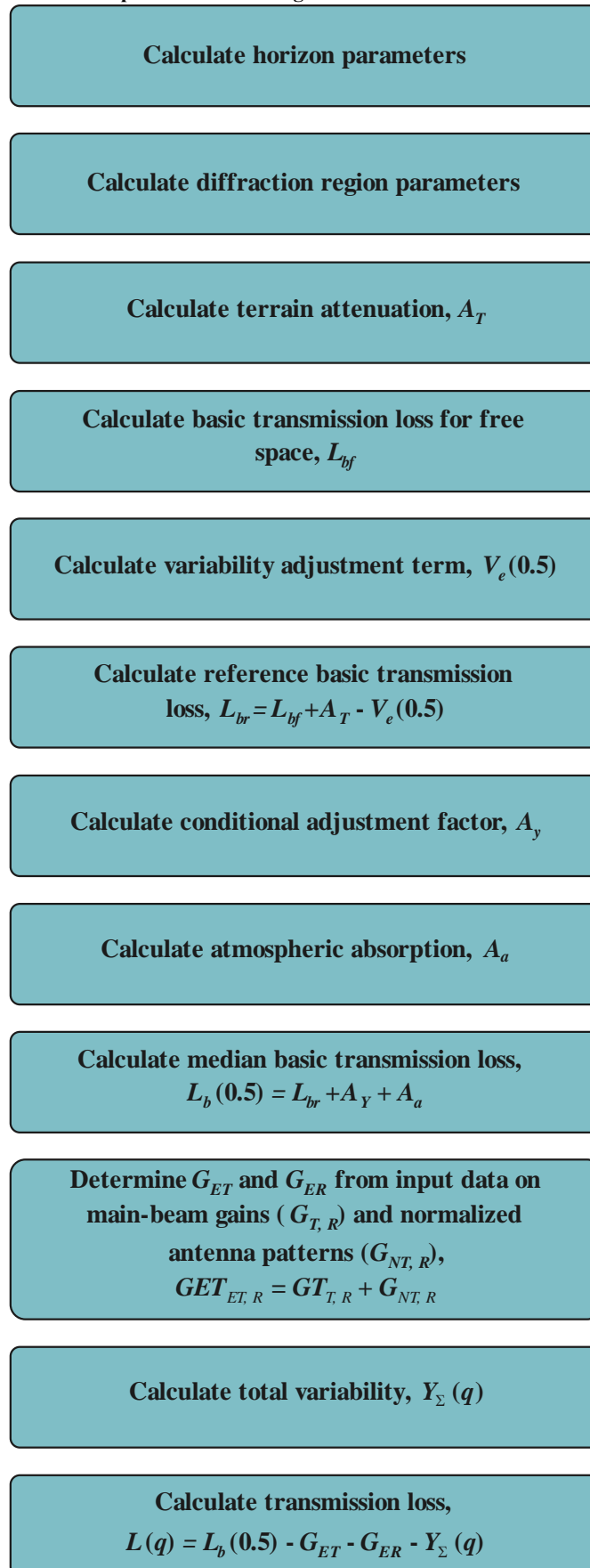$$G_{ET,R} = G_{T,R} + G_{NT,R} \quad \text{dBi} \tag{4}$$

$G_{T,R}$ are the main beam maximum free space antenna gains for the transmitting and the receiving antennas respectively. $G_{NT,R}$ give the relative gain for a defined elevation angle for the transmitting and the receiving antennas respectively. These parameters are inputs to the model.

The variability term from (1), $Y(q)$, includes long term power fading, surface reflection multipath, tropospheric multipath, rain attenuation and ionospheric scintillation. The discussion for these terms is in § 11. The median value for Y_Σ ($q = 0.5$) is equal to zero since the median value of basic transmission loss, $L_b(0.5)$, contains the adjustment terms for long term fading.

Figure 1 shows the flow diagram for calculating the transmission loss, $L(q)$. Calculations for the horizon parameters and the diffraction region parameters are at the top of the flow since those parameters are needed to define the region boundaries.

FIGURE 1

Computational flow diagram for transmission loss

Calculate horizon parameters

Calculate diffraction region parameters

Calculate terrain attenuation, A_T

Calculate basic transmission loss for free space, L_{bf}

Calculate variability adjustment term, $V_e(0.5)$

Calculate reference basic transmission loss, $L_{br} = L_{bf} + A_T - V_e(0.5)$

Calculate conditional adjustment factor, A_y

Calculate atmospheric absorption, A_a

Calculate median basic transmission loss, $L_b(0.5) = L_{br} + A_Y + A_a$

Determine G_{ET} and G_{ER} from input data on main-beam gains ($G_{T,R}$) and normalized antenna patterns ($G_{NT,R}$), $GET_{ET,R} = GT_{T,R} + G_{NT,R}$

Calculate total variability, $Y_\Sigma(q)$

Calculate transmission loss, $L(q) = L_b(0.5) - G_{ET} - G_{ER} - Y_\Sigma(q)$

Report P.2345 -01

2.2 Power available

Power available is the power available at the terminals of the receiving antenna under matched conditions with losses in the receiving system neglected. Power available levels exceeded for a fraction of time q, $P_a(q)$, is calculated by:

$$P_a(q) = e.i.r.p. + G_R + G_{NT} + G_{NR} - L_b(0.5) + Y_\Sigma(q) \quad \text{dBW} \tag{5}$$

where:

$$e.i.r.p. = P_{TR} + G_T \quad \text{dBW} \tag{6}$$

e.i.r.p. is the equivalent isotropically radiated power. P_{TR} is the total power radiated by the transmitting antenna referenced to 1 W. $G_{T,R}$ are the maximum gains of the transmitting and receiving antennas respectively as discussed in § 2.1 and $G_{NT,R}$ are the gains from (4). The variability, $Y_\Sigma(q)$, was discussed in § 2.1 and is calculated in (219). The relative gains G_{NT} and G_{NR} allow for directivity when the antennas are not pointed at each other.

2.3 Power density

The power density, $S_R(q)$, in decibels relative to 1 watt per square metre exceeded for the fraction of time q uses parameters discussed in §§ 2.1 and 2.2 and the effective area, A_I, of an isotropic antenna.

$$S_R(q) = e.i.r.p. + G_{NT} - L_b(q) + Y_\Sigma(q) - A_I \quad \text{dB W/sq m} \tag{7}$$

A_I is calculated by:

$$A_I = 10 \log_{10}\left(\frac{\lambda_m^2}{4\pi}\right) \quad \text{dB sq m} \tag{8}$$

where λ_m is the wavelength in metres for the defined frequency in MHz.

$$\lambda_m = \frac{299.7925}{f} \quad \text{m} \tag{9}$$

2.4 Desired-to-undesired signal ratio

Desired-to-undesired signal ratios available for a fraction of time q, $D/U(q)$, at the terminals of a lossless receiving antenna are calculated by:

$$D/U(q) = D/U(0.5) + Y_{DU}(q) \quad \text{dB} \tag{10}$$

where

$$D/U(0.5) = [P_a(0.5)]_{Desired} - [P_a(0.5)]_{Undesired} \quad \text{dB} \tag{11}$$

and

$$Y_{DU}(q) = \pm\sqrt{[Y_\Sigma(q)]_{Desired}^2 + [Y_\Sigma(1-q)]_{Undesired}^2} \quad \text{dB} \tag{12}$$

$$- \text{ for } q \geq 0.5$$

$$+ \text{ otherwise}$$

Use (5) to calculate $P_a(0.5)$ for both desired and undesired signals with parameters for desired and undesired signals respectively and with $Y_\Sigma(0.5) = 0$.

3   Horizon geometry

Horizons for both terminals are calculated from the input parameters used to determine the lower terminal horizon. The higher terminal horizon is either considered to be the same as the lower terminal horizon or as a smooth earth when the lower terminal is shadowed by the smooth earth from the higher terminal.
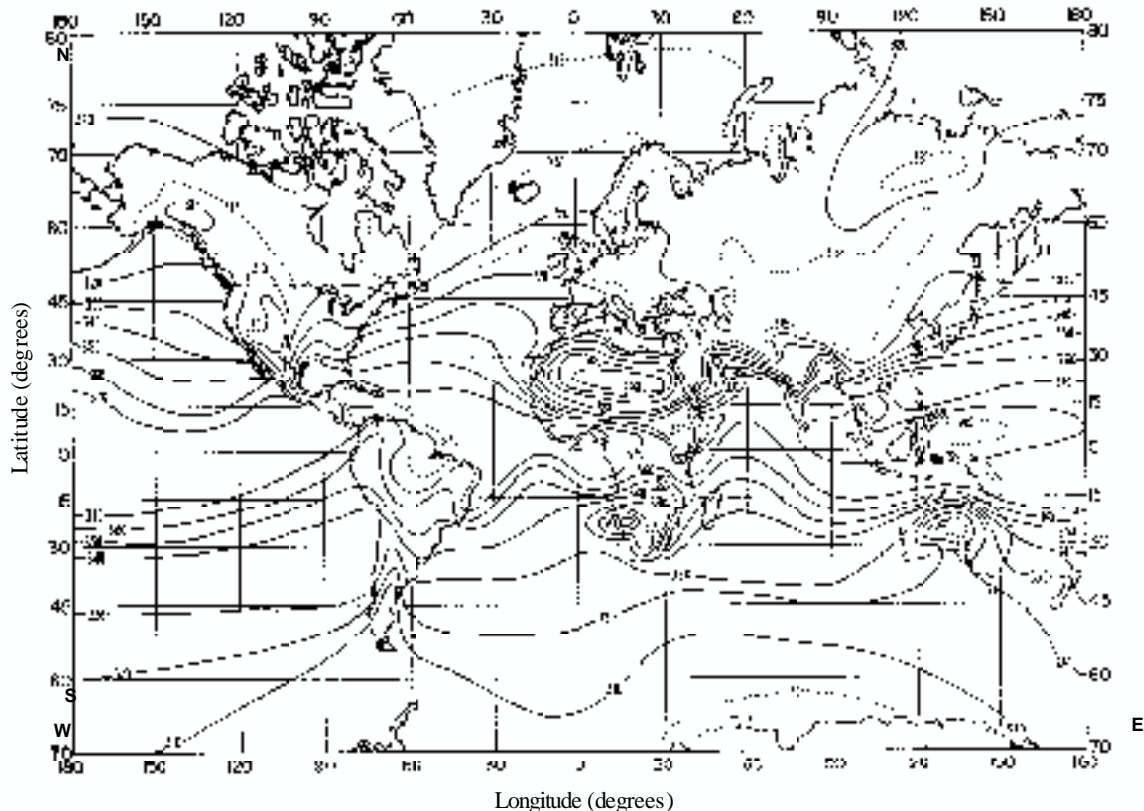
3.1   Effective earth radius

To calculate the effective earth radius, a, adjust the actual earth radius, a_0, with the surface refractivity associated with the effective reflecting surface. Starting with the monthly mean surface refractivity, N_0, calculate the surface refractivity, N_s, for the reflecting surface height, h_r.

$$N_s = greater\ of \begin{cases} N_0 \exp(-\,0.1057\,h_r) \\ \quad\quad or \\ \quad\quad 200 \end{cases} \quad N - units \tag{13}$$

Using $a_0 = 6\,370$ km calculate the effective earth radius.

$$a\ =\ a_0\,[1\ -\ 0.04665\ \exp\ (0.005577\ N_s)]^{-1} \quad km \tag{14}$$

FIGURE 2

Sea level surface refractivity from Recommendation ITU-R P.453-10

Report P.2345-02

Both N_0 and h_r are input parameters. Figure 2 shows the sea level surface refractivity.

4 High antenna height

For high antennas (> 3 km), the effective earth radius can overestimate the amount of ray bending. A solution for this is to calculate ray tracing through an exponential atmosphere. The refractivity varies with the height above mean sea level, h, as:

$$N = N_s \exp\left[-\log_e\left(\frac{N_s}{N_s + \Delta N}\right)(h - h_r)\right] \qquad N - \text{units} \tag{15}$$

where h and h_r are input parameters, N_s is calculated in (13) and

$$\Delta N = -7.32 \exp(0.005577\, N_s) \quad N - \text{units/km} \tag{16}$$

The ray tracing algorithm calculates the change in the ray through a horizontally stratified atmosphere with layer heights above h_r of 0.01, 0.02, 0.05, 0.1, 0.2, 0.305, 0.5, 0.7, 1, 1.524, 2, 3.048, 5, 7, 10, 20, 30.48, 50, 70, 90, 110, 225, 350 and 475 km. above 475 km the rays are assumed to be straight relative to the true earth radius a_0. The ray tracing algorithm is in Attachment 1.

4.1 Smooth earth horizons

Antenna heights input to the method have relationships as shown in Fig. 3. Antenna heights above the effective reflection surface are calculated by:
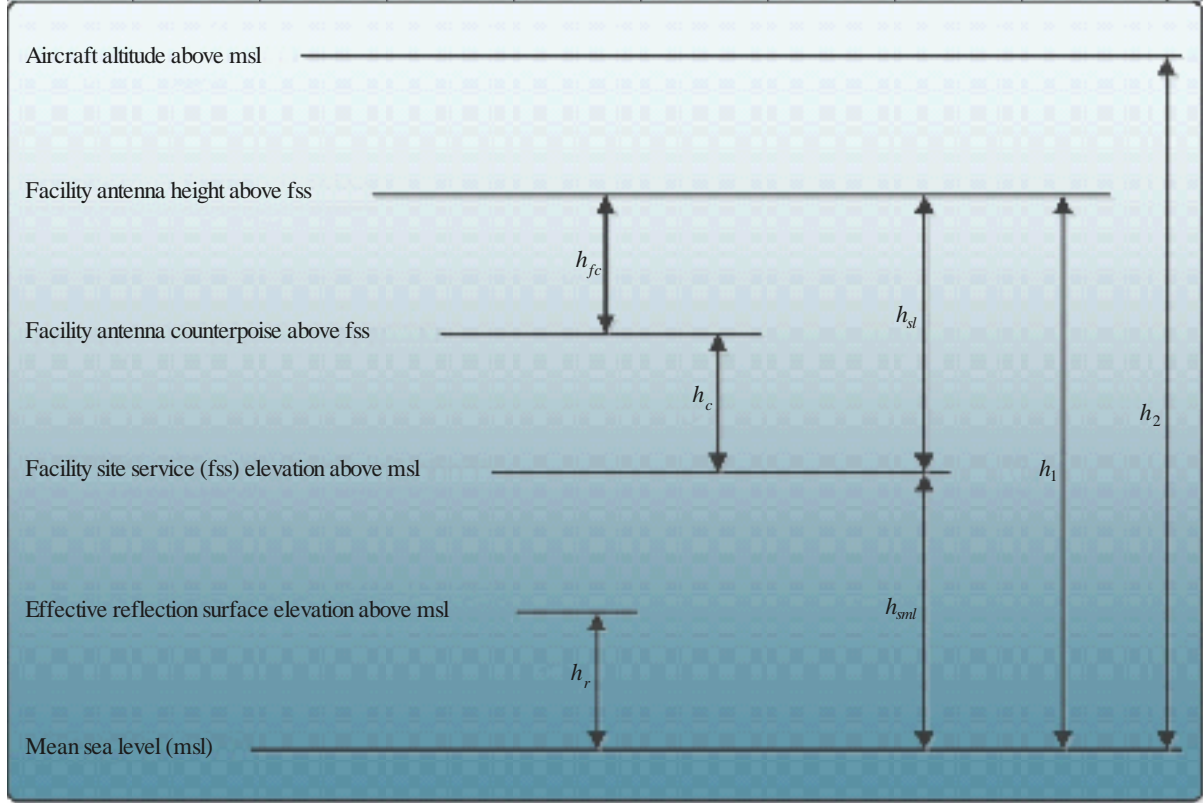
$$h_{r1} = h_{sl} + h_{sml} - h_r \quad \text{km} \tag{17}$$

$$h_{1,2} = h_{r1,2} + h_r \qquad \text{km} \tag{18}$$

Antenna heights $h_{1,2}$ are the heights above mean sea level for antennas 1 and 2 and $h_{r1,2}$ are the antenna heights above the reflective surface for antennas 1 and 2 respectively. The height of antenna 1 above a counterpoise or ground plane, if present, is calculated by:

$$h_{fc} = h_{sl} - h_c \qquad \text{km} \tag{19}$$

FIGURE 3

Input antenna heights and surface elevations

Aircraft altitude above msl

Facility antenna height above fss

Facility antenna counterpoise above fss

Facility site service (fss) elevation above msl

Effective reflection surface elevation above msl

Mean sea level (msl)

Valid input constraints

$0 \leq h_r \leq 4\text{km}$

$0 \leq h_{sml} \leq 4 \text{ km}$

$0.0005 \text{ km} \quad < h_{sl}$

$h_1 \leq h_2$

Note that aircraft altitude is elevation above msl while the facility antenna height is measured with respect to fss.
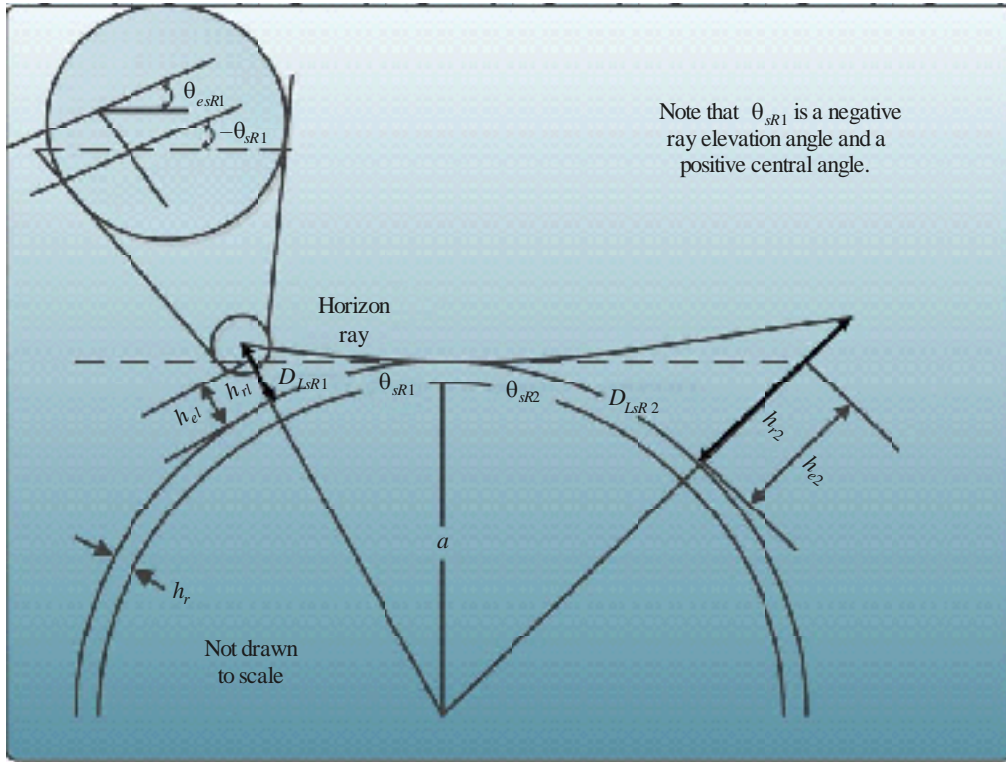
Report P.2345 -03

For those scenarios where the effective earth geometry overestimates ray bending, effective antenna heights, $h_{e1,2}$ become heights that produce the smooth earth horizon distances from each terminal, $d_{LsR1,2}$, calculated with the ray tracing algorithm. Figure 4 shows that the effective heights are lower than the actual heights. When determining the smooth earth distances, the initial take-off angle is $0°$ and the surface refractivity, N_s, is calculated from N_0 in (13). After determining the smooth earth distances, $d_{LsR1,2}$, use those values and from (14) to calculate the differences in the actual antenna heights and the effective antenna heights, $\Delta h_{e1,2}$, as follows:

$$\theta_{sR1,2} = \frac{d_{LsR1,2}}{a} \quad \text{rad} \tag{20}$$

$$h_{e1,2} = lesser\ of \begin{cases} h_{r1,2} \\ \quad \text{or} \\ 0.5\ d_{LsR1,2}^2/a \quad \text{if } \theta_{sR1,2} \leq 0.1 \text{ rad} \\ a[\sec(\theta_{sR1,2}) - 1] \qquad \text{otherwise} \end{cases} \quad \text{km} \tag{21}$$

$$\Delta h_{e1,2} = h_{r1,2} - h_{e1,2} \quad \text{km} \tag{22}$$

FIGURE 4

Effective height geometry

The final smooth earth distances, $d_{Ls1,2}$, are either the values determined by ray tracing, $d_{LsR1,2}$, with high antennas or the values calculated by effective earth geometry, $d_{LsE1,2}$:

$$d_{LsE1,2} = \sqrt{2a\,h_{e1,2}} \quad \text{km} \tag{23}$$

$$d_{Ls1,2} = \begin{cases} d_{LsR1,2} & \text{if } \Delta h_{e1,2} > 0 \\ d_{LsE1,2} & \text{otherwise} \end{cases} \quad \text{km} \tag{24}$$

$$d_{Ls} = d_{Ls1} + d_{Ls2} \quad \text{km} \tag{25}$$

The ray elevation angles, $\theta_{es1,2}$, become either the ray elevation angles from ray tracing, $\theta_{esR1,2}$, for high antennas or the negative of the ray elevation angles calculated with the final smooth earth distances, $\theta_{s1,2}$:

$$\theta_{s1,2} = \frac{d_{Ls1,2}}{a} \quad \text{rad} \tag{26}$$

$$\theta_{es1.2} = \begin{cases} \theta_{esR1,2} & \text{if } \Delta h_{e1,2} > 0 \\ -\theta_{s1,2} & \text{otherwise} \end{cases} \quad \text{rad} \tag{27}$$

4.2   Facility radio horizon

There are four sets of parameters that can produce the horizon for the lower or facility antenna. These parameters are: a) any two horizon parameters (distance, elevation or elevation angle); b) any one horizon parameter and the terrain parameter Δh; c) Δh alone; or d) smooth earth parameters. Figure 5 shows the facility horizon geometry.

For case 1 where at least two horizon parameters are specified, the horizon parameters for distance, d_{LE1}, horizon elevation, h_{LE1}, and horizon elevation angle, θ_{eE1}, are related by:
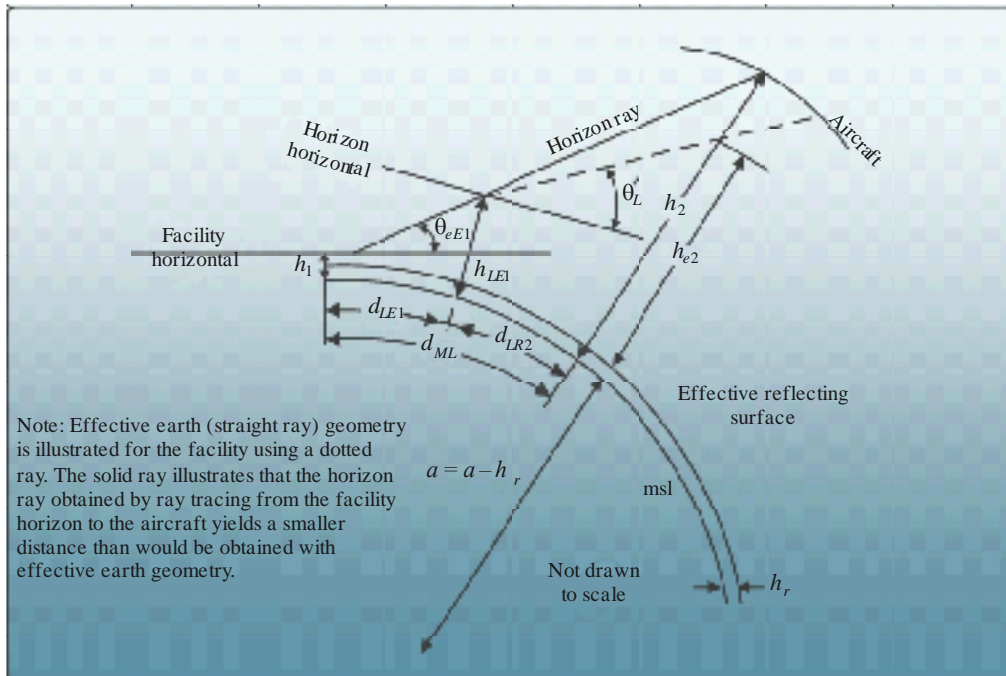
$$d_{LE1} = \pm \sqrt{2a(h_{LE1} - h_1) + a^2 \tan^2\theta_{eE1}} - a\,\tan\theta_{eE1} \quad \text{km} \tag{28}$$

$$h_{LE1} = h_1 + \frac{d_{LE1}^2}{2a} + d_{LE1} \tan \theta_{eE1} \qquad \text{km} \qquad (29)$$

$$\theta_{eE1} = \tan^{-1}\left(\frac{h_{LE1} - h_1}{d_{LE1}} - \frac{d_{LE1}}{2a}\right) \qquad \text{km} \qquad (30)$$

where a is from (14). The choice of the ± in (28) should produce the smallest positive value for h_{LE1} in (29).

FIGURE 5

Facility radio horizon geometry

Report P.2345 -05

One can use the terrain parameter Δh which is an input parameter and d_{Ls1} from (24) to estimate d_{LE1} and θ_{eE1} when those horizon parameters are not specified. When using h_e here, use 0.005 km if h_e falls below that number.

$$d_h = d_{Ls1} \exp\left(-0.07 \sqrt{\Delta h / h_e}\right) \qquad \text{km} \qquad (31)$$

$$d_{LE1} = \begin{cases} 0.1\, d_{Ls1} & \text{if } d_h < 0.1\, d_{Ls1} \\ 3\, d_{Ls1} & \text{if } d_h > 3\, d_{Ls1} \\ d_h & \text{otherwise} \end{cases} \qquad \text{km} \qquad (32)$$

$$\theta_{eE1} = \text{lesser of} \begin{cases} \frac{0.5}{d_{Ls1}}\left[1.3\, \Delta h \left(\frac{d_{Ls1}}{d_{LE1}} - 1\right) - 4\, h_{e1}\right] \\ \text{or} \\ 0.2094 \end{cases} \qquad \text{rad} \qquad (33)$$

where d_{Ls1} is from (24).

In the case of high antennas, however, the accurate calculation of more than one horizon parameter is dependent on ray tracing results. Figure 6 shows the full logic flow diagram for calculating the parameters for the lower or facility horizon. The full method for calculating horizon parameters is:

1　　　　Calculate the horizon parameters using equations (28) through (33), but consider the values to be initial values.

2　　　　Use h_1 from (18) and h_{e1} from (21) to test the values from step 1.

$$h_{e1} > 3 \text{ km} \quad \text{and} \quad \begin{pmatrix} \theta_{eE1} > 0 \text{ and } h_1 > h_{LE1} \\ \text{or} \\ \theta_{eE1} \leq 0 \text{ and } h_1 < h_{LE1} \end{pmatrix} \tag{34}$$

When these conditions are true, set the parameters as in Fig. 5 for smooth earth. Otherwise keep the parameter values in step 1.

3   When the test conditions in step 2 are false, use the following values:

$$d_{L1} = \begin{cases} d_{LE1} & \text{if } \Delta h_{e1} = 0 \\ \text{use ray tracing otherwise} \end{cases} \quad \text{km} \tag{35}$$

$$h_{L1} = h_{LE1} \quad \text{km} \tag{36}$$
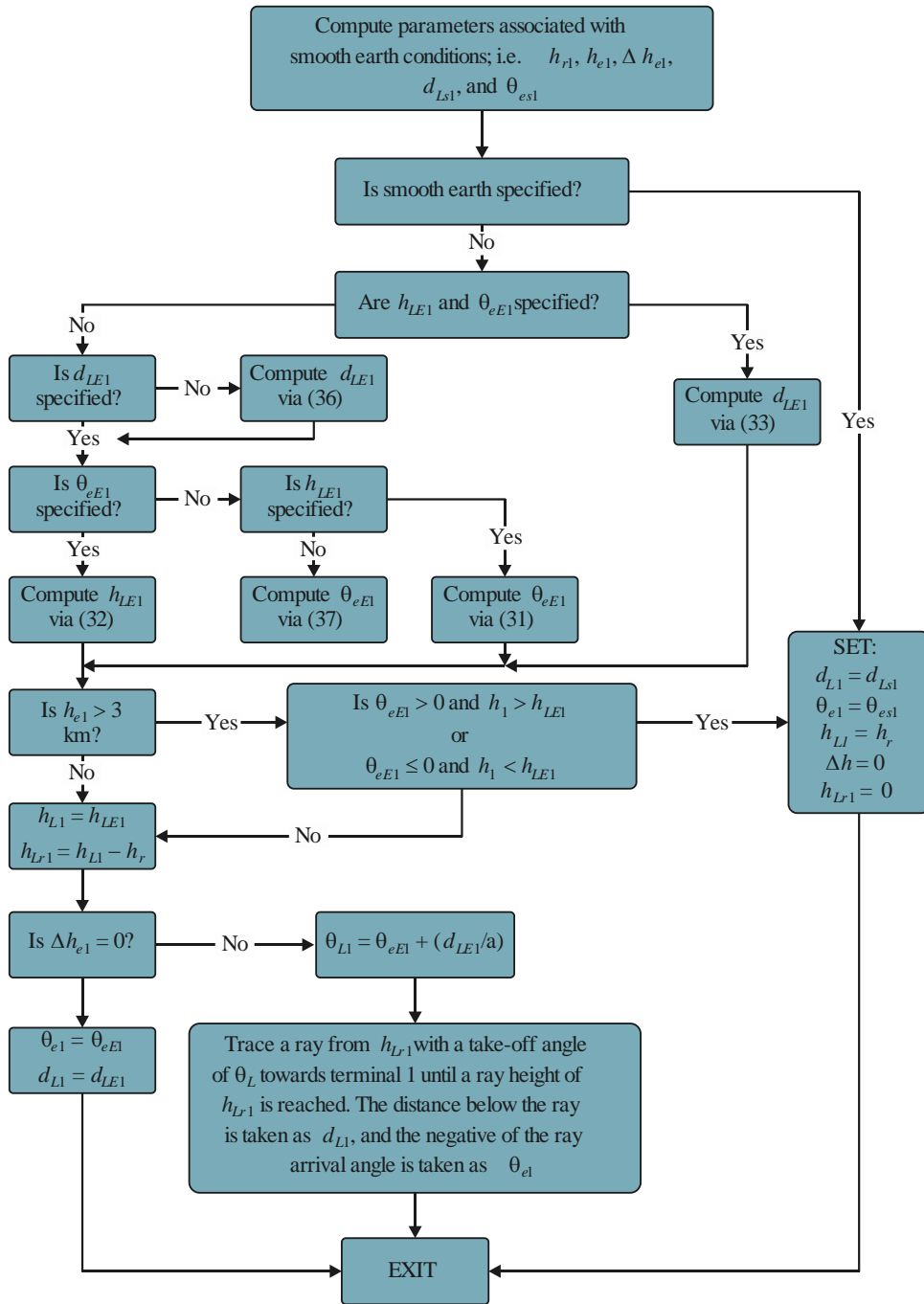
$$h_{Lr1} = h_{L1} - h_r \quad \text{km} \tag{37}$$

$$\theta_{e1} = \begin{cases} \theta_{eE1} & \text{if } \Delta h_{e1} = 0 \\ \text{use ray tracing otherwise} \end{cases} \quad \text{rad} \tag{38}$$

For ray tracing in (35) and (38), start at the horizon elevation, h_{Lr1}, with a take-off angle of $-\theta_L$.

$$\theta_L = \theta_{eE1} + \frac{d_{LE1}}{a} \quad \text{rad} \tag{39}$$

FIGURE 6

Logic flow to calculate facility horizon parameters

Report P.2345-06

Continue through the ray tracing algorithm until the lower antenna height, h_{r1}, is reached. Then the negative of the arrival angle is θ_{e1} and the great circle distance traversed by the ray is d_{L1}.

The great circle distance from h_{LE1} to the aircraft altitude h_2, d_{LR2}, is calculated via ray tracing using a take-off angle of θ_L at h_{LE1}. The maximum LoS distance, d_{ML}, is calculated by:

$$d_{ML} = \begin{cases} d_{Ls1} + d_{Ls2} & \text{for smooth earth} \\ a\left[\cos^{-1}\left(\frac{(a+h_{e1})\cos\theta_{e1}}{(a+h_{e2})}\right) - \theta_{e1}\right] & \text{if } \Delta h_{e2} = 0 \\ d_{L1} + d_{LR2} & \text{otherwise} \end{cases} \quad \text{km} \quad (40)$$

4.3 Higher antenna (aircraft or satellite) horizon

In the IF77 the higher antenna horizon is defined as either a common horizon with the lower antenna horizon (as in an obstacle horizon) or as a smooth earth horizon. Figure 7 shows the geometry for calculating the great circle distance from the horizon to the higher antenna.

Using the great circle distance between the lower and the higher antennas, d, which is an input parameter, the great circle horizon distance for the higher antenna, d_{L2}, is calculated by:

$$d_{sL} = \sqrt{2a\, h_{Lr1}} \quad \text{km} \tag{41}$$

$$d_{LM} = d_{L1} + d_{sL} + d_{Ls2} \quad \text{km} \tag{42}$$

$$d_{L2} = \begin{cases} d - d_{L1} & \text{if } d_{ML} \le d \le d_{LM} \\ d_{Ls2} & \text{otherwise} \end{cases} \quad \text{km} \tag{43}$$

The value h_{Lr1} is the height of the obstacle horizon for the lower antenna and d_{sL} is the smooth earth horizon distance for the obstacle. The value a, is from (14), d_{L1} is from (35) and d_{Ls2} is from (24).

The horizon height for the higher antenna, h_{L2}, is the obstacle height of the lower antenna from the reflecting surface or the smooth earth horizon height.

$$h_{Lr2} = \begin{cases} h_{Lr1} & \text{if } d_{ML} < d < d_{LM} \\ 0 & \text{otherwise} \end{cases} \quad \text{km} \tag{44}$$

$$h_{L2} = h_{Lr2} + h_r \quad \text{km} \tag{45}$$

where h_r is the surface reflection height which is an input parameter. The horizon ray elevation angle is relative to the horizontal at the higher antenna where the angle is positive if it is above the horizontal.

$$\theta_{e2} = \tan^{-1}\left(\frac{h_{Lr2} - h_{e2}}{d_{L2}} - \frac{d_{L2}}{2a}\right) \quad \text{rad} \tag{46}$$

FIGURE 7

Geometry for the higher antenna radio horizon

Report P.2345 -07
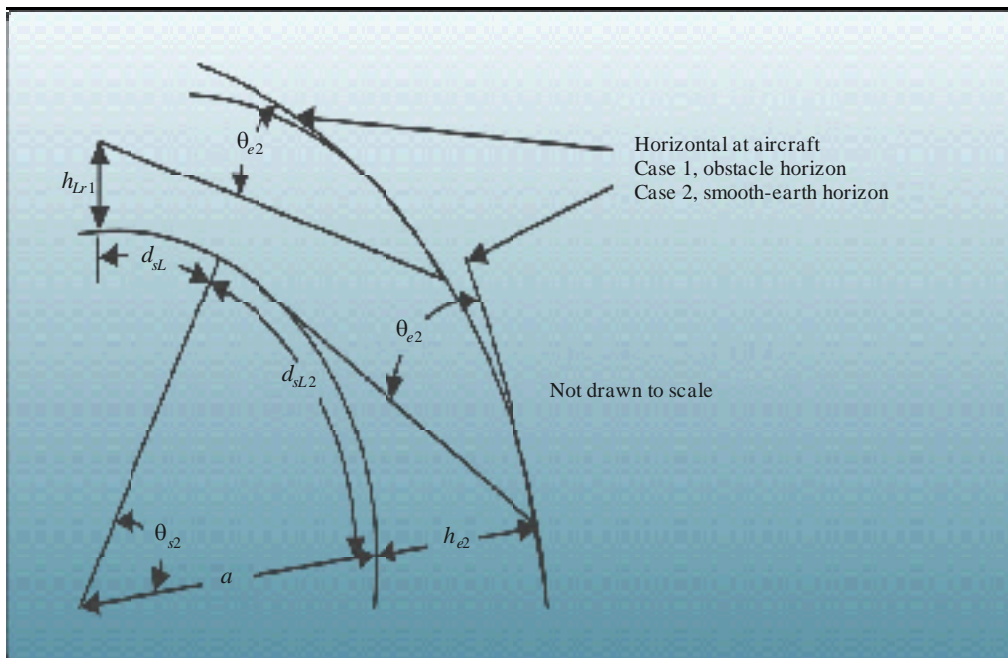
5 Diffraction region

The IF77 method assumes that diffraction attenuation, A_d, is linear with distance when other parameters are fixed. To establish the linear relationship, the method determines a diffraction value at two distances. The first distance, d_{ML}, is the maximum LoS distance and the second distance, d_A, is the shortest beyond-the-horizon distance defined by the facility horizon obstacle and the smooth earth horizon for the receiving antenna. Figure 8 shows the geometry of the paths. Values for both smooth earth diffraction and knife-edge diffraction in each case are calculated and then combined. The first two sections discuss rounded earth diffraction and knife-edge diffraction respectively. The third section shows how to combine the two diffraction pieces.

5.1 Rounded earth diffraction

The two paths used in the case of rounded earth diffraction are path F-O-ML and path O-A from Fig. 8.

The following set of equations produce straight-line attenuation values versus distance.

$$h_{ep1} = \begin{cases} h_{e1} & \text{for path F} - 0 - \text{ML} \\ h_{Lr1} & \text{for path 0} - \text{A} \end{cases} \quad \text{km} \tag{47}$$

where h_{e1} is from (21) and h_{Lr1} is from (37). The height h_{ep2} equals h_{e2} from (21) for both paths.

FIGURE 8

Paths used to determine diffraction attenuation
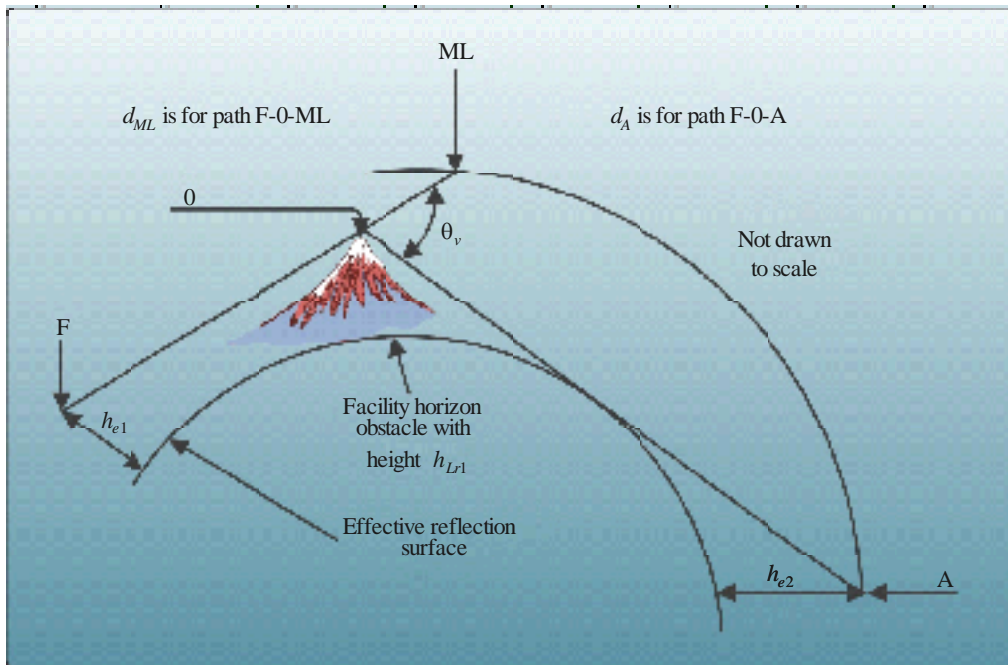
Report P.2345 -08

$$d_{Lp1} = \begin{cases} d_{L1} & \text{for path F} - 0 - \text{ML} \\ d_{LO1} = d_{sL} & \text{for path 0} - \text{A} \end{cases} \quad \text{km} \tag{48}$$

$$d_{Lp2} = \begin{cases} d_{ML} - d_{L1} & \text{for path F} - 0 - \text{ML} \\ d_{LO2} = d_{Ls2} & \text{for path 0} - \text{A} \end{cases} \quad \text{km} \tag{49}$$

The parameters for these equations include d_{L1} from (35), d_{sL} from (41), d_{ML} from (40) and d_{Ls2} from (24). The path parameters for rounded earth diffraction are the attenuation line intercept (A_p), the attenuation path slope (M_p) and the height gain function ($G_{\hbar p1,2}$). For the following equations, the values for the F-O-ML path, A_F, M_F, and $G_{\hbar F1,2}$, will equal A_p, M_p and $G_{\hbar 1,2}$ respectively using h_{ep1} from (47), h_{ep2} equal to h_{e2} from (21) and $d_{Lp1,2}$ values for the F-O-ML path as determined in (48) and (49). The values for the O-A path, A_A, M_A and $G_{\hbar A1,2}$ will equal A_p, M_p and $G_{\hbar 1,2}$ respectively using h_{ep1} from (47), h_{ep2} equal to h_{e2} from (21) and $d_{Lp1,2}$ values for the O-A path as determined in (48) and (49).

Constants for the equations are the effective earth radius (a from (14)), the frequency (f in MHz), the conductivity for the type of surface (σ from Table 1) and the dielectric constant (ε from Table 1).

TABLE 1

Surface types and constants [4]

Type	Conductivity (mhos/m)	Dielectric Constant
Poor ground	0.001	4
Average ground	0.005	15
Good ground	0.02	25
Sea water	5*	81*
Fresh water	0.01*	81*
Concrete	0.01	5
Metal	10^7	10

*More appropriate values are calculated if surface sea temperature is specified.

$$\theta_3 = 0.5 \, (a \, f)^{-1/3} \quad \text{rad} \tag{50}$$

$$\theta_4 = 3\theta_3 \quad \text{rad} \tag{51}$$

$$d_{Lp} = d_{Lp1} + d_{Lp2} \quad \text{km} \tag{52}$$

$$d_3 = d_{Lp} + a\theta_3 \quad \text{km} \tag{53}$$

$$d_4 = d_{Lp} + a\theta_4 \quad \text{km} \tag{54}$$

$$a_{1,2} = \frac{d_{Lp1,2}^2}{2h_{ep1,2}} \quad \text{km} \tag{55}$$

$$a_{3,4} = \frac{(d_{3,4} - d_{LP})}{\theta_{3,4}} \quad \text{km} \tag{56}$$

$$K_{d1,2,3,4} = 0.36278 \, (f a_{1,2,3,4})^{-1/3} \, [(\varepsilon - 1)^2 + (18\,000\sigma/f)^2]^{-1/4} \tag{57}$$

$$K_{1,2,3,4} = \begin{cases} K_{d1,2,3,4} & \text{for horizontal polarization} \\ K_{d1,2,3,4} \, [\varepsilon^2 + (18\,000\sigma/f)^2]^{1/2} & \text{for vertical polarization} \end{cases} \tag{58}$$

$$K_{F1,2} = \text{lesser } of \; K_{1,2} \text{ or } 0.99999 \tag{59}$$

$$B_{1,2,3,4} = 416.4 \, f^{1/3} \left(1.607 - K_{1,2,3,4}\right) \tag{60}$$

$$X_{1,2} = B_{1,2} \, a_{1,2}^{-2/3} \, d_{Lp1,2} \quad \text{km} \tag{61}$$

$$X_{3,4} = B_{3,4}\, a_{3,4}^{-2/3}\left(d_{3,4} - d_{Lp1,2}\right) + X_1 + X_2 \quad \text{km} \tag{62}$$

$$G_{1,2,3,4} = 0.05751\, X_{1,2,3,4} - 10\, \log_{10} X_{1,2,3,4} \tag{63}$$

$$W_{1,2} = 0.0134\, X_{1,2}\, \exp\left(-0.005\, X_{1,2}\right) \tag{64}$$

$$y_{1,2} = 40\, \log_{10}\left(X_{1,2}\right) - 117 \quad \text{dB} \tag{65}$$

$$F_{1,2} = \begin{cases} y_{1,2} \text{ or} -117 (\text{whichever has the lesser absolute value}) \text{ for } 0 \le K_{F1,2} \le \ 10^{-5} \\ y_{1,2} \qquad\qquad\qquad \text{for } 10^{-5} \ \le \ K_{F1,2} \ \text{and} \ -450\left(\log_{10} K_{F1,2}\right)^{-3} \le X_{1,2} \text{ dB} \\ 20\, \log_{10}\left(K_{F1,2}\right) - 15 + \frac{2.5\,(10)^{-5}\, X_{1,2}^2}{K_{F1,2}} \qquad\qquad\qquad\qquad \text{otherwise} \end{cases} \tag{66}$$

$$F_{X1,2} = \begin{cases} F_{1,2} & \text{for } 0 \le \ X_{1,2} \ \le 200 \\ W_{1,2}\, y_{1,2} + \left(1 - W_{1,2}\right) G_{1,2} & \text{for } 200 \le \ X_{1,2} \ \le 2\,000 \quad \text{dB} \\ G_{1,2} & \text{for } 2\,000 \ \le \ X_{1,2} \end{cases} \tag{67}$$

$$A_{3,4} = G_{3,4} - F_{X1} - F_{X2} - 20 \quad \text{dB} \tag{68}$$

The values for A_p and M_p are:

$$M_p = \frac{A_4 - A_3}{d_4 - d_3} \qquad \text{dB/km} \tag{69}$$

$$A_p = A_4 - M_p d_4 \qquad \text{dB} \tag{70}$$

Rounded earth diffraction attenuation the path F-O-ML uses M_F equal to M_p and A_F equal to A_p with the values of (67, 68) associated with the F-O-ML path in (47, 48, 49).

$$A_{rML} = A_F + M_F d \qquad \text{dB} \tag{71}$$

The value d is the great circle path distance in km which is an input parameter. Rounded earth diffraction attenuation the path O-A uses A_A equal to A_p and M_A equal to M_p with the values of (67) and (68) associated with the O-A path in (47), (48) and (49).

$$A_{rA} = A_A + M_A(d_{LO1} + d_{LO2}) \qquad \text{dB} \tag{72}$$

Here are the equations for $G_{fip1,2}$ that equals either $G_{fiF1,2}$ or $G_{fiO1,2}$ depending on whether one uses values in (47), (48) and (49) associated with F-O-ML or O-A respectively.

$$B_{N1,2} = 1.607 - K_{1,2} \tag{73}$$

$$f_{1,2} = 2.235\, B_{N1,2}^2 \left(\frac{f^2}{a_{1,2}}\right)^{1/3} h_{ep1,2} \tag{74}$$

$$f_{c1,2} = 0.3\, \sqrt{d_{Lp1,2}\lambda} \tag{75}$$

where λ is from (9).

$$G_{W1,2} = \begin{cases} 0 & \text{if } h_{ep1,2} \ge 2 f_{c1,2} \\ 1 & \text{if } h_{ep1,2} \le f_{c1,1} \\ 0.5\left(1 + \cos\left[\frac{\pi\,(h_{ep1,2} - f_{c1,2})}{f_{c1,2}}\right]\right) & \text{otherwise} \end{cases} \tag{76}$$

$$
G_{ℏ1,2} = \begin{cases}
0 \quad \text{whenever } h_{ep1,2} \geq 2f_{c1,2} \\
-6.6 - 0.013\, ℏ_{1,2} - 2\, \log_{10} ℏ_{1,2} \quad \text{whenever } ℏ_{1,2} \geq 2.5 \\
\qquad \text{or when } K_{1,2} \leq 0.01 \\
1.2 - 13.5\, ℏ_{1,2} + 15\, \log_{10} ℏ_{1,2} \quad \text{if } ℏ_{1,2} < 0.3 \\
-6.5 - 1.67\, ℏ_{1,2} + 6.8\, \log_{10} ℏ_{1,2} \quad \text{if } 0.3 \leq ℏ_{1,2} < 2.5 \\
\qquad \text{or when } 0.01 < K_{1,2} \leq 0.5 \\
T - 25\,(T - B)\,(0.05 - K_{1,2}) \\
\qquad \text{where} \\
T = -13.9 + 24.1\, ℏ_{1,2} + 3.1\, \log_{10} ℏ_{1,2} \quad \text{if } ℏ_{1,2} < 0.25 \\
T = -5.9 - 1.9\, ℏ_{1,2} + 6.6\, \log_{10} ℏ_{1,2} \quad \text{if } 0.25 \leq ℏ_{1,2} < 2.5 \\
B = 1.2 - 13.5\, ℏ_{1,2} + 15\, \log_{10} ℏ_{1,2} \quad \text{if } ℏ_{1,2} < 0.3 \\
B = -6.5 - 1.67\, ℏ_{1,2} + 6.8\, \log_{10} ℏ_{1,2} \quad \text{if } 0.3 \leq ℏ_{1,2} < 2.5 \\
\qquad \text{or when } K_{1,2} > 0.5 \\
T - 20\,(T - B)\,(0.1 - K_{1,2}) \\
\qquad \text{where} \\
T = -13 \quad \text{if } ℏ_{1,2} < 0.1 \\
T = -4.7 - 2.5\, ℏ_{1,2} + 7.6\, \log_{10} ℏ_{1,2} \quad \text{if } 0.1 \leq ℏ_{1,2} < 2.5 \\
B = -13.9 + 24.1\, ℏ_{1,2} + 3.1\, \log_{10} ℏ_{1,2} \quad \text{if } ℏ_{1,2} < 0.25 \\
B = -5.9 - 1.9\, ℏ_{1,2} + 6.6\, \log_{10} ℏ_{1,2} \quad \text{if } 0.25 \leq ℏ_{1,2} < 2.5
\end{cases} \quad \text{dB} \quad (77)
$$

where the values associated with $K_{1,2}$ are from curve fitting to gain curves [5]. The height gain functions are calculated as follows:

$$
G_{ℏp1,2} = G_{h1,2}\, G_{W1,2} \quad \text{dB} \tag{78}
$$

$$
G_{ℏF1,2} = G_{ℏp1,2} \quad \text{dB} \quad \text{for path F} - \text{O} - \text{ML} \tag{79}
$$

$$
G_{ℏA1,2} = G_{ℏp1,2} \quad \text{dB} \quad \text{for path O} - \text{A} \tag{80}
$$

5.2 Knife-edge diffraction

Knife-edge diffraction attenuation is a combination of the knife-edge diffraction attenuations for paths F-O-ML and O-A as in the rounded earth diffraction. For the knife-edge diffraction attenuation for path F-O-ML, A_{KML}:

$$
A_{KML} = 6 - G_{ℏF1} - G_{ℏF2} \quad \text{dB} \tag{81}
$$

where $G_{ℏF1,2}$ are from (79). The knife-edge diffraction attenuation for the path O-A, A_{KA}, is calculated by the following sequence of equations:

$$
d_{LsA} = d_{LO1} + d_{LO2} \quad \text{km} \tag{82}
$$

The values $d_{LO1,2}$ are from (48) and (49).

$$
\theta_v = \theta_{e1} + \theta_{e2} + \frac{d_{L1} + d_{LsA}}{a} \quad \text{rad} \tag{83}
$$

The values $\theta_{e1,2}$ and d_{L1} are from Fig. 5.

$$v = 5.1658 \, \sin(0.5 \, \theta_v) \, \sqrt{\frac{f \, d_{LsA} \, d_{L1}}{d_{LsA} + d_{L1}}} \quad \text{rad} \tag{84}$$

The values C_v and S_v are calculated from Fresnel integrals.

$$C_v = \int_0^v \cos\left(\frac{\pi t^2}{2}\right) dt \tag{85}$$

$$S_v = \int_0^v \sin\left(\frac{\pi t^2}{2}\right) dt \tag{86}$$

$$f_v = 0.5 \, \sqrt{[1 - (C_v + S_v)]^2 + (C_v - S_v)^2} \tag{87}$$

$$A_{KA} = A_{rA} - G_{fiML1} - G_{fiA1} - 20 \, \log_{10} f_v \quad \text{dB} \tag{88}$$

The value A_{rA} is from (72) and the values G_{fiML1} and G_{fiA1} are from (79) and (80) for paths F-O-ML and O-A respectively.

5.3   Diffraction attenuation

Rounded earth diffraction attenuation and knife-edge diffraction attenuation combine to form the total diffraction attenuation, A_d. The blending factor, W, is calculated from:

$$W = \begin{cases} 1 & \text{when } d_{ML} \geq d_{Ls} \quad \text{(rounded earth only)} \\ 0 & \text{when } d_{ML} \leq 0.9 \, d_{Ls} \quad \text{(knife} - \text{edge only)} \\ 0.5 \left[1 + \cos\left(\frac{\pi \, (d_{Ls} - d_{ML})}{0.1 \, d_{Ls}}\right)\right] & \text{otherwise} \end{cases} \tag{89}$$

where the maximum LoS distance, d_{ML}, is from (40) and the total smooth earth distance, d_{Ls}, is from (25). The diffraction attenuation for path F-O-ML, A_{ML}, uses the blending factor:

$$A_{ML} = \begin{cases} A_{rML} & \text{if } W > 0.999 \\ A_{KML} & \text{if } W < 0.001 \quad \text{dB} \\ (1 - W)A_{KML} + W A_{rML} & \text{otherwise} \end{cases} \tag{90}$$

where A_{rML} is from (71) calculated with d_{ML} and A_{KML} is from (81). The facility-to-antenna 2, d_A, distance is calculated from:

$$d_A = d_{L1} + d_{LsA} \quad \text{km} \tag{91}$$

where d_{L1} is from (34) and d_{LsA} is from (80). The diffraction attenuation for path O-A, A_A, also, uses the blending factor, W:

$$A_A = \begin{cases} A_{rA} & \text{if } W > 0.999 \\ A_{KA} & \text{if } W < 0.001 \quad \text{dB} \\ (1 - W)A_{KA} + W A_{rA} & \text{otherwise} \end{cases} \tag{92}$$

where $A_{rA} = A_{rML}$ from (71) with $d = d_A$ and A_{KA} is from (88). The values for the diffraction attenuation, A_d, and M_d are:

$$M_d = \frac{A_{ML} - A_A}{d_{ML} - d_A} \quad \text{dB/km} \tag{93}$$

$$A_d = A_{ML} + M_d(d - d_{ML}) \text{ dB} \tag{94}$$

The value d is the great circle path distance in km which is an input parameter. The terrain attenuation, A_T, uses A_d in § 7.

6 Line-of-sight region

For paths shorter than the maximum LoS range (i.e. $d < d_{ML}$), calculations for the LoS attenuation, A_{LoS}, start with a two ray model involving the phasor sum of the direct and the earth-reflected rays. This scenario, also, includes the short term fading statistics, Y_π, from § 10.2. Diffraction makes a contribution to A_{LoS} for distances less than the maximum LoS distance but greater than the LoS transition distance (i.e. $d_0 < d < d_{ML}$). Some of the parameters affected by a counterpoise include the counterpoise component in this section, but the discussion on counterpoise is in Attachment 1. For any parameter in this section that has a "g" subscript, there is a parameter with a "c" subscript that uses parameters related to a counterpoise that will are discussed in this section or in Attachment 1.

6.1 Two-ray path length geometry

Figure 9 shows the geometry for the two-ray model used on the LoS region. The value Δr is the difference between the direct ray, r_0, and the length of the reflected ray, $r_{12} = r_1 + r_2$.

$$\Delta r = r_{12} - r_0 \quad \text{km} \tag{95}$$

The following set of equations determines Δr and path length d for various values of the grazing angle, ψ. This calculation is repeated for different values of ψ until there is sufficient coverage for Δr and d. the counterpoise parameters are included here, but will be used in Attachment 1.

$$z = \frac{a_0}{a} - 1 \tag{96}$$

$$k_a = \frac{1}{(1 + z \cos \psi)} \tag{97}$$

$$a_a = a_0 k_a \quad \text{km} \tag{98}$$

$$\Delta h_{a1,2} = \Delta h_{e1,2} \frac{(a_a - a_0)}{(a - a_0)} \quad \text{km} \tag{99}$$

$$H_1 = \begin{cases} h_{r1} - \Delta h_{a1} & \text{for earth} \\ h_{fc} & \text{for counterpoise} \end{cases} \quad \text{km} \tag{100a}$$

$$H_2 = \begin{cases} h_{r2} - \Delta h_{a2} & \text{for earth} \\ h_{r2} - \Delta h_{a2} - h_c & \text{for counterpoise} \end{cases} \quad \text{km} \tag{100b}$$

where a_0 is the actual earth radius of 6 370 km, h_c is an input parameter and h_{fc} is from (19).

$$z_{1,2} = a_a + H_{1,2} \quad \text{km} \tag{101}$$

$$\theta_{1,2} = \cos^{-1}\left(\frac{a_a \cos \psi}{z_{1,2}}\right) - \psi \quad \text{rad} \tag{102}$$

$$D_{1,2} = z_{1,2} \sin \theta_{1,2} \quad \text{km} \tag{103}$$

$$H'_{1,2} = \begin{cases} D_{1,2} \tan \psi & \text{for } \psi < 1.56 \text{ rad} \\ H_{1,2} & \text{otherwise} \end{cases} \quad \text{km} \tag{104}$$

$$\alpha = \begin{cases} \tan^{-1}\left[\dfrac{(H'_2 - H'_1)}{D_1 + D_2}\right] & \text{for } \psi < 1.56 \text{ rad} \\ \psi & \text{otherwise} \end{cases} \quad \text{km} \tag{105}$$

$$r_0 = \begin{cases} \dfrac{(D_1 + D_2)}{\cos \alpha} & \text{for } \psi < 1.56 \text{ rad} \\ H_2 - H_1 & \text{otherwise} \end{cases} \quad \text{km} \tag{106}$$

FIGURE 9

Spherical earth with two ray path geometry

$$\theta_{h1,2} = \pm\,\alpha - \theta_{1,2}$$
(use + for θ_{h1})

$-\theta_2$

r_0

θ_{n1}

α

r_2

θ_1

H_2 H_2'

r_1

H_1 Not drawn
to scale

H_1' Ψ Ψ

d

a_a

θ_1 θ_2

$R_{12} = r_1 + r_2$

$$\Delta r = \frac{4H_1'\,H_2'}{R_{12} + r_0}$$

$$\Delta r \approx 2H_1'H_2'/d$$

d_1 d_2

Note: relationships between the various geometric parameters shown here were
previously provided in IF-73 (3, Sec. A.4.2).
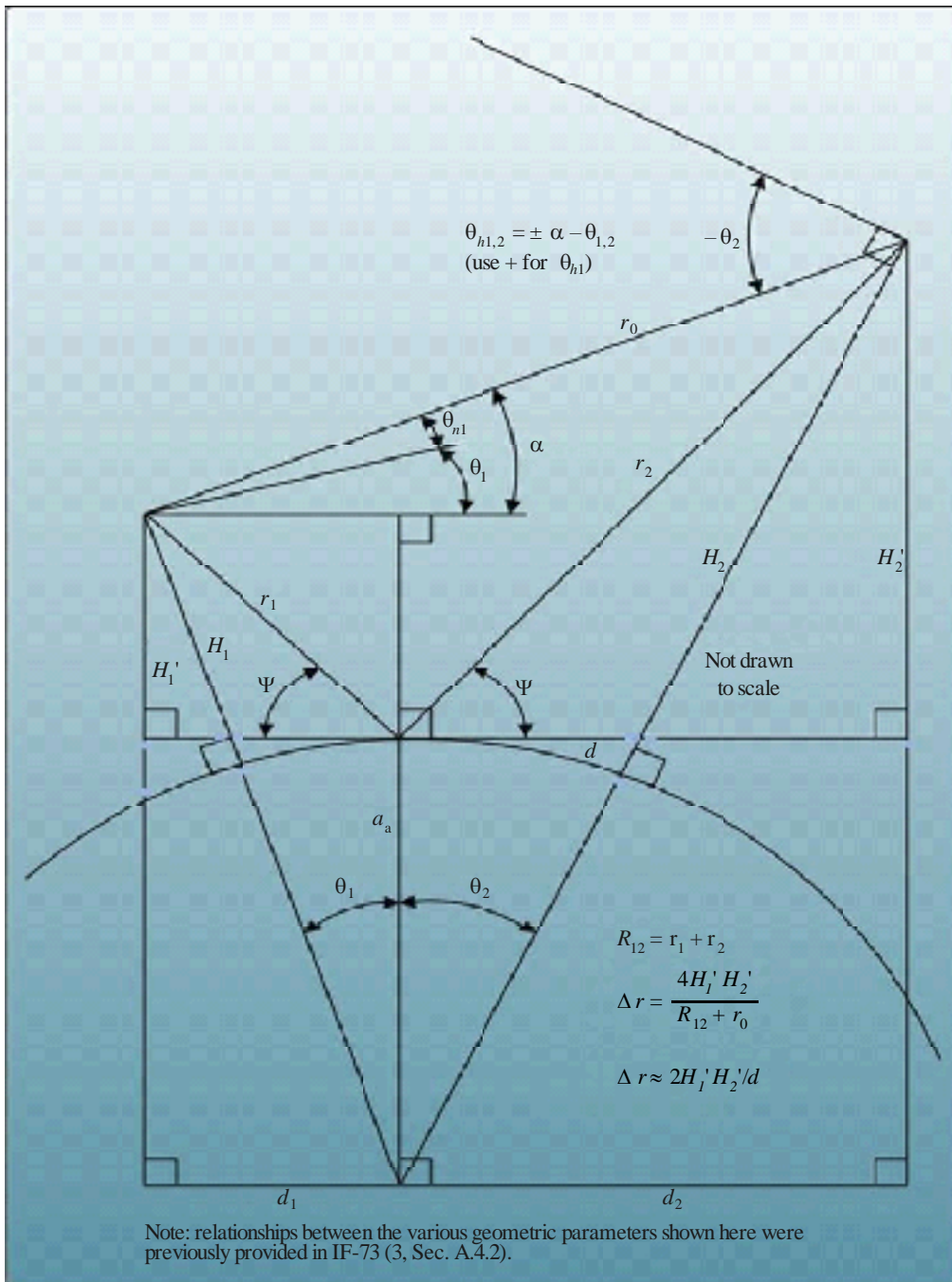
Report P.2345 -09

$$r_{12} = \begin{cases} \dfrac{(D_1 + D_2)}{\cos\psi} & \text{for } \psi < 1.56 \text{ rad} \\[2mm] H_1 + H_2 & \text{otherwise} \end{cases} \quad \text{km} \tag{107}$$

$$\Delta r = \frac{4\,H'_1 H'_2}{(r_0 + r_{12})} \quad \text{km} \tag{108}$$

There are two types of Δr, Δr_g refers to earth parameters and equals Δr from (108) when using the earth parameters from (100a) and (100b) to calculate $H'_{1,2}$. The value Δr_c refers to counterpoise parameters and equals Δr from (108) when using the counterpoise parameters from (100a) and (100b) to calculate $H'_{1,2}$.

$$\theta_{h1} = \alpha - \theta_1 \quad \text{rad} \tag{109a}$$

$$\theta_{h2} = -(\alpha + \theta_2) \quad \text{rad} \tag{109b}$$

$$\theta_{r1,2} = -(\psi + \theta_{h1,2}) \quad \text{rad} \tag{110}$$

$$\theta_0 = \theta_{r1} + \theta_{r2} \qquad \text{rad} \tag{111}$$

$$d = a_a \theta_0 \quad \text{km} \tag{112}$$

This set of equations to calculate the great circle distance d uses an adjusted effective earth radius, a_a, and adjusted effective antenna heights, $H_{1,2}$, that vary with ψ since the values a from (14) and $h_{r1,2}$ from (17) are not appropriate when cos ψ is not near to a value of 1. The value Δr is calculated by (108) rather than (95), because r_0 and r_{12} may be very large and almost equal.

Except where there is a specific reference to the counterpoise case, any calculations based on Δr, including equations (108) through (111), are from the earth reflection case (e.g. $\Delta r = \Delta r_g$).

6.2 Effective Reflection Coefficient

The magnitude of the effective reflection coefficient, R_{Tg}, includes the divergence, D_v, and ray length factor, F_r, from § 6.2.1; the surface roughness factor, $F_{\sigma h}$, from § 6.2.2; antenna gain pattern factor, g_{Rg}, from § 6.2.3; plane earth reflection coefficient magnitude, R_g, from § 6.2.4; and a counterpoise factor, f_g, from Attachment 1. Where there is no counterpoise, f_g equals 1.

$$R_{Tg} = D_v F_r F_{\sigma h} f_g g_{Rg} R_g \tag{113}$$

6.2.1 Divergence and ray length factors

The divergence factor, D_v, accounts for a reduction in the magnitude of the reflection from a curved surface as compared to a reflection from a flat surface. In the case where the reflected ray is much longer than the direct ray, such as two close aircraft antennas, the ray length factor, F_r, accounts for the reduction in the magnitude of the reflected ray.

The equations to calculate D_v and F_r are:

$$r_{1,2} = \begin{cases} H_{1,2} & \text{if } \psi = 90° \\ \dfrac{D_{1,2}}{\cos \psi} & \text{otherwise} \end{cases} \quad \text{km} \tag{114}$$

where $H_{1,2}$ are from (100a) and (100b), the grazing angle, ψ, is from Fig. 9, and $D_{1,2}$ are from (103).

$$R_r = \frac{r_1 r_2}{r_{12}} \qquad \text{km} \tag{115}$$

where r_{12} is from (107).

$$D_v = \left[1 + \frac{2R_r(1 + (\sin\psi)^2)}{a_a \sin\psi} + \left(\frac{2R_r}{a_a}\right)^2\right]^{-\frac{1}{2}} \tag{116}$$

where a_a is from (98).

$$F_r = \frac{r_0}{r_{12}} \tag{117}$$

where r_0 is from (106).

6.2.2   Surface roughness factors

There are surface roughness factors for specular, $F_{\sigma h}$, and diffuse, $F_{d\sigma h}$, reflections. The calculations for these factors are:

$$\Delta h_d = \Delta h_m \left[1 - 0.8 \exp(-0.02\,d)\right] \quad\quad \text{m} \tag{118}$$

Here the Δh_m value is the terrain parameter Δh in metres. The Δh value is an input parameter. The great circle distance, d, is from (112).

$$\sigma_h = \begin{cases} 0.25\, H_{1/3} & \text{for water} \\ 0.39\, \Delta h_d & \text{for } \Delta h_d \leq 4\,m \\ 0.78\, \Delta h_d \exp\left(-0.5\, \Delta h_d^{1/4}\right) & \text{otherwise} \end{cases} \quad \text{m} \tag{119}$$

where $H_{1/3}$ is a value for significant wave height based on the sea state for a water reflecting surface. This parameter is chosen from Table 2.

$$\delta = \sigma_h \sin\frac{\psi}{\lambda_m} \quad\quad \text{m} \tag{120}$$

where the grazing angle, ψ, from Fig. 9 is a starting parameter for calculating Δr in § 5.1. The wavelength in metres, λ_m, is from (9).

$$F_{\sigma h} = \exp(-2\pi\delta) \tag{121}$$

TABLE 2

Estimates of parameters for sea states [4]

Sea [a] State Code	Descriptive Terms [a]	Average Wave Height Range Meters (feet)	$H_{1/3}$ [b] Meters (feet)	σ_h [c] Meters (feet)
0	Calm (glassy)	0 (0)	0 (0)	0 (0)
1	Calm (rippled)	0 - 0.1 (0 - 0.33)	0.09 (0.3)	0.00 (0.08)
2	Smooth (wavelets)	0.1 - 0.5 (0.33 - 1.6)	0.43 (1.4)	0.11 (0.35)
3	Slight	0.5 - 1.25 (1.6 - 4.0)	1 (3.3)	0.25 (0.82)
4	Moderate	1.25 - 2.5 (4 - 8)	1.9 (6.1)	0.46 (1.5)
5	Rough	2.5 - 4 (8 - 13)	3 (10)	0.76 (2.5)
6	Very rough	4 - 6 (13 - 20)	4.6 (15)	1.2 (3.8)
7	High	6 - 9 (20 - 30)	7.9 (26)	2 (6.5)
8	Very high	9 - 14 (30 - 46)	12 (40)	3 (10)
9	Phenomenal	>14 (>46)	>14 (>45)	>3.5 (>11)

(a) Based on international meteorological code [42, code 3700].

(b) Estimates significant wave heights, average of highest one-third, $H_{1/3}$ [53, table 1].

(c) Estimated using a formulation provided by Moskowitz [41, (1)] with $H_{1/3}$ estimates.

$$F_{d\sigma h} = \begin{cases} 0.01 + 946\,\delta^2 & \text{if } \delta < 0.00325 \\ 6.15\,\delta & \text{if } 0.00325 \leq \delta \leq 0.0739 \\ 0.45 + \sqrt{0.000843 - (\delta - 0.1026)^2} & \text{if } 0.0739 \leq \delta \leq 0.1237 \\ 0.601 - 1.06\,\delta & \text{if } 0.1237 \leq \delta \leq 0.3 \\ 0.01 + 0.875\exp(-3.88\,\delta) & \text{otherwise} \end{cases} \qquad (122)$$

The determination of $F_{d\sigma h}$ is curve fitting to measured data [6]. The diffuse reflection coefficient, R_d, uses $F_{d\sigma h}$, the plane earth reflection coefficient magnitude, R_g, from § 6.2.4, the ray length factor, F_r, from (117), the counterpoise factor, f_g, from (293) and the antenna gain pattern factor, g_{Rg}, from § 6.2.3. When there is no counterpoise, f_g equals 1.

$$R_d = F_r F_{d\sigma h} f_g g_{Rg} R_g \qquad (123)$$

6.2.3 Antenna pattern gain factors

The antenna gain factors $g_{D,R}$ and $g_{Rh,v}$ allow for situations where antenna gains effective for the direct ray path are different from the gains effective for the reflected ray path. Figure 10 shows the relationship between the two ray paths and the gains. The gains are relative voltage gains and are measured relative to the boresight of the their respective antennas (i.e. for boresight, $g_{D,R} = g_{R1,2} = 1$ V/V). Relative gain values can be determined from antenna patterns (i.e. Fig. 11).

FIGURE 10

Antenna gain notation and correspondence between ray take-off angles and gains
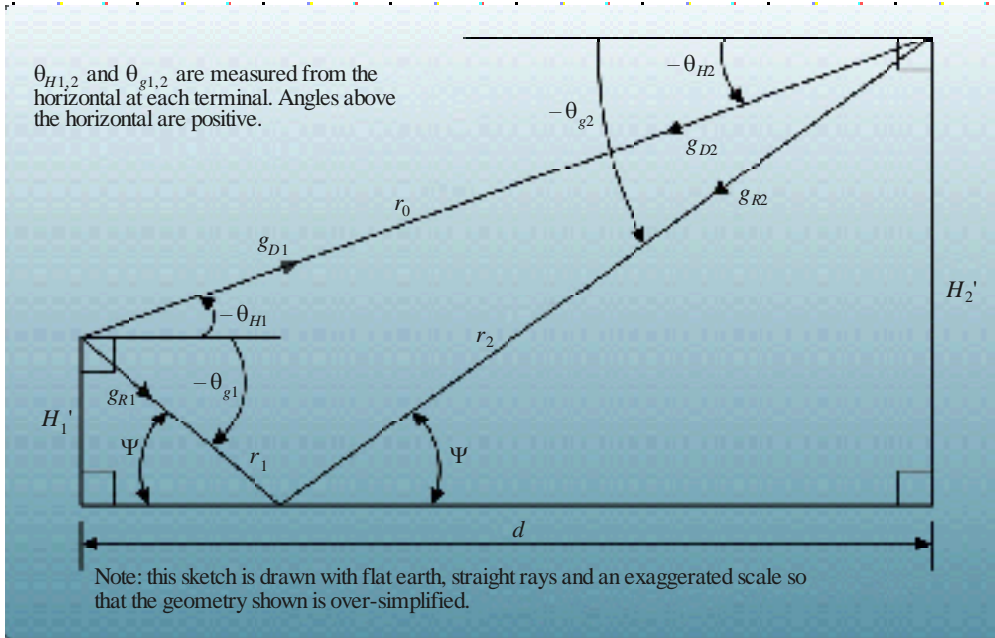
Report P.2345 -10

These gains are complex quantities, but are treated as scalars in this method since, in many practical applications, the relative phase between the direct and reflected rays is expected to be zero or is unknown. The voltage gains are ratios that are dimensionless, but are different from power ratios that are also dimensionless. Decibel gains are related to these gains by:

$$G_{R1,2} = 20 \ \log_{10} g_{R1,2} \quad \text{dB} \tag{124}$$

Here $G_{R1,2} \leq 0$ because $0 < g_{R1,2} \leq 1$. The calculations for $g_{D,R}$ are:

$$g_D = \begin{cases} g_{D1}g_{D2} & \text{for linear polarization} \\ 0.5 \left[g_{hD1}g_{hD2} + g_{vD1}g_{vD2} \right] & \text{for elliptical polarization} \end{cases} \tag{125}$$

$$g_R = \begin{cases} 1 & \text{for isotropic and/or elliptical polarization} \\ g_{R1}g_{R2} & \text{otherwise} \end{cases} \tag{126}$$

Isotropic implies that, for the radiation angle of interest, $g_{R1} = g_{D1}$ and $g_{R2} = g_{D2}$. Elliptical polarization uses both the horizontally polarized ($g_{hD1,2}$ and $g_{hR1,2}$) and vertically polarized ($g_{vD1,2}$ and $g_{vR1,2}$) components of the antennas. Table 3 shows values for $g_{D1,1}$.

The gain factor g_{Rv} involves the vertical polarization gains, $g_{vR1,2}$.

$$g_{Rv} = \begin{cases} 1 & \text{for isotropic antennas} \\ g_{vR1}g_{vR2} & \text{otherwise} \end{cases} \tag{127}$$

The gain factor g_{Rh} is the same for horizontal polarization gains.

$$g_{Rh} = \begin{cases} 1 & \text{for isotropic antennas} \\ g_{hR1} g_{hR2} & \text{otherwise} \end{cases} \tag{128}$$

FIGURE 11

Normalized antenna gain vs. elevation angle [2]
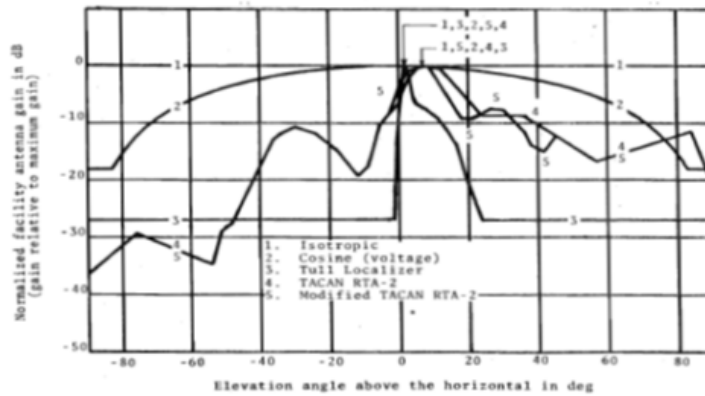
Report P.2345-11

The antenna patterns in Fig. 11 are vertical plane patterns. Adjusting $G_{T,R}$ from (4) can change gain variations in azimuth. The values $G_{NT,R}$ for (4) are:

$$G_{NT} = \begin{cases} 20 \log_{10} g_{D1} & \text{if the lower antenna is transmitting} \\ 20 \log_{10} g_{D2} & \text{otherwise} \end{cases} \tag{129}$$

$$G_{NR} = \begin{cases} 20 \log_{10} g_{D1} & \text{if the lower antenna is receiving} \\ 20 \log_{10} g_{D2} & \text{otherwise} \end{cases} \tag{130}$$

The elevation angles associated with the gain factors are in Table 3.

TABLE 3

Gain factors for elevation angles [1]

Factor	Elevation Angle
g_{D1}	θ_{H1} for LoS, θ_{e1} from Fig. 6 otherwise
g_{D2}	θ_{H2} for LoS, θ_{e2} from (44) otherwise
g_{R1}, g_{vR1}, g_{hR1}	θ_{g1}
g_{R2}, g_{vR2}, g_{hR2}	θ_{g2}

Calculations for these angles are:

$$\theta_{L1,2} = \left(\theta_{es1,2} + \theta_{s1,2} \right) \left(\frac{a_a - a_0}{a - a_0} \right) \qquad \text{rad} \tag{131}$$

where $\theta_{es1,2}$ are from (27), $\theta_{s1,2}$ are from (26), a_a is from (98) and a is from (14). The value a_0 is the actual earth radius at 6 370 km.

$$\theta_{H1,2} = \theta_{h1,2} + \theta_{L1,2} \quad \text{rad} \tag{132}$$

$$\theta_{g1,2} = \theta_{r1,2} + \theta_{L1,2} \quad \text{rad} \tag{133}$$

where $\theta_{h1,2}$ is from (109a) and (109b) and $\theta_{r1,2}$ is from (110). The angles $\theta_{L1,2}$ force an element of ray tracing in the elevation angles at the smooth earth horizon and prorate the values elsewhere.

The values $H_{1,2}$ in (100a) and (100b) have the option for a value based on a counterpoise. This, in turn affects $\theta_{h1,2}$ and $\theta_{r1,2}$. The counterpoise case is discussed further in Attachment 1. The parameter g_{Rg} from (123) equals g_R from (126) associated with the $H_{1,2}$ value for ground reflection.

6.2.4   Plane earth reflection coefficients

The dielectric constant, ε, and conductivity, σ, of the reflective surface determine the plane earth reflection coefficient, $R \exp(-j\varphi)$.

For water:

$$\varepsilon = \frac{\varepsilon_s - \varepsilon_0}{1 + (2\pi f T)^2} + \varepsilon_0 \tag{134}$$

$$\sigma = \frac{f^2 T(\varepsilon - \varepsilon_0)}{2\,865} + \sigma_i \quad \text{mho/m} \tag{135}$$

The dielectric constant, ε_0, represents electronic and atomic polarizations and equals 4.9. The value ε_s is the static dielectric constant; the frequency, f, is in MHz; the relaxation time, T, is in μs and σ_i is the ionic conductivity. The values for ε_s, T and σ_i for water are from Table 4.

TABLE 4

Surface dielectric constant and conductivity for water [2]

For Fresh Water

	0°C	10°C	20°C
ε_s [d]	88	84	80
T[μs] [d]	1.87×10^{-5}	1.36×10^{-5}	1.01×10^{-5}
σ_i [mho/m] [a]	0.01	0.01	0.01

For Sea Water [e]

	0°C	10°C	20°C
ε_s	75	72	69
T[μs]	1.69×10^{-5}	1.21×10^{-5}	9.2×10^{-6}
σ_i [mho/m]	3.0	4.1	5.2

For all other surfaces, the appropriate dielectric constant, ε, and conductivity, σ, are from Table 5.

TABLE 5

Surface types and constants [4]

Type	Conductivity (mhos/m)	Dielectric Constant
Poor ground	0.001	4
Average ground	0.005	15
Good ground	0.02	25
Sea water	5*	81*
Fresh water	0.01*	81*
Concrete	0.01	5
Metal	10^7	10

*More appropriate values are calculated if surface sea tempera-
ture is specified.

The formulation for $R \exp(-j\varphi)$ is as follows:

$$\varepsilon_c = \varepsilon - j60\,\lambda_m \sigma \qquad (136)$$

where λ_m is from (9).

$$Y_c = \sqrt{\varepsilon_c - \cos^2\psi} \qquad (137)$$

where the grazing angle, ψ, from Fig. 9 is a starting parameter for Δr in § 5.1.

$$R_v \exp[-j(\pi - c_v)] = \frac{\varepsilon_c \sin\psi - Y_c}{\varepsilon_c \sin\psi + Y_c}\,g_R \qquad (138a)$$

where g_R is from (126).

$$R_h \exp[-j(\pi - c_h)] = \frac{\sin\psi - Y_c}{\sin\psi + Y_c}\,g_R \qquad (138b)$$

$$R_e \exp[-j(\pi - c_e)] = 0.5\left[g_{Rh}R_h \exp[-j(\pi - c_h)]\right] + \left[g_{Rv}\,R_v \exp[-j(\pi - c_v)]\right] \qquad (138c)$$

where $g_{Rv,h}$ are from (127) and (128), and

$$R \exp(-j\phi) = \begin{cases} R_v \exp[-j(\pi - c_v)] & \text{for vertical polarization} \\ R_h \exp[-j(\pi - c_h)] & \text{for horizontal polarization} \\ R_e \exp[-j(\pi - c_e)] & \text{for elliptical polarization} \end{cases} \qquad (139)$$

For elliptical polarization, both antennas must have the sense and circular polarization is a special case of elliptical polarization.

When the parameters in equations (134) through (139) use reflection parameters related to earth or ground, the reflection coefficient, $R \exp(-j\varphi)$ becomes:

$$R_g \exp(-j\phi_g) = R \exp(-j\phi) \qquad (140)$$

For the counterpoise case, the reflection coefficient becomes $R_c \exp(-j\varphi_g)$, see Attachment 1. This is true where the geometry used to calculated gain factors in § 5.2.3 use the $H_{1,2}$ values from (100a) and (100b).

The total phase lag between the direct ray and the reflected ray is:

$$\Phi_{Tg} = \frac{2\,\pi\,\Delta r_g}{\lambda} + \Phi_g + \Phi_{kg} + \frac{\pi v_g^2}{2} \qquad \text{rad} \tag{141}$$

The value Δr_g equals Δr from (108). The parameters φ_{kg} and v_g are not necessary when there is no counterpoise since they are part of the phase lag associated with the knife-edge diffraction over the edge of a counterpoise. The values for φ_{kg} and v_g are discussed in Attachment 1.

6.3   Line-of-sight transition distance, d_0

The LoS transition distance, d_0, is the largest distance in the LoS region where the diffraction component is negligible. This parameter is determined as follows:

$$\theta_{h5} = 2\,\sin^{-1}\left[\frac{0.5}{5.1658}\sqrt{\frac{d_{ML}}{f\,d_{L1}(d_{ML}-d_{L1})}}\right] \qquad \text{rad} \tag{142}$$

where d_{ML} is from (40), f is frequency in MHz, and d_{L1} is from Fig. 6.

$$\theta_5 = \theta_{h5} - \tan^{-1}\left[\frac{h_1 - h_{L1}}{d_{L1}} - \frac{d_{L1}}{2a}\right] \qquad \text{rad} \tag{143}$$

where h_{L1} is from Fig. 6, a is from (14), and h_1 is the lower antenna height above mean sea level as shown in Fig. 3.

$$h_{em} = h_2 - \Delta h_{e2} \qquad \text{km} \tag{144}$$

where h_2 is the higher antenna height above mean sea level as shown in Fig. 3 and Δh_{e2} is from (22).

$$d_{L5} = -a\,\tan(\theta_5) + \sqrt{(a\,\tan\theta_5)^2 + 2a(h_{em2}-h_{L1})} \qquad \text{km} \tag{145}$$

$$d_5 = d_{L5} + d_{L1} \qquad \text{km} \tag{146}$$

$$\theta_{e5} = \tan^{-1}\left(\frac{h_{L1} - h_{em2}}{d_{L5}} - \frac{d_{L5}}{2a}\right) \qquad \text{rad} \tag{147}$$

$$\theta_6 = \theta_{e1} + \theta_{e5} + \frac{d_5}{a} \qquad \text{rad} \tag{148}$$

The value θ_{e1} is from (38).

$$v_5 = 5.1658\,\sin(0.5\,\theta_6)\sqrt{\frac{f\,d_{L1}d_{L5}}{d_5}} \tag{149}$$

The value v_5 is the upper limit of the Fresnel integrals:

$$C_5 = \int_0^{v_5} \cos\left(\frac{\pi t^2}{2}\right) dt \tag{150}$$

$$S_5 = \int_0^{v_5} \sin\left(\frac{\pi t^2}{2}\right) dt \tag{151}$$

$$f_5 = 0.5\sqrt{[1 - (C_5 + S_5)]^2 + (C_5 - S_5)^2} \tag{152}$$

$$A_{K5} = -20\log_{10} f_5 \quad \text{dB} \tag{153}$$

$$A_{r5} = A_F + M_F d_5 \quad \text{dB} \tag{154}$$

where M_F and A_F equal M_p and A_p from (69, 70) for the F-O-ML path respectively.

$$A_5 = \begin{cases} A_{r5} & \text{if } W > 0.99 \\ A_{K5} & \text{if } W < 0.001 \quad \text{dB} \\ (1-W)A_{K5} + WA_{r5} & \text{otherwise} \end{cases} \tag{155}$$

where W is from (89), and

$$d_d = d_{ML} - \frac{A_{ML}(d_{ML} - d_5)}{A_{ML} - A_5} \quad \text{km} \tag{156}$$

where A_{ML} is from (90) and d_{ML} is from (40). The parameter d_d is too short for the LoS transition distance when both antennas have low heights, therefore:

$$d_0 = \begin{cases} d_{L1} & \text{when } d_{L1} > d_d \\ d_{\lambda/6} & \text{when } d_{\lambda/6} > d_{L1} \text{ and } d_d \quad \text{km} \\ d_d & \text{otherwise} \end{cases} \tag{157}$$

where d_{L1} is the horizon distance for the lower antenna in Fig. 6. The parameter $d_{\lambda/6}$ is the largest distance using the two ray model from § 6.1 where the reflection coefficient is −1. This is the distance in the set of equations (96) through (108) where Δr equals $\lambda/6$ (λ is the wavelength.).

6.4 Line-of-sight attenuation, A_{LoS}

LoS attenuation, A_{LoS}, is calculated as follows:

$$F_{fs} = \begin{cases} 1 & \text{if lobing is used and } \Delta r_g < 10\lambda \\ 1 & \text{if } \Delta r_g \leq 0.5\,\lambda \text{ and } \left|g_D + R_{Tg}\exp(-j\phi_{Tg})\right| < g_D \\ 0 & \text{otherwise} \end{cases} \tag{158}$$

where Δr_g equals Δr from (106), λ is from (9), g_D is determined in § 5.2.3, R_{Tg} is from (113) and φ_{Tg} is from (141).

$$W_{R0} = \left|g_D + F_{fs}R_{Tg}\exp(-j\phi_{Tg}) + R_{Tc}\exp(-j\phi_{Tc})\right|^2 + 0.0001\,g_D \tag{159}$$

The term $R_{Tc}\exp(-j\varphi_{Tc})$ is due to a counterpoise and is calculated in Attachment 1 if a counterpoise is present. When there is no counterpoise, the term is equal to zero.

$$A_{R0} = 10\log_{10}\left(\frac{g_D^2}{W_{R0}}\right) \quad \text{dB} \tag{160}$$

$$M_L = \frac{A_{ML} - A_0}{d_{ML} - d_0} \qquad \text{dB/km} \tag{161}$$

where A_{ML} is from (90), d_{ML} is from (40) and d_0 is from (157). The parameter A_0 equals A_{R0} with the g_D and W_{R0} values evaluated for $d = d_0$.

$$A_{LOS} = \begin{cases} A_{R0} & \text{if } d < d_0 \\ A_0 + M_L(d - d_0) & \text{if } d_0 \leq d \leq d_{ML} \end{cases} \qquad \text{dB} \tag{162}$$

where d is from (112). The lobing mentioned in (158) is discussed in Attachment 1.

7 Scattering region

This formulation to calculate the tropospheric scattering attenuation, A_s, contains a ray tracing technique that makes it appropriate for use with high antennas. The equation for tropospheric scattering attenuation is:

$$A_s = S_e + S_v + 10 \log_{10}(\kappa\theta^3/l_s) \qquad \text{dB} \tag{163}$$

S_e is a scattering efficiency term and S_v is a scattering volume term. The terms κ, θ and l_s are the wave number, the scattering angle and the total ray length through the scattering volume respectively.

The ray tracing technique for calculating the scattering angle, θ, begins as:

$$\theta_{a1,2} = \frac{\left[\frac{(h_{Lr1,2} - h_{e1,2})}{a + h_{e1,2}} + 2 \sin\left(\frac{d_{L1,2}}{2a}\right)^2\right]}{\left[\sin\left(\frac{d_{L1,2}}{a}\right)\right]} \qquad \text{rad} \tag{164}$$

The heights $h_{Lr1,2}$ are from (37) and (49) and $h_{e1,2}$ are from (21) respectively. The value a is from (14) and $d_{L1,2}$ are from (34) and (43).

$$d_s = d - d_{L1} - d_{L2} \quad \text{km} \tag{165}$$

where the great circle distance, d, is an input parameter.

$$\theta_s = \theta_{a1} + \theta_{a2} + \frac{d_s}{a} \qquad \text{rad} \tag{166}$$

$$d_{z1} = \frac{\left[\left(\frac{d_s}{2a} + \theta_{a2}\right) d_s + h_{L2} - h_{L1}\right]}{\theta_s} \qquad \text{rad} \tag{167}$$

$$d_{z2} = d_s - d_{z1} \qquad \text{km} \tag{168}$$

Here we introduce the upper limit of the gradient of the ray tracing, $A_m = 157 * 10^{-6}$ km^{-1} which relates to the edge of super refractivity. Gradients larger than A_m can produce ducting.

$$dN = A_m - a^{-1} \qquad \text{km}^{-1} \tag{169}$$

$$\gamma_e = \frac{N_s * 10^{-6}}{dN} \qquad \text{km} \tag{170}$$

where N_s is from (13).

$$z_{a1,2} = \frac{1}{2a}\left(\frac{d_{z1,2}}{2}\right)^2 + \theta_{a1,2}\left(\frac{d_{z1,2}}{2}\right) + h_{Lr1,2} \qquad \text{km} \qquad (171)$$

$$z_{b1,2} = \frac{1}{2a} d_{z1,2}^2 + \theta_{a1,2}\, d_{z1,2} + h_{Lr1,2} \qquad \text{km} \qquad (172)$$

$$Q_{o1,2} = A_m - dN \exp\left(-\frac{h_{Lr1,2}}{\gamma_e}\right) \qquad \text{per km} \qquad (173)$$

$$Q_{a1,2} = A_m - dN \exp\left(-\frac{z_{a1,2}}{\gamma_e}\right) \qquad \text{per km} \qquad (174)$$

$$Q_{b1,2} = A_m - dN \exp\left(-\frac{z_{b1,2}}{\gamma_e}\right) \qquad \text{per km} \qquad (175)$$

$$Z_{a1,2} = \frac{(7Q_{o1,2} + 6Q_{a1,2} - Q_{b1,2})}{24}\left(\frac{d_{z1,2}}{2}\right)^2 + \theta_{a1,2}\frac{d_{z1,2}}{2} + h_{Lr1,2} \qquad \text{km} \qquad (176)$$

$$Z_{b1,2} = \frac{(Q_{o1,2} + 2\,Q_{a1,2})}{6}\, d_{z1,2}^2 + \theta_{a1,2}\, d_{z1,2} + h_{Lr1,2} \qquad \text{km} \qquad (177)$$

$$Q_{A1,2} = A_m - dN \exp\left(-\frac{z_{a1,2}}{\gamma_e}\right) \qquad \text{per km} \qquad (178)$$

$$Q_{B1,2} = A_m - dN \exp\left(-\frac{z_{b1,2}}{\gamma_e}\right) \qquad \text{per km} \qquad (179)$$

$$\theta_{A1,2} = \frac{(Q_{o1,2} + 4\,Q_{A1,2} + Q_{B1,2})}{6}\, d_{z1,2} + \theta_{a1,2} \qquad \text{rad} \qquad (180)$$

$$\theta = \theta_{A1} + \theta_{A2} \qquad \text{rad} \qquad (181)$$

The value θ is the scattering angle for the tropospheric scattering attenuation, A_s, from (163).

$$Z_{A1,2} = \frac{(Q_{o1,2} + 2\,Q_{A1,2})}{6}\, d_{z1,2}^2 + \theta_{a1,2}\, d_{z1,2} + h_{Lr1,2} \qquad \text{km} \qquad (182)$$

$$X_a = \frac{(Z_{A2} - Z_{A1})}{\theta} \qquad \text{km} \qquad (183)$$

$$d_{Z1} = d_{z1} + X_a \qquad \text{km} \qquad (184)$$

$$d_{Z2} = d_{z2} - X_a \qquad \text{km} \qquad (185)$$

$$h_v = \frac{(\theta_{A1}Z_{A2} + \theta_{A2}Z_{A1})}{\theta} \qquad \text{km} \qquad (186)$$

The value, h_v, is the height of the scattering volume.

$$X_{A1,2} = (h_{e1,2} - h_{L1,2})^2 + 4(a + h_{e1,2})(a + h_{L1,2}) \sin\left(\frac{d_{L1,2}}{2a}\right)^2 \qquad \text{km} \qquad (187)$$

$$l_{1,2} = X_{A1,2}^{\frac{1}{2}} + d_{Z1,2} \qquad \text{km} \qquad (188)$$

$$l = l_1 + l_2 \qquad \text{km} \qquad (189)$$

The value, l, is the total ray length for the tropospheric scattering attenuation, A_s, from (163).

$$\varepsilon_1 = (5.67 * 10^{-6}) N_s^2 - (2.32 * 10^{-3}) N_s + 0.031 \qquad (190)$$

$$\varepsilon_2 = 0.0002 N_s^2 - 0.06 N_s + 6.6 \qquad (191)$$

$$\vartheta = 0.1424 \left\{ 1 + \frac{\varepsilon_1}{\exp\left[\left(\frac{h_v}{4}\right)^6\right]} \right\} \qquad \text{per km} \qquad (192)$$

$$S_e = 83.1 - \frac{\varepsilon_2}{1 + 0.07716 h_v^2} + 20 \log_{10}\left[\left(\frac{0.1424}{\vartheta}\right)^2 \exp(\vartheta h_v)\right] \qquad \text{dB} \qquad (193)$$

$$s = \frac{(l_1 - l_2)}{l} \qquad (194)$$

S_e is the scattering efficiency term for the tropospheric scattering attenuation, A_s, from (163) and s is the modulus of asymmetry.

$$\eta = \frac{\vartheta \theta l}{2} \qquad (195)$$

$$\kappa = \frac{2\pi}{\lambda} \qquad \text{per km} \qquad (196)$$

where λ is the wavelength in km. This is equal to $\lambda_m/1000$ where λ_m is from (9). The value κ is the wave number.

$$\rho_{1,2} = 2\kappa\theta h_{e1,2} \qquad (197)$$

$$A = (1 - s^2)^2 \qquad (198)$$

$$X_{v1} = (1 + s)^2 \eta \qquad (199)$$

$$X_{v2} = (1 - s)^2 \eta \qquad (200)$$

$$q_{1,2} = X_{v1,2}^2 + \rho_{1,2}^2 \qquad (201)$$

$$B_s = 6 + 8s^2 + 8 \frac{(1 + s)X_{v2}^2 \rho_2^2}{q_2^2} + 8 \frac{(1 - s)X_{v1}^2 \rho_1^2}{q_1^2}$$
$$+ 2(1 - s^2)\left(1 + \frac{2X_{v1}^2}{q_1}\right)\left(1 + \frac{2X_{v2}^2}{q_2}\right) \qquad (202)$$

$$C_s = 12 \left(\frac{\rho_1 + \sqrt{2}}{\rho_1} \right)^2 \left(\frac{\rho_2 + \sqrt{2}}{\rho_2} \right)^2 \left(\frac{\rho_1 + \rho_2}{\rho_1 + \rho_2 + 2\sqrt{2}} \right) \tag{203}$$

$$S_v = 10 \log_{10} \left(\frac{(A\eta^2 + B_s\eta)q_1q_2}{\rho_1^2\rho_1^2} + C_s \right) \quad \text{dB} \tag{204}$$

S_v is the scattering volume term for the tropospheric scattering attenuation, A_s, from (163).

8 Terrain attenuation

Calculations for the terrain attenuation, A_T, change for different regions.

$$A_T = \begin{cases} A_{LOS} & \text{for } d < d_{ML} \\ \left[\begin{array}{ll} A_d & \text{if } A_{sx} \geq A_{dx} \\ A_{sx} + \dfrac{A_{sx} - A_{ML}}{d_x - d_{ML}} (d - d_x) & \text{otherwise} \end{array} \right] & \text{for } d_{ML} \leq d \leq d_x \\ \left[\begin{array}{c} \text{lesser } of \ A_d \text{ or } A_s \\ \text{where } A_s \text{ has been selected for a shorter distance} \end{array} \right] & \text{for } d_x < d \end{cases} \quad \text{dB} \tag{205}$$

A_{LoS} is from (162). The value d is a specified parameter except in the LoS region where it is from (112). A_d is from (94). $A_{sx} = A_s$ from (163) and $A_{dx} = A_d$ from (94) both for $d = d_x$. A_{ML} is from (90) and d_{ML} is from (40).

The distance, d_x, is the shortest distance beyond the radio horizon at which $A_s > 20$ dB and $M_s \leq M_d$. M_s is the slope of the curve for A_s versus distance determined by successive A_s calculations (§ 7). M_d is from (93).

9 Free space loss

The free space loss calculation is:

$$L_{bf} = 32.45 + 20 \log_{10}(fr) \tag{206}$$

where f in MHz is an input parameter and r is calculated below.

For LoS paths, calculate r_{WH}.

$$r_{WH} = [(h_2 - h_1)^2 + 4(h_1 + a_0)(h_2 + a_0)[\sin(0.5 \, d/a_0)]^2]^{\frac{1}{2}} \quad \text{km} \tag{207}$$

The heights $h_{1,2}$ are the heights of the lower and higher antennas, respectively, from mean sea level from Fig. 3. The value a_0 is the actual earth radius of 6 370 km and the great circle distance, d, is from (112) for LoS paths.

$$r = \text{greater of } r_0 \text{ or } r_{WH} \quad \text{km} \tag{208}$$

where r_0 is from (106).

For all other paths, calculate the two values, $r_{L1,2}$:

$$r_{L1,2} = \left[(h_{1,2} - h_{L1,2})^2 + 4(h_{1,2} + a_0)(h_{L1,2} + a_0)[\sin(0.5 \, d_{L1,2}/a_0)]^2 \right]^{\frac{1}{2}} \quad \text{km} \tag{209}$$

Heights $h_{L1,2}$ are from (36) and (45) respectively. Distances $d_{L1,2}$ are calculated in § 4.

$$r_{BH} = r_{L1} + r_{L2} + d_s \quad \text{km} \tag{210}$$

where d_s is from (165).

$$r = \text{greater of } d \text{ or } r_{BH} \quad \text{km} \tag{211}$$

where d is from (112).

10 Atmospheric absorption

Estimating the median atmospheric absorption combines the amount of absorption of oxygen and water vapour for a given frequency with the ray length through the identified atmospheric layers. The absorption is calculated from the surface absorption rates and ray lengths as:

$$A_a = \Upsilon_{oo} R_{eo} + \Upsilon_{ow} R_{ew} \quad \text{dB} \tag{212}$$

The figures of the geometry of the ray lengths are in Fig. 12.

FIGURE 12

Geometry associated with atmospheric absorption

Report P.2345-12
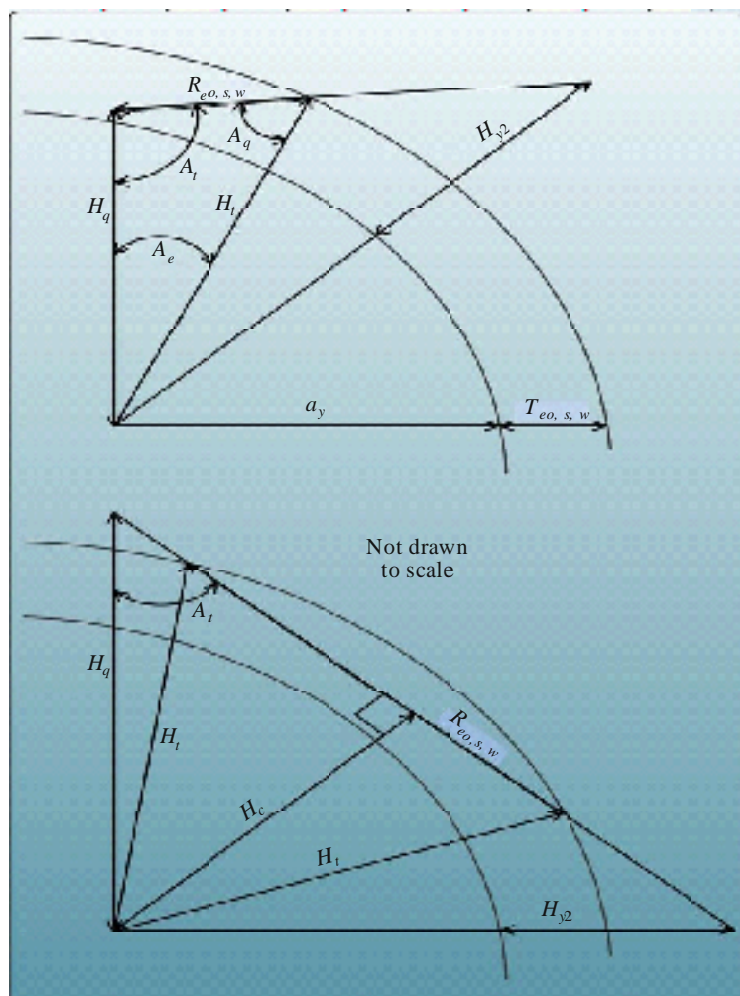
10.1   Surface absorption rates

Effective ray lengths for oxygen and water vapour combined with the surface absorption rates give an estimate for attenuation due to atmospheric absorption. Curves for the surface absorption rates for oxygen and water vapour, Υ_{oo} and Υ_{ow} respectively, for frequency are on Fig. 13. Data from the graph in Fig. 13 are available in table form in Attachment 2.

FIGURE 13

Surface values of atmospheric absorption by oxygen and water vapour [5]

Pressure 760 mm Hg
Temperature 20°C
Water vapor density 10g/m³

Report P.2345 -13
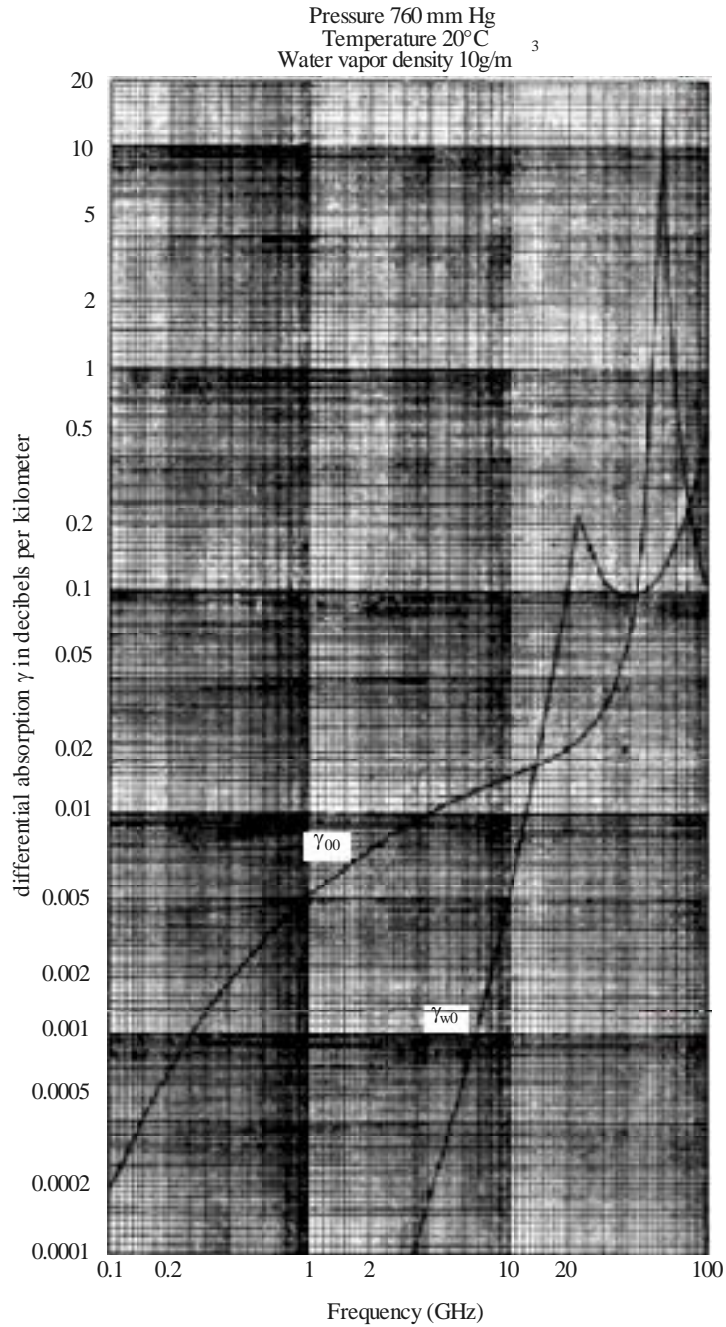
10.1.1 Determining ray length

The geometry for determining ray length through the appropriate layers of the atmosphere is illustrated in Fig. 12. The values T_{eo} and T_{ew} are 3.25 km and 1.36 km respectively.

Calculate A_t and H_z

$$A_t = \beta + (0.5\,\pi) \tag{213}$$

$$H_z = \text{lesser of} \begin{cases} T_{eo,w} + a_\Upsilon \\ H_{\Upsilon2} + a_\Upsilon \end{cases} \tag{214}$$

For $H_{\gamma1} < T_{eo,w}$

$$A_q = \sin^{-1}\left[\frac{(H_{\Upsilon1} + a_\Upsilon)\sin A_t}{H_z}\right] \tag{215}$$

$$A_e = \pi - (A_t + A_q) \tag{216}$$

$$R_{eo,w} = \begin{cases} T_{eo,w} - H_{\Upsilon1} & \text{if } A_q < 0.02 \text{ rad} \\ \dfrac{(H_{\Upsilon1} + a_\Upsilon)\sin A_e}{\sin A_q} & \text{otherwise} \end{cases} \quad \text{km} \tag{217}$$

For $T_{eo,w} < H_{\Upsilon1}$

$$H_c = (H_{\Upsilon1} + a_\Upsilon)\sin A_t \tag{218}$$

$$R_{eo,w} = \begin{cases} 0 & \text{if } T_{eo,w} + a_\Upsilon \leq H_c \text{ or } A_t \leq \pi/2 \\ 2(T_{eo,w} + a_\Upsilon)\sin\left[\cos^{-1}\left(H_c \Big/ (T_{eo,w} + a_\Upsilon)\right)\right] & \text{otherwise} \end{cases} \quad \text{km} \tag{219}$$

10.1.2 Line-of-sight paths ($d \leq d_{ML}$)

Atmospheric absorption calculations for LoS paths use the following values:

- $H_{\Upsilon1,2} = H_{1,2}$ from (100 a and b)
- $a_\Upsilon = a_a$ from (14)
- $\beta = \theta_{h1}$ from (109a)

10.1.3 Single horizon paths ($d_{ML} \leq d \leq d_{L1} + d_{Lo1}$)

The single horizon paths use two sets of starting parameters. $R_{1eo,w}$ and $R_{2eo,w}$ equal $R_{eo,w}$ in the calculations above for the two sets of initial parameters. $R_{eo,w}$ is the sum of $R_{1eo,w}$ and $R_{2eo,w}$.

Atmospheric absorption calculations for $R_{1eo,w}$ use the following values:

- $H_{\Upsilon1} = $ lesser of h_{e1} or h_{Lr1}
- $H_{\Upsilon2} = $ greater of h_{e1} or h_{Lr1}
- $a_\Upsilon = a$ from (14)
- $\beta = \theta_{e1}$ from (38) if $H_{\Upsilon1} = h_{e1}$ and θ_L from (39) otherwise

Atmospheric absorption calculations for $R_{2eo,w}$ use the following values:

- $H_{\Upsilon 1}$ = lesser of h_{e2} or h_{Lr2}
- $H_{\Upsilon 2}$ = greater of h_{e2} or h_{Lr2}
- a_{Υ} = a from (14)
- $\beta = \theta_{e2}$ from (38) if $H_{\Upsilon 1} = h_{e2}$ and θ_L from (39) otherwise

10.1.4   Two horizon paths

Two-horizon paths also use two sets of starting parameters. Again, $R_{1eo,w}$ and $R_{2eo,w}$ equal $R_{eo,w}$ in the calculations above for the two sets of initial parameters and $R_{eo,w}$ is the sum of $R_{1eo,w}$ and $R_{2eo,w}$.

Atmospheric absorption calculations for $R_{1eo,w}$ use the following values:

- $H_{\Upsilon 1}$ = lesser of h_{e1} or h_v
- $H_{\Upsilon 2}$ = greater of h_{e1} or h_v
- a_{Υ} = a from (14)
- $\beta = \theta_{e1}$ from (36) if $H_{\Upsilon 1} = h_{e1}$ and $-\tan^{-1}\theta_{A1}$ (θ_{A1} from (178)) otherwise

Atmospheric absorption calculations for $R_{2eo,w}$ use the following values:

- $H_{\Upsilon 1}$ = lesser of h_{e2} or h_v
- $H_{\Upsilon 2}$ = greater of h_{e2} or h_v
- a_{Υ} = a from (14)
- $\beta = \theta_{e2}$ from (37) if $H_{\Upsilon 1} = h_{e2}$ and $-\tan^{-1}\theta_{A2}$ (θ_{A2} from (176)) otherwise

11   Variability

Total variability, $Y(q)$, for this method includes terms for long-term (hourly median) variability, $Y_e(q)$ and short-term variability from multipath, $Y_{\pi}(q)$, rain attenuation, $Y_r(q)$, and ionospheric scintillation, $Y_I(q)$. The terms are combined by:

$$Y_{\Sigma}(q) = \pm \sqrt{Y_e^2(q) + Y_{\pi}^2(q) + Y_r^2(q) + Y_I^2(q)} \qquad (220)$$

$$+ \text{ for } q \le 0.5$$

$$- \text{ otherwise}$$

For an hourly median availability, all the short-term variabilities are set to zero. Variability due to rain attenuation is considered equal to zero when $q \le 0.98$ since the assumption is that rain attenuation occurs during 2 percent of the time. Also, variability due to ionospheric scintillation is considered equal to zero except for satellite paths that pass through the ionosphere at about 350 km above sea level.

11.1   Variability due to long-term fading

The variable, $Y_e(q)$, represents long-term or hourly median fading. This is a signed value such that positive values with $q \le 0.5$ indicate a decrease in transmission loss or an increase in received power. Long-term fading has two components. One component is due to seasonal changes and the other component is due to climatic changes. The long-term fading uses an effective distance, d_e, calculated as follows:

$$d_e = \begin{cases} \dfrac{130\,d}{d_q} & \text{for } d \le d_q \\ 130 + d - d_q & \text{otherwise} \end{cases} \quad \text{km} \tag{221}$$

where d is the great circle distance that is a specified parameter or, in the LoS region, is from (112) and d_q is calculated by

$$d_q = d_{Lq} + \left[65\,(100/f)^{1/3} \right] \quad \text{km} \tag{222}$$

where f is frequency in MHz and d_{Lq} is the total smooth earth horizon distance determined by ray tracing in Attachment 1 for an effective earth radius of 9 000 km. The equations to calculate the gain factors, g (0.1 or 0.9, f), associated with $Y_e(q)$ are:

$$g(0.1, f) = \begin{cases} 0.21 \sin[5.22 \log(f/200)] + 1.28 & \text{for } 60 \le f \le 1\,600 \text{ MHz} \\ 1.05 & \text{for } f > 1\,600 \text{ MHz} \end{cases} \tag{223}$$

$$g(0.9, f) = \begin{cases} 0.18 \sin[5.22 \log(f/200)] + 1.23 & \text{for } 60 \le f \le 1\,600 \text{ MHz} \\ 1.05 & \text{or } f > 1\,600 \text{ MHz} \end{cases} \tag{224}$$

The calculations for the reference levels of the hourly Y median variability, $Y_0(0.1)$ and $Y_0(0.9)$, and for the parameter, $V(0.5)$ start with the equation for f_2.

$$f_2 = f_\infty + \left[(f_m - f_\infty) \exp\left(-c_2 d_e^{n_2}\right) \right] \tag{225}$$

feeds into:

$$\left. \begin{array}{l} V(0.5) \\ Y_0(0.1) \\ -Y_0(0.9) \end{array} \right\} = \left[c_1 d_e^{n_1} - f_2 \right] \exp\left(-c_3 d_e^{n_3}\right) + f_2 \quad \text{dB} \tag{226}$$

The values c_1, c_2, c_3, n_1, n_2, n_3, f_m and f_∞ are from Table 6 (all hours all year) for Y_0 (0.1), Table 7 (all hours all year) for Y_0 (0.9) or Table 8 (Climate 1) for $V(0.5)$. Other options for determining these parameters are using time blocks (§ 11.1.1), climates (§11.1.2) or mixed distributions (§10.1.3).

$$Y(0.1 \text{ or } 0.9) = g(0.1 \text{ or } 0.9, f)\, Y_0(0.1 \text{ or } 0.9) \quad \text{dB} \tag{227}$$

Use $Y(0.1)$ and $Y(0.9)$ to calculate other percentiles for the hourly median received power.

TABLE 6

Constants for calculating $Y_0(0.1)$ [5]

Time Block	c_1	$\dfrac{d_e \text{ in km.}}{c_2}$	c_3	n_1	n_2	n_3	f_m	f_∞
4	1.22^{-2}	9.81^{-6}	1.09^{-8}	1.36	2.00	3.58	10.8	5.5
5	2.58^{-4}	3.41^{-6}	2.01^{-11}	2.05	2.25	4.78	8.0	4.0
6	3.84^{-3}	4.22^{-5}	7.76^{-9}	1.57	1.76	3.66	9.6	5.2
7	7.95^{-3}	3.76^{-5}	3.19^{-8}	1.47	1.76	3.40	11.2	5.5
S *	4.47^{-3}	1.66^{-5}	2.06^{-8}	1.55	1.90	3.48	9.98	5.1
1	1.09^{-4}	1.21^{-6}	8.29^{-8}	2.28	2.29	3.26	9.6	2.8
2	1.04^{-5}	4.28^{-8}	3.51^{-8}	2.71	2.91	3.41	9.15	2.8
3	2.02^{-4}	1.45^{-6}	4.27^{-8}	2.15	2.28	3.37	9.4	2.8
8	1.70^{-4}	7.93^{-7}	1.29^{-7}	2.19	2.37	3.18	9.5	3.0
W *	2.46^{-4}	1.74^{-7}	1.27^{-8}	2.11	2.64	3.62	9.37	2.8
A *	5.25^{-4}	1.57^{-6}	4.70^{-7}	1.97	2.31	2.90	10.0	5.4

Time Blocks "S", "W", and "A" are all hours summer, all hours winter, and all hours all year respectively. See Table III.1 for definitions of the other time blocks.
Small digits represent the exponent of the number, for example $2.33^{-2} = 2.33 \times 10^{-2}$.

TABLE 7

Constants for calculating $Y_0(0.9)$ [5]

Time Block	c_1	$\dfrac{d_e \text{ in km.}}{c_2}$	c_3	n_1	n_2	n_3	f_m	f_∞
4	1.84^{-4}	2.22^{-6}	3.65^{-16}	2.09	2.29	6.82	8.0	4.0
5	3.80^{-4}	4.76^{-6}	8.39^{-17}	1.92	2.19	7.10	6.6	3.3
6	1.81^{-3}	5.82^{-6}	6.37^{-13}	1.67	2.15	5.38	8.4	4.1
7	3.19^{-3}	2.51^{-6}	5.03^{-9}	1.60	2.27	3.69	10.0	4.4
S *	7.42^{-4}	5.55^{-5}	4.37^{-8}	1.84	1.69	3.28	8.25	4.0
1	1.72^{-4}	6.39^{-8}	2.93^{-10}	2.10	2.79	4.24	8.2	2.4
2	1.05^{-5}	7.00^{-13}	7.64^{-9}	2.59	4.80	3.68	7.05	2.8
3	3.64^{-5}	3.74^{-9}	3.53^{-7}	2.40	3.28	2.94	7.8	2.2
8	1.64^{-6}	1.43^{-7}	3.14^{-7}	3.08	2.66	3.03	8.6	2.6
W *	3.45^{-6}	1.25^{-8}	7.50^{-7}	2.87	3.07	2.82	7.92	2.45
A *	2.93^{-4}	3.78^{-8}	1.02^{-7}	2.00	2.88	3.15	8.2	3.2

Time Blocks "S", "W", and "A" are all hours summer, all hours winter, and all hours all year, respectively. See Table III.1 for definitions of other time blocks.
Small digits represent the exponent of the number, for example, $4.97^{-4} = 4.97 \times 10^{-4}$.

TABLE 8

Constants for calculating $V(0.5)$ [5]

d_e in km

Climate	c_1	c_2	c_3	n_1	n_2	n_3	f_m	f_∞
1. Continental Temperate	1.59^{-5}	1.56^{-11}	2.77^{-8}	2.32	4.08	3.25	3.9	0
2. Maritime Temperate Overland	1.12^{-4}	1.26^{-20}	1.17^{-11}	1.68	7.30	4.41	1.7	0
3. Maritime Temperate Oversea	1.18^{-4}	3.33^{-13}	3.82^{-9}	2.06	4.60	3.75	7.0	3.2
4. Maritime Subtropical Overland	1.09^{-4}	5.89^{-18}	2.21^{-7}	2.06	6.81	2.97	5.8	2.2
5. Maritime Subtropical Oversea	(deleted)							
6. Desert (Sahara) (Computes - $V(0.5)$)	8.85^{-7}	2.76^{-14}	2.25^{-12}	2.80	4.82	4.78	8.4	8.2
7. Equatorial	3.45^{-7}	3.74^{-12}	6.97^{-8}	2.97	4.43	3.14	1.2	-8.4
8. Continental Subtropical	1.59^{-5}	1.56^{-11}	2.77^{-8}	2.32	4.08	3.25	3.9	0

$$Y(q) = \begin{cases} cY(0.1) & \text{for } q < 0.5 \\ 0 & \text{for } q = 0.5 \quad \text{dB} \\ cY(0.9) & \text{for } q > 0.5 \end{cases} \tag{228}$$

The distribution calculations to obtain values for c are in Attachment 1. The values of c for $q < 0.1$ are in Table 9 and the values of c for $q > 0.9$ are in Table 10.

TABLE 9

Factor c for q [2]

Climate Number	$q = 0.01$	$q = 0.001$	$q = 0.001$
1, 6 & 8*	1.95	2.73	3.33
2	1.79	2.27	2.66
3	2.20	3.30	3.70
4	1.82	2.41	2.90
5*	----	----	----
7a & 7b	2.15	3.05	3.80

TABLE 10

Factor c for q [2]

q	c *
0.95	1.28
0.99	1.82
0.995	2.01
0.999	2.41
0.9995	2.57
0.9999	2.90

*For $q > 0.9$ c values follow a log-normal distribution for all climates.

There is a correction factor for the elevation angle of the lower antenna, $f_{\theta h}$.

$$f_{\theta h} = \begin{cases} 0.5 - \pi^{-1} \tan^{-1}[20 \log_{10}(32 \, \theta_{h1})] & \text{for LoS paths with } \theta_{h1} > 0 \\ 1 & \text{otherwise} \end{cases} \quad (229)$$

The value θ_{h1} is from (109a).

$$Y_{eI}(q) = f_{\theta h} Y(q) \quad \text{dB} \quad (230)$$

$$V_e(0.5) = f_{\theta h} V(0.5) \quad \text{dB} \quad (231)$$

When using lobing, calculate Y_T.

$$Y_T = L_b - \left[L_{bf} - V_e(0.5) - 20 \log_{10}\left(R_{Tg} + R_{Tc}\right)\right] \quad \text{dB} \quad (232)$$

Where $L_b(0.5)$ is from (2), L_{bf} is from (205), and R_{Tg} is from (113). The value for R_{Tc} equals zero when there is no counterpoise; otherwise it is calculated in Attachment 1.

$$A_{YI} = L_{bf} - 3 - L_{br} - Y_{eI}(0.1) \quad (233)$$

L_{br} is from (3). The value A_{YI} is zero when using lobing and the higher antenna is within 10 lobes of its radio horizon.

$$A_Y = \begin{cases} 0 & \text{if } A_{YI} \leq 0 \\ 10 & \text{if } A_{YI} \geq 10 \\ A_{YI} & \text{otherwise} \end{cases} \quad (234)$$

The calculations for the long-term variability, $Y_e(q)$ are:

$$Y_e(q \geq 0.1) = Y_{eI}(q) \quad \text{dB} \quad (235)$$

$$Y_e(q < 0.1) = \begin{cases} \text{lesser of } [Y_{eI}(q) \text{ or } Y_T] & \text{for lobing} \\ \text{lesser of } \left[Y_{eI}(q) \text{ or } L_{br} + A_Y - (L_{bf} - c_Y)\right] & \text{otherwise} \end{cases} \quad (236)$$

where c_Y is 6, 5.8, and 5 dB for q values of 0.0001, 0.001, 0.01 respectively.

11.1.1   Time blocks

This method has options to calculate variabilities for blocks of time and seasonal groupings. These time blocks are defined in Table 11 and are associated with a continental temperate climate. To add the effects of time blocks to the long-term variability, one uses values in Tables 6, 7 and 8 that are appropriate to the time block desired and use those values to calculate $V(0.5)$, $Y_0(0.1)$ and $Y_0(0.9)$ in (225). To combine time blocks use the technique for mixing distributions described in § 11.5.

TABLE 11

Time block ranges [1]

NO.	MONTHS	HOURS
1	Nov. - Apr.	0600 - 1300
2	Nov. - Apr.	1300 - 1800
3	Nov. - Apr.	1800 - 2400
4	May - Oct.	0600 - 1300
5	May - Oct.	1300 - 1800
6	May - Oct.	1800 - 2400
7	May - Oct.	0000 - 0600
8	Nov. - Apr.	0000 - 0600
Summer	May - Oct.	ALL-HOURS
Winter	Nov. - Apr.	ALL-HOURS

11.1.2 Climates

There are options for different climates as defined in (238) and (239). Table 12 provides the values b_1, b_2, b_3, c_1, and c_2 for the following equations to use in calculating the long-term variability.

$$\left.\begin{array}{c} V(0.5) \\ Y_0(0.1) \\ -Y_0(0.9) \end{array}\right\} = \frac{(d_e/b_1)^2}{1 + (d_e/b_1)^2}\left[c_1 + \frac{c_2}{1 + [(d_e - b_2)/b_3]^2}\right] \quad \text{dB} \qquad (237)$$

The value, d_e, is from (220).

$$g(0.1, f) = \begin{cases} 1 & \text{for all climates except 2, 4 and 6} \\ 0.18\ \sin[5\ \log_{10}(f/200)] + 1.06 & \text{for } 60 \le f \le 1\,500 \text{ MHz climates 2 and 6} \\ 1 & \text{suggested for } 60 \le f \le 200 \text{ MHz climate 4} \\ 0.10\ \sin[5\ \log_{10}(f/200)] + 1.02 & \text{for } 200 \le f \le 1\,500 \text{ MHz climate 4} \\ 0.93 & \text{for } f > 1\,500 \text{ MHz climates 2, 4 and 6} \end{cases} \qquad (238)$$

$$g(0.9, f) = \begin{cases} 1 & \text{for all climates except 6} \\ 0.13\ \sin[5\ \log_{10}(f/200)] + 1.04 & \text{for } 60 \le f \le 1\,500 \text{ MHz in climate 6} \\ 0.92 & \text{for } f > 1\,500 \text{ Mhz in climate 6} \end{cases} \qquad (239)$$

where f is the input frequency in MHz. These values are then used in (225) and (229) to calculate Y_e (q) as in § 11.1. Section 11.6 describes how to combine the distributions for multiple climates.

TABLE 12

Constants to calculate $v(0.5)$, $Y_0(0.1)$, and $Y_0(0.9)$ [2]

Climate	Parameter	b_1	b_2	b_3	c_1	c_2
1. Equatorial	$V(0.5)$	144.9	190.3	133.8	-9.67	12.7
	$Y_0(0.1)$	636.9	134.8	95.6	2.70	131.1
	$Y_0(0.9)$	762.2	123.6	94.5	-2.73	-204.4
2. Continental subtropical	$V(0.5)$	228.9	205.2	143.6	-0.62	9.19
	$Y_0(0.1)$	138.7	143.7	98.6	8.8	19.9
	$Y_0(0.9)$	100.4	172.5	136.4	-3.41	-9.83
3. Maritime subtropical	$V(0.5)$	262.6	185.2	99.8	1.26	15.5
	$Y_0(0.1)$	165.3	225.7	129.7	12.9	12.3
	$Y_0(0.9)$	138.2	242.2	178.6	-7.83	-8.52
4. Desert	$V(0.5)$	84.1	101.1	98.6	-9.21	9.05
	$Y_0(0.1)$	464.4	93.1	94.2	4.72	204.2
	$Y_0(0.9)$	139.1	132.7	193.5	-2.54	-16.8
5. *Mediterranean	-----	-----	-----	-----	-----	-----
6. Continental temperate	$V(0.5)$	228.9	205.2	143.6	-0.62	9.19
	$Y_0(0.1)$	93.2	135.9	113.4	6.04	10.4
	$Y_0(0.9)$	93.7	186.8	133.5	-3.43	-9.17
7a. Maritime temperate overland	$V(0.5)$	141.7	315.9	167.4	-0.39	2.86
	$Y_0(0.1)$	216.0	152.0	122.7	11.0	17.9
	$Y_0(0.9)$	187.8	169.6	108.9	-8.79	-13.3
7b. Maritime temperate oversea	$V(0.5)$	2222.0	164.8	116.3	3.15	857.9
	$Y_0(0.1)$	136.2	188.5	122.9	10.8	10.5
	$Y_0(0.9)$	609.8	119.9	106.6	-10.9	-217.6
8. *Polar		Use climate 6				

* For climates numbers 5 and 8, Mediterranean and Polar, values are not available; a substitute for Polar is suggested for use unless more definite information is available from other sources.

11.2 Variation due to multipath

The variable, Y_π, represents short-term (less than an hour) fading due to multipath. This fading is a result of both surface reflection and tropospheric multipath and generally follows a Nakagami-Rice distribution.

11.2.1 Surface reflection multipath

Surface reflection multipath contributes to the short-term variability of LoS paths. This method uses both the specular and diffuse components of the surface multipath mechanism. These components as well as the tropospheric multipath components make up the short-term fading, $Y_\pi(q)$, component of the total variability for the model.

The model uses the following fading formulas to incorporate the surface reflection multipath elements into $Y_\pi(q)$:

$$F_{A_Y} = \begin{cases} 1 & \text{if } A_Y \le 0 \\ 0.1 & \text{if } A_Y \ge 9 \\ 0.5\left[1.1 + 0.9\cos\left(\frac{\pi A_Y}{9}\right)\right] & \text{otherwise} \end{cases} \tag{240}$$

where A_Y is from (232) and

$$F_{\Delta r} = \begin{cases} 1 & \text{if } \Delta r_g \ge \dfrac{\lambda}{2} \\ 0.1 & \text{if } \Delta r_g \le \dfrac{\lambda}{6} \\ \dfrac{1.1 - 0.9\cos[3\pi(\Delta r_g - \lambda/6)/\lambda]}{2} & \text{otherwise} \end{cases} \tag{241}$$

where Δr_g equals Δr from (108) when using ground parameters and λ is the wavelength in km where the wavelength in metres, λ_m, is from (9).

The reflection contributions are R_S^2 for the relative contribution of the specular component and R_d^2 is the contribution of the diffuse component. These values are calculated by:

$$R_s = R_{Tg}\,(F_{AY}F_{\Delta r}) \tag{242}$$

where R_{Tg} is from (113) and

$$R_d = R_{Tg}\left(\frac{F_{d\sigma h}}{F_{\sigma h}D_v}\right) \tag{243}$$

where $F_{d\sigma h}$ is from (121), $F_{\sigma h}$ is from (122) and D_v is from (116).

The relative power level, W_R, from the surface reflection components is calculated by:

$$W_R = \begin{cases} \dfrac{(R_s^2 + R_d^2)}{g_D^2} & \text{for LoS } (d \le d_{ML}) \\ 0 & \text{otherwise} \end{cases} \tag{244}$$

where d is the path length from (112), d_{ML} is from (40), and g_D is from (125).

11.2.2 Tropospheric multipath

Tropospheric multipath is caused by elevated layers in the troposphere and is part of the short-term variability. This mechanism is only used when working with time availability for instantaneous levels exceeded. Tropospheric multipath determines relative power level W_a which the method uses to determine the short-term multipath fading, $Y_\pi(q)$.

The fading component from tropospheric multipath is calculated as:

$$F = 10\log_{10}\left(f\,R_{ew}^3\right) - 84.26 \quad \text{dB} \tag{245}$$

when $d \le d_{ML}$. The input frequency f is in MHz, R_{ew} is calculated in § 10.1 for different paths, d is from (112) and d_{ML} is the maximum LoS distance from (40). The variable F is not calculated for $d \ge d_{ML}$.

NOTE – The values for K_{LoS} are from Table 13 for column $Y_\pi(0.99)$. K_{ML} is determined for F values with $d = d_{ML}$.

$$K_{LOS} = \begin{cases} 40 \text{ dB} & \text{if } F \leq 0.14 \\ -20 \text{ dB} & \text{if } F \geq 18.4 \\ \text{obtained from Table 13 otherwise} \end{cases} \tag{246}$$

The values for K_{LoS} are K values from Table 13 for column $Y\pi(0.99)$ for $-F$.

TABLE 13

Characteristics of Nakagami-Rice phase interference fading distribution [5]

K	$\tilde{Y}_\pi$	σ_{Y_π}	$Y_\pi(0.005)$	$Y_\pi(0.01)$	$Y_\pi(0.02)$	$Y_\pi(0.05)$	$Y_\pi(0.1)$	$Y_\pi(0.9)$	$Y_\pi(0.95)$	$Y_\pi(0.98)$	$Y_\pi(0.99)$	$Y_\pi(0.995)$	$Y_\pi(0.1) - Y_\pi(0.9)$
db	db	db	db	db	db	db	db	db	db	db	db	db	db
40	-0.0002	0.061	0.1568	0.1417	0.1252	0.1004	0.0784	-0.0790	-0.1016	-0.1270	-0.1440	-0.1596	0.1574
35	-0.0007	0.109	0.2768	0.2504	0.2214	0.1778	0.1352	-0.1411	-0.1815	-0.2272	-0.2579	-0.2860	0.2763
30	-0.0022	0.194	0.4862	0.4403	0.3898	0.3136	0.2453	-0.2525	-0.3254	-0.4082	-0.4638	-0.5151	0.4978
25	-0.0069	0.346	0.8460	0.7676	0.6811	0.5496	0.4312	-0.4538	-0.5868	-0.7391	-0.8421	-0.9374	0.8850
20	-0.0217	0.616	1.4486	1.3184	1.1738	0.9524	0.7508	-0.8218	-1.0696	-1.3572	-1.5544	-1.7389	1.5726
18	-0.0343	0.776	1.7840	1.6264	1.4508	1.1846	0.9332	-1.0453	-1.3660	-1.7416	-2.0014	-2.2461	1.9785
16	-0.0543	0.980	2.1856	1.9963	1.7847	1.4573	1.1558	-1.3326	-1.7506	-2.2463	-2.5931	-2.9231	2.4884
14	-0.0859	1.238	2.6605	2.4355	2.1829	1.7896	1.4247	-1.7028	-2.2526	-2.9156	-3.3872	-3.8422	3.1275
12	-0.136	1.569	3.2136	2.9491	2.6507	2.1831	1.7455	-2.1808	-2.9119	-3.8143	-4.4715	-5.1188	3.9263
10	-0.214	1.999	3.8453	3.5384	3.1902	2.6408	2.1218	-2.7975	-3.7820	-5.0372	-5.9833	-6.9452	4.9193
8	-0.334	2.565	4.5493	4.1980	3.7975	3.1602	2.5528	-3.5861	-4.9287	-6.7171	-8.1418	-9.6386	6.1389
6	-0.507	3.279	5.3093	4.9132	4.4591	3.7313	3.0307	-4.5714	-6.4059	-8.9732	-11.0972	-13.4194	7.6021
4	-0.706	4.036	6.0955	5.6559	5.1494	4.3315	3.5366	-5.7101	-8.1216	-11.5185	-14.2546	-17.1017	9.2467
2	-0.866	4.667	6.8613	6.3811	5.8252	4.9219	4.0366	-6.7874	-9.6278	-13.4690	-16.4258	-19.4073	10.8240
0	-0.941	5.094	7.5411	7.0246	6.4248	5.4449	4.4782	-7.5267	-10.5553	-14.5401	-17.5512	-20.5618	12.0049
-2	-0.953	5.340	8.0697	7.5228	6.8861	5.8423	4.8088	-8.0074	-11.0005	-15.0271	-18.0527	-21.0706	12.8162
-4	-0.942	5.465	8.4231	7.8525	7.1873	6.0956	5.0137	-8.0732	-11.1876	-15.2273	-18.2573	-21.2774	13.0869
-6	-0.929	5.525	8.6309	8.0435	7.3588	6.2354	5.1233	-8.1386	-11.2606	-15.3046	-18.3361	-21.3565	13.2619
-8	-0.922	5.551	8.7394	8.1417	7.4451	6.3034	5.1749	-8.1646	-11.2893	-15.3349	-18.3669	-21.3880	13.3395
-10	-0.918	5.562	8.7918	8.1881	7.4857	6.3341	5.1976	-8.1753	-11.3005	-15.3466	-18.3788	-21.4000	13.3729
-12	-0.916	5.567	8.8155	8.2090	7.5031	6.3474	5.2071	-8.1792	-11.3048	-15.3512	-18.3834	-21.4046	13.3863
-14	-0.916	5.569	8.8258	8.2179	7.5106	6.3531	5.2112	-8.1804	-11.3065	-15.3529	-18.3852	-21.4064	13.3916
-16	-0.915	5.570	8.8301	8.2216	7.5136	6.3552	5.2128	-8.1811	-11.3072	-15.3537	-18.3860	-21.4072	13.3929
-18	-0.915	5.570	8.8319	8.2232	7.5149	6.3561	5.2135	-8.1813	-11.3075	-15.3540	-18.3863	-21.4075	13.3948
-20	-0.915	5.570	8.8326	8.2238	7.5154	6.3565	5.2137	-8.1814	-11.3076	-15.3541	-18.3864	-21.4076	13.3951
-∞	-0.915	5.570	8.8331	8.2242	7.5158	6.3567	5.2139	-8.1815	-11.3077	-15.3542	-18.3865	-21.4077	13.3954

$$K_t = \begin{cases} K_{LOS} & \text{if } d \leq d_{ML} \\ -20 & \text{if } \theta_s > 0.02618 \text{ rad} \\ K_{ML} + \dfrac{(-20 - K_{ML})\theta_s}{0.02618} & \text{otherwise} \end{cases} \tag{247}$$

where θ_s is the scattering angle from (166). This angle is negative in the LoS region. K_t determines the relative power, W_a. The value K_{ML} is the same as the value K_{LoS} when R_{ew} is evaluated at d_{ML}.

$$W_a = 10^{-K_t/10} \tag{248}$$

11.2.3 Variation due to multipath

The model uses the relative powers W_R and W_a to calculate the ratio between the direct ray component and the Rayleigh fading component, K.

$$K = -10 \log_{10}(W_R + W_a) \quad \text{dB} \tag{249}$$

K is then the value to determine the Nakagami-Rice probability distribution for $Y_\pi(q)$ from Fig. 14.

FIGURE 14

Nakagami-Rice probability distribution of instantaneous fading associated with phase interference [5]

q is the probability that $Y_\pi \pm (W_\pi - W_m)$ exceeds $Y_\pi(q)$,
as *K* decreases without limit, the Nakagami-Rice distribution approaches the rayleigh distribution

k = ratio in decibels between the steady component of
the received power and rayleigh fading component
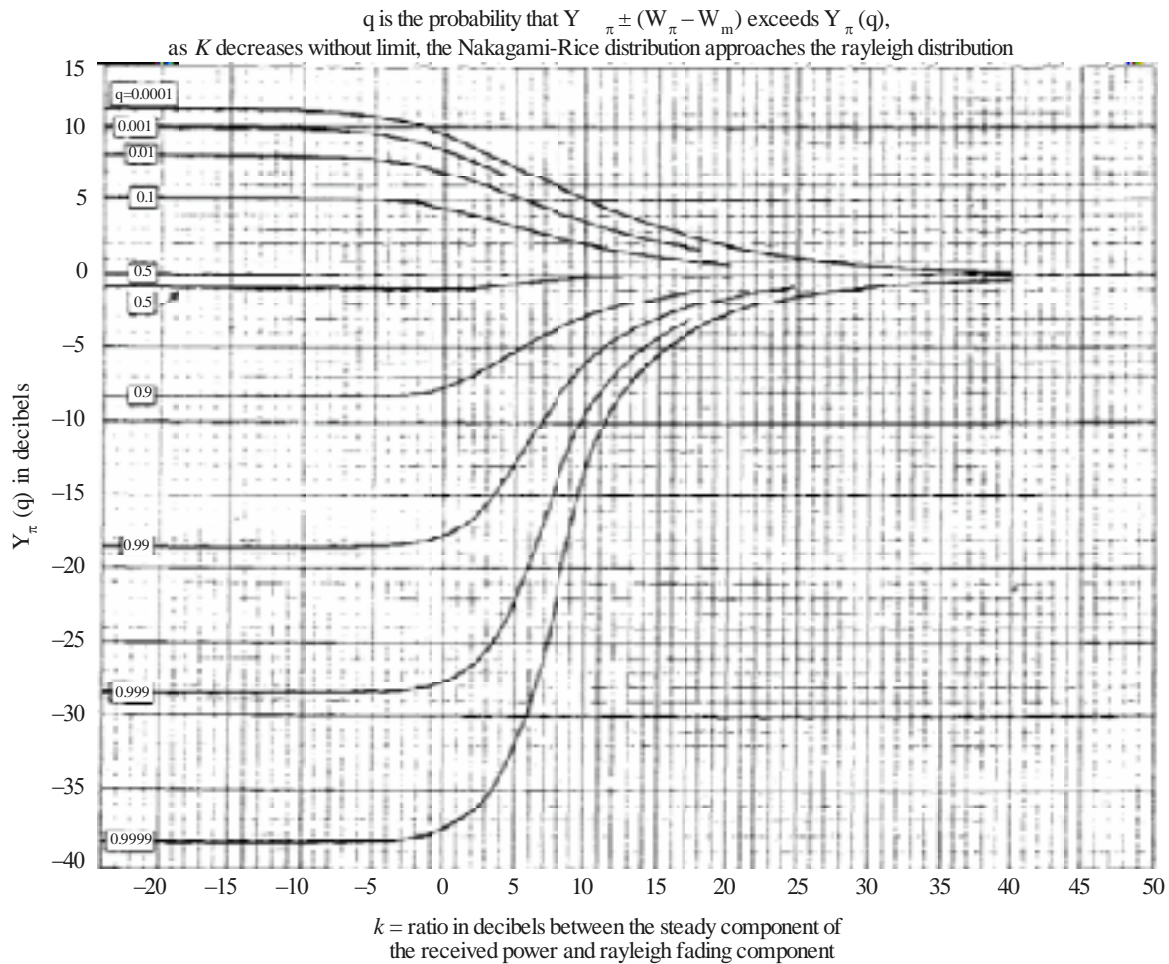
Report P.2345-14

11.3 Rain attenuation

There are two options for determining rain attenuation, Y_r. The first option requires rain zone and storm size input values. There are three storm sizes which are small, medium and large (5, 10, or 20 km, respectively). This method assumes only one storm in any path. There are five steps for calculating Y_r using this option.

1   Determine point rain rates (rate at a particular point of observation). Table 14 identifies the point rain rates for a rain zone chosen from Fig. 15 and for a time percentage. Note that for all $q \leq 0.98$, the point rain rate equals zero which makes $Y_r(q)$ equal zero.

2   Determine path average rain rates. Take the point rain rate value and the identified storm size to find the path average rain rate from Table 15.

3   Determine the attenuation rate, $A_{rr}(q)$. Use the path average rain rate from step 3 and the frequency to find the attenuation rate from Table 16. Use linear interpolation to calculate the rate.

4   Determine the in-storm ray length. The ray length within T_{es}, R_{es}, is calculated using the following parameters and calculations from the geometry in Fig. 12.

Line of sight paths *(d ≤ d$_{ML}$)*

Atmospheric absorption calculations for LoS paths use the following values:

- $H_{\gamma 1,2} = H_{1,2}$ from (98)

- $a_\gamma = a_a$ from (14)

- $\beta = \theta_{h1}$ from (107a)

Single horizon paths $(d_{ML} \le d \le d_{L1} + d_{L01})$

The single horizon paths use one set of starting parameters. Atmospheric absorption calculations for Res use the following values:

- $H_{\gamma 1}$ = lesser of h_{e1} or h_{Lr1}

- $H_{\gamma 2}$ = greater of h_{e1} or h_{Lr1}

- $a_\gamma = a$ from (14)

- $\beta = \theta_{e1}$ from (37) if $H_{\gamma 1} = h_{e1}$ and θ_L from (38) otherwise

Two-horizon paths $(d_{L1} + d_{L01} \le d)$

Two-horizon paths also use one set of starting parameters. Atmospheric absorption calculations for R_{es} use the following values:

- $H_{\gamma 1}$ = lesser of h_{e1} or h_v

- $H_{\gamma 2}$ = greater of h_{e1} or h_v

- $a_\gamma = a$ from (14)

- $\beta = \theta_{e1}$ from (37) if $H_{\gamma 1} = h_{e1}$ and $-\tan^{-1} \theta_{A1}$ (θ_{A1} from (176)) otherwise

Calculate A_t and H_z

$$A_t = \beta + (0.5\,\pi) \tag{250}$$

$$H_z = \text{lesser of} \begin{cases} T_{es} + a_\gamma \\ H_{\gamma 1} + a_\gamma \end{cases} \tag{251}$$

TABLE 14

Point rain rates (mm/hr) not exceeded for a fraction of time, q [2]

Rain Zone

r	1	2	3	4	5	6
≤.98	0	0	0	0	0	0
.99	0.17	0.25	0.31	0.54	0.75	1.0
.995	0.62	0.98	1.54	2.07	2.7	3.35
.998	1.8	3.1	4.8	6.2	7.8	9.4
.999	3.2	5.4	8.8	11.7	14.0	17.0
.9995	5.1	9.6	14.5	19.0	23.5	28.5
.9998	8.2	17.0	25.0	33.0	40.0	48.0
.9999	11.3	22.8	34.0	44.5	54.0	67.0
.99995	14.6	29.5	43.0	57.0	68.0	84.0
.99998	18.8	37.8	56.0	73.0	91.0	112.0
.99999	24.0	44.0	64.0	86.0	110.0	160.0

For $H_{\gamma 1} < T_{es}$

$$A_q = \sin^{-1}\left[\frac{(H_{\gamma 1} + a_\gamma)\sin A_t}{H_z}\right]$$ (252)

$$A_e = \pi - (A_t + A_q)$$ (253)

$$R_{es} = \begin{cases} T_{es} - H_{\gamma 1} & \text{if } A_q < 0.02 \text{ rad} \\ \dfrac{(H_{\gamma 1} + a_\gamma)\sin A_e}{\sin A_q} & \text{otherwise} \end{cases} \quad \text{km}$$ (254)

For $T_{es} < H_{\gamma 1}$

$$H_c = (H_{\gamma 1} + a_\gamma)\sin A_t$$ (255)

$$R_{es} = \begin{cases} 0 & \text{if } T_{es} + a_\gamma \leq H_c \text{ or } A_t \leq \pi/2 \\ 2(T_{es} + a_\gamma)\sin\left[\cos^{-1}\left(H_c\big/(T_{es} + a_\gamma)\right)\right] & \text{otherwise} \end{cases} \quad \text{km}$$ (256)

T_{es} equals the storm size input value. The in-storm length r_s is determined by

$$r_s = \begin{cases} T_{es} & \text{if } R_{es} \geq T_{es} \\ R_{es} & \text{otherwise} \end{cases}$$ (257)

5   Determine rain attenuations values. The rain attenuation variability, $Y_r(q)$, for $q > 0.98$ is calculated by:

$$Y_r(q) = -A_{rr}r_s$$ (258)

FIGURE 15

Rain zones of the world [4]

Latitude (degrees)
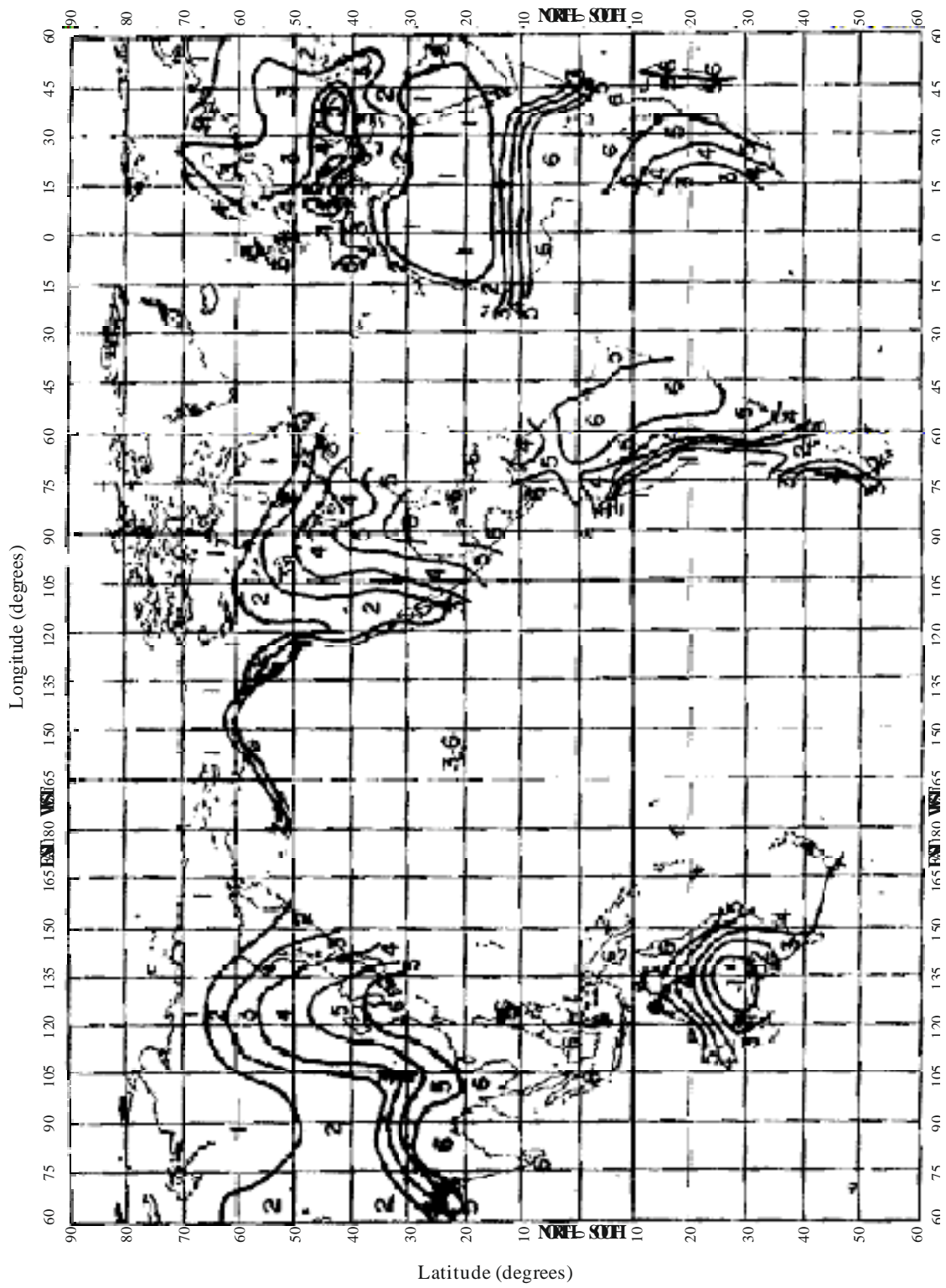
TABLE 15

Path average-to-point rain rate ratio [2]

Point Rain Rate in mm/hr	Storm Size Estimated 5 km	Storm Size Estimated 10 km	Storm Size Estimated 20 km
10	1.0	1.0	1.0
15	0.96	0.916	0.835
18	0.94	0.865	0.73
20	0.93	0.85	0.70
23	0.915	0.83	0.66
27	0.899	0.797	0.61
30	0.888	0.775	0.58
33	0.878	0.755	0.564
37	0.865	0.730	0.54
40	0.860	0.720	0.53
44	0.850	0.704	0.51
50	0.840	0.683	0.493
55	0.833	0.670	0.480
60	0.824	0.650	0.470
65	0.818	0.640	0.452
70	0.813	0.627	0.440
80	0.805	0.610	0.422
90	0.798	0.592	0.408
100	0.790	0.575	0.392
115	0.780	0.565	0.378
140	0.770	0.550	0.357
155	0.765	0.540	0.350
185	0.760	0.528	0.325
200	0.758	0.520	0.310

TABLE 16

Attenuation in mm/km for various rain rates [2]

Rainfall Rate		Frequency in GHz											
mm/hr	in/hr	100	60	30	20	15	10	7.5	6	5	4.3	3	2
0.00	0.00	0.00	0.00	0.00	0.00	0.00	0.00	0.00	0.00	0.00	0.00	0.00	0.00
0.25	0.01	0.25	0.16	0.03	0.01	0.006	0.002	0.0008	0.0004	0.000	0.000	0.000	0.000
1.25	0.05	1.29	0.76	0.21	0.09	0.04	0.01	0.004	0.002	0.001	0.0008	0.0004	0.000
2.5	0.10	2.19	1.43	0.45	0.20	0.10	0.03	0.01	0.005	0.003	0.002	0.0007	0.0003
5	0.20	3.68	2.63	0.93	0.43	0.23	0.07	0.03	0.01	0.006	0.003	0.001	0.0006
12.5	0.49	7.08	5.46	2.43	1.18	0.71	0.24	0.08	0.03	0.02	0.009	0.003	0.001
25	0.98	11.7	9.86	4.87	2.49	1.53	0.60	0.22	0.09	0.04	0.020	0.007	0.002
50	1.97	19.6	17.0	9.59	5.15	3.28	1.45	0.59	0.24	0.10	0.050	0.010	0.005
100	3.94	33.7	29.4	18.4	10.4	6.77	3.43	1.55	0.64	0.26	0.120	0.030	0.010
150	5.91	46.8	40.9	26.8	15.7	10.2	5.49	2.71	1.13	0.47	0.210	0.050	0.020
200	7.87	61.0	56.0	34.0	22.0	14.5	8.10	4.10	1.80	0.73	0.34	0.082	0.036

11.4 Variation due to scintillation

Propagation paths that pass through an altitude of about 350 km in the ionosphere include a variability associated with ionospheric scintillation, $Y_I(q)$. This method uses two types of calculations to determine the variability. One specifies the variability by selecting a scintillation index group. The other uses a weighted mixture of distributions selected for specific cases. This method also allows $Y_I(q)$ to change with latitude of earth stations of a geostationary satellite.

One can find the variability due to scintillation for time percentage q on Fig. 16. Data values from the graph in Fig. 16 are in table form in Attachment 2. The index group is calculated by

$$S_I = \frac{\left(P_{peak} - P_{min}\right)}{\left(P_{peak} + P_{min}\right)} \times 100\% \tag{259}$$

For a geostationary satellite, $Y_I(q)$ can change to reflect the latitude of earth facilities along the sub-satellite meridian. Start with the value associated with the latitude and time percentage from Fig. 16. This technique uses data measured at 136 MHz ($Y_{136}(q)$). To calculate $Y_I(q)$, find the index n by

$$n = \begin{cases} 1 & \text{for } \theta_{FL} \leq 17° \\ 1 + \dfrac{(\theta_{FL} - 17)}{7} & \text{for } 17° < \theta_{FL} < 24° \\ 2 & \text{for } 24° < \theta_{FL} < 45° \\ 1 + \dfrac{(52° - \theta_{FL})}{7} & \text{for } 45° < \theta_{FL} < 52° \\ 1 & \text{for } \theta_{FL} \geq 52° \end{cases} \tag{260}$$

where θ_{FL} is the magnitude of the earth facility latitude in degrees. Equation (261) shows the conversion from $Y_{136}(q)$ to $Y_I(q)$.

$$Y_I(q) = (136/f)^n Y_{136}(q) \tag{261}$$

This method has a process for mixing scintillation indices. The process for mixing the distributions is described in § 11.5.

FIGURE 16

Signal level distribution for ionospheric scintillation index groups
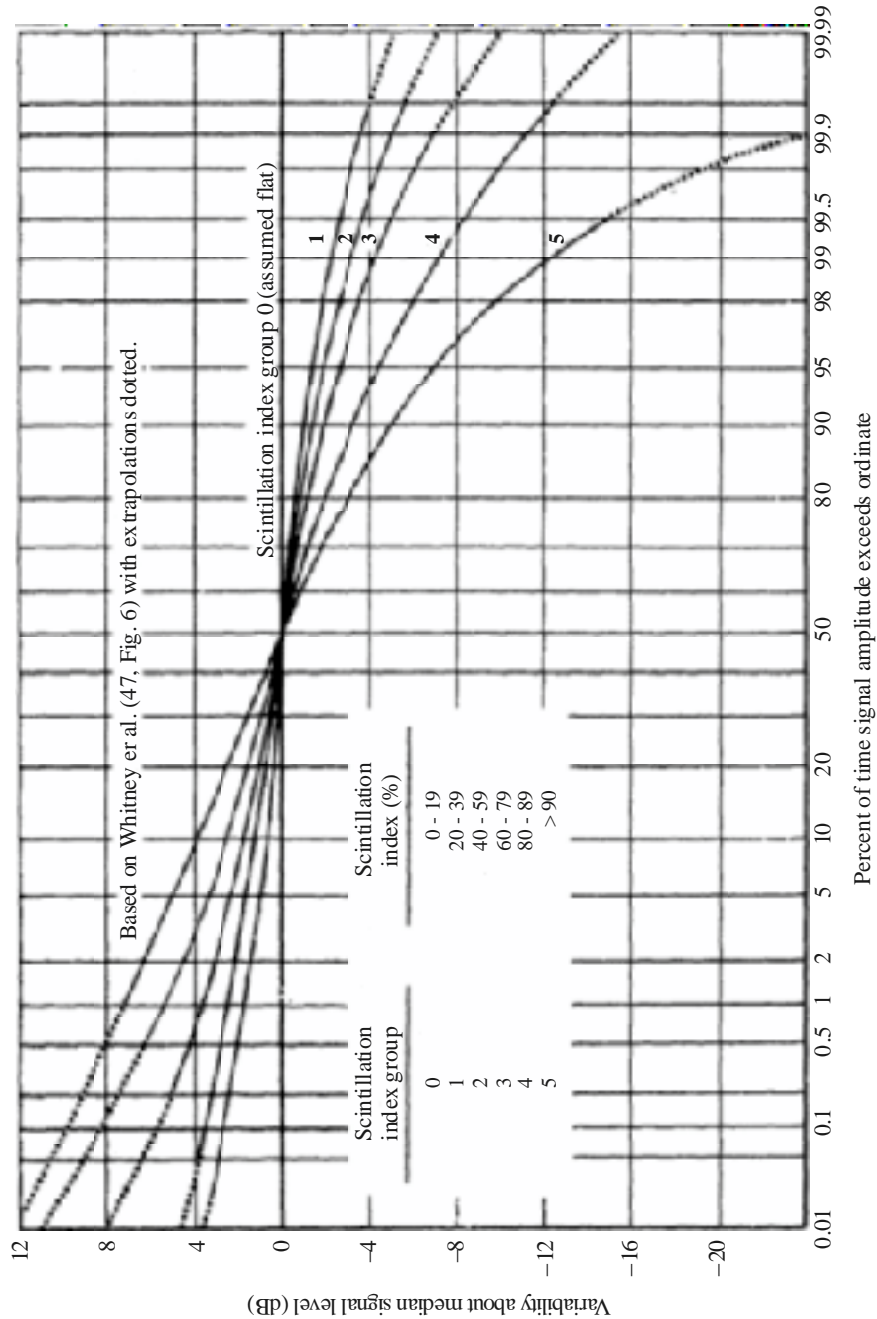
Report P.2345 - 16

11.5 Mixing distributions

This process combines distributions for time blocks (§ 11.1.1) to produce distributions for summer and winter or across boundaries for different climate types. The process can, also, be used for combining distributions for fading associated with ionospheric scintillation index groups (§ 11.4).

1   Select M (> 10) levels of variability that cover the entire range of the variable (e.g. transmission loss) ($V_1,…V_i, …, V_M$).

2   Identify the fraction of time (weighting factor) over which each distribution is applicable $(W_1, \ldots W_i, \ldots, W_N)$.

3   Determine the time percentage applicable for the variable level is not to be exceeded $(q_{11}, \ldots, q_{ij}, \ldots, q_{MN})$.

4   Calculate the time percentages for each level of variability from step 1.

$$q_1 = q_{11}W_1 + \ldots + q_{1j}W_j + \ldots + q_{1N}W_N$$

.

.

.

$$q_i = q_{i1}W_1 + \ldots + q_{ij}W_j + \ldots + q_{iN}W_N$$

.

.

.

$$q_M = q_{M1}W_1 + \ldots + q_{Mj}W_j + \ldots + q_{MN}W_N$$

For distributions of long-term variability, the variability functions are from:

$$V_C(q) = [V(0.5) + Y(q)]|_C \tag{262}$$

The $|_C$ indicates that $V(0.5)$ and $V(q)$ are the appropriate values for the conditions associated with the situation C. After the mixing, $Y(q)$ is calculated by

$$Y(q) = V(q) - V(0.5) \tag{263}$$

For scintillation index values covering an identified condition, the $Y_I(q)$ from the mixing is the value for the condition.

Attachment 1

1   Ray tracing

In cases where there are high (3 km) antennas, the ray bending technique used in IF77 may overestimate ray bending. In these cases, the IF77 method uses a ray tracing technique which is covered in this section.

This algorithm assumes a horizontally stratified atmosphere defines the layer heights beginning at h_r and rising for layers in km of 0.0, 0.01, 0.02, 0.05, 0.1, 0.2, 0.5, 0.7, 1.0, 1.524, 2, 3.048, 5, 7, 10, 20, 30.48, 50, 70, 90, 110, 225, 350 and 475. These values are contained in H_{layers} (I). The initial elevation angle can be negative. Any angle that is excessively negative is set to the grazing angle for a smooth earth.

For each element of H_{layers}:

$$EN(I) = \exp\left(-C_e\, H_{layers}(I)\right) N_s\, 10^{-6} \tag{264}$$

where C_e is from equation (16) and N_s is from equation (15).

$$N_I(I) = 1. + EN(I) \tag{265}$$

$$R(I) = (a_0 + h_r). + H_{layers}(I) \tag{266}$$

$$h_{RT1} = a_s + h_r + h_{r1} \quad \text{km} \tag{267}$$

$$h_{RT2} = a_s + h_r + h_{r2} \quad \text{km} \tag{268}$$

$$N_1 = N_s\, 10^{-6} \exp(-C_e\, h_{r1}) \tag{269}$$

$$N_2 = N_s\, 10^{-6} \exp(-C_e\, h_{r2}) \tag{270}$$

$$N_{I1} = 1 + N_1 \tag{271}$$

$$N_{I2} = 1 + N_2 \tag{272}$$

Starting with element 2 of H_{layers} ($I = 2$):

$$A(I) = \frac{\log_e R_I(I) - \log_e R_I(I-1)}{\log_e R(I) - \log_e R(I-1)} \tag{273}$$

Starting at the first H_{layers} value above h_{r1} for each layer indicated by index I until the H_{layers} value is greater than h_{r2}:

$$X = \frac{h_{RT1}}{2\, R(I)} \tag{274}$$

$$Y = 2 \sin^2(2\, \theta_{RT}) \tag{275}$$

where θ_{RT} is the absolute value of the take-off angle.

$$Z = \frac{R(I) - h_{RT1}}{h_{RT1}} \tag{276}$$

$$W = \frac{(N_1 - N_{RT}) \cos \theta_{RT}}{N_I(I)} \tag{277}$$

$$\theta_I(I) = 2 \sin^{-1}\left(\sqrt{[X(Y + Z - W)]}\right) \tag{278}$$

$$X_A = \frac{-A_I(I)}{A_I(I) + 1} \tag{279}$$

$$\theta_{all} = \theta_{all}\theta\left[(\theta_I(I) - \theta_I(I-1))X_A\right] \tag{280}$$

$$X_B = \frac{N_I(last)\,R_I(last)}{h_{r2}} \tag{281}$$

When equations (274) to (281) are done for the value of $H_{layers} > h_{r2}$ or the index, I, equals 25, angle at the higher antenna and the great circle distance between antennas 1 and 2 are:

$$\theta_F = \begin{cases} \theta_I(I) & \text{if } h_{r2} < 475 \text{ km} \\ \cos^{-1}[\cos(\theta_I(I))X_B] & \text{otherwise} \end{cases} \tag{282}$$

$$d_{RT} = a_s(\theta_F + \theta_{all}) \tag{283}$$

2 Counterpoise or ground plane

2.1 Effective reflection coefficient

The presence of a counterpoise affects the effective reflection coefficient of the system. The effective reflection coefficient related to a counterpoise, R_{Tc}, uses a divergence, D_v, ray length factors, F_r, a surface roughness factor, $F_{\sigma h}$, counterpoise factor, f_c, antenna gain factor for the counterpoise, g_c, and the plane earth reflection coefficient magnitude, R_c.

$$R_{Tc} = \begin{cases} D_v F_r F_{\sigma h} f_c g_{Rc} R_c & \text{for counterpoise present} \\ 0 & \text{otherwise} \end{cases} \tag{284}$$

In the counterpoise case, $D_v F_r F_{\sigma h}$ is assumed equal to unity since the counterpoise would be near the lower antenna and flat. Therefore they are not considered in this section.

2.2 Counterpoise factors

The counterpoise factors reduce the amount of reflection for both the counter poise and the ground reflections when a counterpoise is present. The geometry of the counterpoise is shown in Figs 17 and 18.

$$\theta_{ce} = \tan^{-1}\left(\frac{2\,h_{fc}}{d_c}\right) \tag{285}$$

where h_{fc} is the height of antenna 1 above the counterpoise from equation (20) and d_c is the counterpoise diameter which is an input parameter.

FIGURE 17

Geometry for earth reflection diffraction parameter, v_g, with counterpoise shadowing
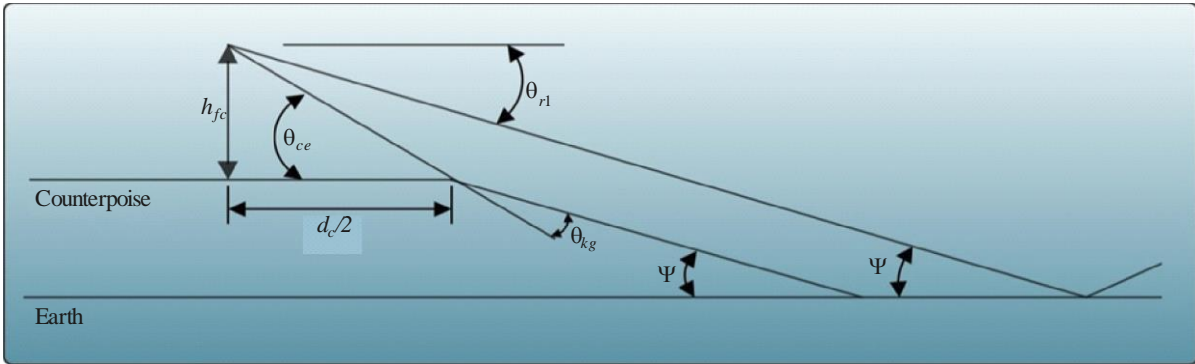
FIGURE 18

Geometry for earth reflection diffraction parameter, v_c, with limited surface of counterpoise
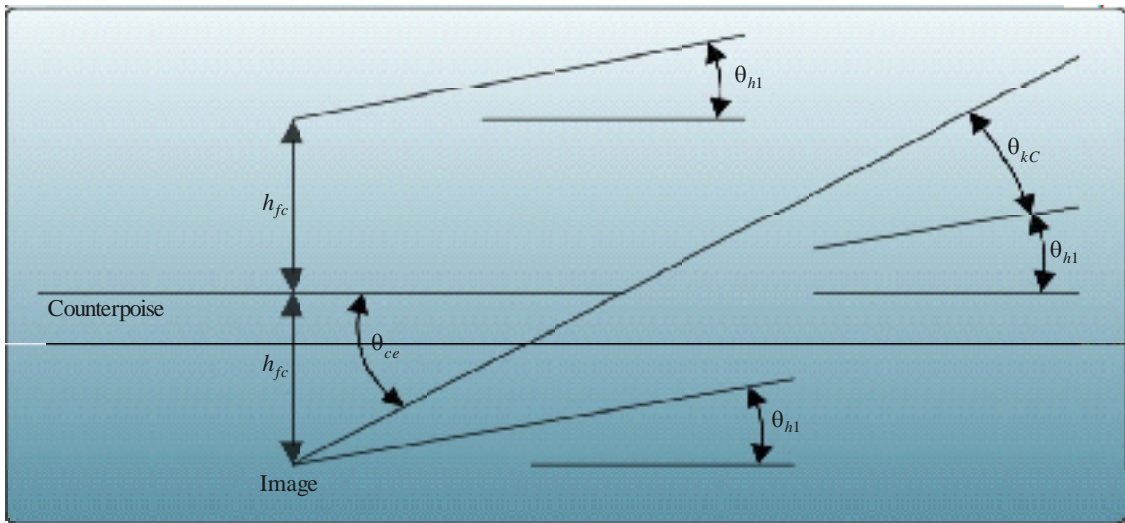
$$r_c = \frac{0.5\, d_c}{\cos \theta_{ce}} \tag{286}$$

$$\theta_{kg} = |\theta_{ce}| - |\theta_{r1}| \tag{287}$$

where θ_{r1} is from equation (110).

$$Y_v = \sqrt{\frac{8\, r_c}{\lambda}} \tag{288}$$

where λ is the wavelength in km equal to $\lambda_m/1\,000$ which λ_m is from (9).

$$\theta_{kc} = |\theta_{ce} - \theta_{h1}| \tag{289}$$

where θ_{h1} is calculated using counterpoise parameters in (100) through (109).

$$v_g = \pm\, Y_v\, \sin\frac{\theta_{kg}}{2} \begin{pmatrix} - & \text{for } |\theta_{r1}| < \theta_{ce} \\ + & \text{otherwise} \end{pmatrix} \tag{290}$$

$$v_c = \pm\, Y_v\, \sin\frac{\theta_{kc}}{2} \begin{pmatrix} - & \text{for } \theta_{h1} > \theta_{ce} \\ + & \text{otherwise} \end{pmatrix} \tag{291}$$

$$C_{g,c} = \int_0^{v_{g,c}} \cos\left(\frac{\pi t^2}{2}\right) dt \tag{292}$$

$$S_{g,c} = \int_0^{v_{g,c}} \sin\left(\frac{\pi t^2}{2}\right) dt \tag{293}$$

where $C_{g,c}$ and $S_{g,c}$ are Fresnel integrals.

$$f_{c,g} = 0.5\,\sqrt{\left[1 - (C_{g,c} + S_{g,c})\right]^2 + (C_{g,c} - S_{g,c})^2} \tag{294}$$

$$\phi_{kg,c} = \tan^{-1}\left(\frac{C_{g,c} - S_{g,c}}{1 - C_{g,c} - S_{g,c}}\right) \tag{295}$$

The value f_g is used in (113), f_c is used for R_{Tc} is equation (282) and $\varphi_{kg,c}$ are used in (158) and (159) in § 6.4.

3 Cumulative distribution

For long term fading in § 10.1, to calculate percentiles for hourly received power starts with the $Y(0.9)$ and $Y(0.1)$ values calculated in equation (223). The assumption for this distribution is that it is normal or nearly normal. The equation for other percentiles is equation (224). The values for c use the $Q_i(q/100)$ values where

$$c = \frac{Q_i(q)}{Q_i(0.9)} \tag{296}$$

for $Y(0.9)$ and a defined q and

$$c = \frac{Q_i(q)}{Q_i(0.1)} \tag{297}$$

for $Y(0.1)$ and a defined q. The value for $q = 0.5$ here is zero and, so, is not included in the calculations. $Q_i(q/100)$ values can be found in Table 17.

TABLE 17

**Approximate inverse complementary cumulative normal distribution values
[Rec. ITU-R 1546 Table 3]**

$q\%$	$Q_i(q/100)$	$q\%$	$Q_i(q/100)$	$q\%$	$Q_i(q/100)$	$q\%$	$Q_i(q/100)$
1	2.327	26	0.643	51	−0.025	76	−0.706
2	2.054	27	0.612	52	−0.050	77	−0.739
3	1.881	28	0.582	53	−0.075	78	−0.772
4	1.751	29	0.553	54	−0.100	79	−0.806
5	1.645	30	0.524	55	−0.125	80	−0.841
6	1.555	31	0.495	56	−0.151	81	−0.878
7	1.476	32	0.467	57	−0.176	82	−0.915
8	1.405	33	0.439	58	−0.202	83	−0.954
9	1.341	34	0.412	59	−0.227	84	−0.994
10	1.282	35	0.385	60	−0.253	85	−1.036
11	1.227	36	0.358	61	−0.279	86	−1.080
12	1.175	37	0.331	62	−0.305	87	−1.126
13	1.126	38	0.305	63	−0.331	88	−1.175
14	1.080	39	0.279	64	−0.358	89	−1.227
15	1.036	40	0.253	65	−0.385	90	−1.282
16	0.994	41	0.227	66	−0.412	91	−1.341
17	0.954	42	0.202	67	−0.439	92	−1.405
18	0.915	43	0.176	68	−0.467	93	−1.476
19	0.878	44	0.151	69	−0.495	94	−1.555
20	0.841	45	0.125	70	−0.524	95	−1.645
21	0.806	46	0.100	71	−0.553	96	−1.751
22	0.772	47	0.075	72	−0.582	97	−1.881
23	0.739	48	0.050	73	−0.612	98	−2.054
24	0.706	49	0.025	74	−0.643	99	−2.327
25	0.674	50	0.000	75	−0.674		

Attachment 2

Abbreviations, acronyms and symbols

This list includes most of the abbreviations, acronyms, and symbols used in this report. The units given for symbols in this list are those required by or resulting from equations as given in this report and are applicable except when other units are specified.

In the following list, the English alphabet precedes the Greek alphabet, letters precede numbers, and lower-case letters precede upper-case letters. Miscellaneous symbols and notations are given after the alphabetical items.

a	effective earth radius calculated from eq. (14) (km)
a_a	an effective earth radius associated with k_a in the two ray model in the LoS region, eq. (98) (km)
a_0	actual earth radius, 6 370 km
$a_{1,2,3,4}$	effective earth radii from diffraction calculations, eq. (55) (56)
a_γ	effective earth radius used in atmospheric absorption from § 10 (km)
A	an intermediate parameter for tropospheric scatter attenuation, eq. (198)
A_a	atmospheric absorption attenuation, eq. (212) (dB)
A_A	diffraction attenuation intercept for path O-A, eq. (92) (dB)
A_d	diffraction attenuation for beyond the horizon paths, eq. (94) (dB)
A_{dx}	A_d at d_x, eq. (205) (dB)
$A_{e,q,t}$	angles from Fig. 12 (rad)
A_F	attenuation path intercept for diffraction path F-O-ML, eq. (71) (dB)
A_I	effective area of an isotropic antenna, eq. (8) (dB sq. m)
A_{KA}	knife-edge diffraction attenuation for O-A path, eq. (88) (dB)
A_{KML}	knife-edge diffraction attenuation for F-O-ML path, eq. (81) (dB)
A_{K5}	knife-edge diffraction attenuation at d_5, eq. (153) (dB)
A_{LoS}	attenuation in the LoS region, eq. (162) (dB)
A_m	upper limit of the ray tracing gradient, eq. (169) (km^{-1})
A_{ML}	diffraction attenuation for F-O-ML path, eq. (90) (dB)
A_0	A_{R0} at d_0, eq. (161) (dB)
A_p	attenuation path intercept for rounded earth diffraction, eq. (70) (km)
A_{rA}	rounded earth diffraction attenuation for the O-A path, eq. (72) (dB)
A_{rF}	rounded earth diffraction attenuation for the F-O-A path, eq. (71) (dB)
A_{rML}	rounded earth diffraction attenuation for the F-O-ML, eq. (71) path
A_{RO}	attenuation in the LoS region where the diffraction effects associated with terrain are negligible, eq. (160) (dB)
$A_{rr}(q)$	attenuation rate associated with rain and a fraction of time, q, step 3 in § 11.3 (dB/km)
A_{r5}	rounded earth diffraction attenuation for the F-O-A path at d_5, eq. (154) (dB)
A_S	forward scatter attenuation, eq. (163) (dB)
A_{SX}	forward scatter attenuation at d_x, eq. (205) (dB)

A_T	terrain attenuation, eq. (205) (dB)
A_Y	conditional adjustment factor used to prevent available signal powers form exceeding levels expected for free space propagation by unrealistic amounts, eq. (234) (dB)
A_{YI}	initial value for conditional adjustment factor, A_Y, eq. (233) (dB)
$A_{3,4}$	intermediate parameters for rounded earth diffraction calculations, eq. (68) (dB)
A_5	combined diffraction attenuation at d_5, eq. (155) (dB)
$b_{1,2,3}$	long term variability parameters for eq. (237) from Table 12
B	intermediate parameter for $G_{fi1,2}$, eq. (77)
$B_{N1,2}$	parameters used for rounded earth calculations, eq. (73)
B_S	intermediate parameter for scattering volume, S_V, eq.(202)
$B_{1,2,3,4}$	intermediate parameters for rounded earth diffraction calculations, eq. (60)
c	cumulative distribution for long term fading calculations, eq. (228) and Attachment 1
$c_{e,h,v}$	phase of plane earth reflection coefficient relative to π for elliptical, horizontal, and vertical polarisations, eqs. (138) (139)
c_Y	variability limiting parameter, eq. (236) (dB)
$c_{1,2,3}$	parameters for long term fading calculations, eqs. (225) (226) (237) from Tables 6, 7, 8
C_S	intermediate parameter for tropospheric scatter calculations, eq. (203)
$C_{v,g,c,5}$	Fresnel integrals, eqs. (85) (292) (152)
D	great circle distance between lower and higher antennas (may be an input or calculated by eq. (112) (km)
d_A	facility to aircraft distance, eq. (91) (km)
d_c	counterpoise diameter, eq. (285) (km)
d_d	initial estimate of d_0, eq. (156) (km)
d_e	effective distance for long term power fading, eq. (221) (km)
d_h	distance used to calculate facility horizon, eq. (31) (km)
$d_{L1,2}$	horizon distances for the lower (1) and higher (2) antennas § 4.2, § 4.3 (km)
d_{LE1}	horizon distances for the lower (1) and higher (2) antennas based on effective earth radius, eq. (32) (km)
d_{LM}	greatest distance between the lower and higher antennas where there is a common horizon, eq. (42) (km)
$d_{LO1,2}$	smooth earth horizon distances for lower path O-A, eqs. (48) (49) (km)
d_{Lp}	total horizon distance for the path for diffraction, eq. (52) (km)
$d_{Lp1,2}$	radio horizon distances for lower (1) and higher (2) antennas for the path for diffraction, eqs. (48) (49) (km)
d_{Lq}	total smooth earth horizon distance determined by ray tracing, equals d_{RT} for $a_S = 9\,000$ km, eq. (283) (km)
d_{LR2}	horizon distance for higher antenna discussed before eq. (40) (km)
d_{Ls}	total smooth earth horizon distance between the lower and higher antennas, eq. (25) (km)
d_{LsA}	smooth earth horizon distance for O-A path, eq. (82) (km)
$d_{Ls1,2}$	smooth earth horizon distance for the lower (1) and higher (2) antennas, eq. (24) (km)
$d_{LsE1,2}$	effective smooth earth horizon distances for the lower (1) and higher (2) antennas, eq. (23) (km)

$d_{LsR1,2}$	smooth earth horizon distances for the lower (1) and higher (2) antennas § 4.1 Fig. 3 (km)
$d_{LO1,2}$	smooth earth horizon distances for path O-A in eqs. (48) (49) (km)
$d_{L1,2}$	total smooth earth horizon distance between the lower and higher antennas, eq. (25) (km)
d_{L5}	intermediate distance in LoS region, eq. (145) (km)
d_{ML}	maximum LoS distance from the lower antenna, eq. (40) (km)
d_q	intermediate distance in calculating d_e, eq. (222) (km)
d_s	scattering distance, eq. (165) (km)
d_{sL}	smooth earth horizon distance with an obstacle horizon, eq. (41) (km)
d_x	distance just beyond the radio horizon discussed after eq. (205) (km)
$d_{z1,2}$	distances used in tropospheric scatter calculations, eqs. (167) (168) (km)
$d_{Z1,2}$	distances used in tropospheric scatter calculations, eqs. (184) (185) (km)
$D/U\,(q)$	desired to undesired signal ratio, eq. (10) (dB)
D_v	divergence factor, eq. (116)
d_0	largest distance in the LoS region where the diffraction component is negligible, eq. (157) (km)
$d_{3,4}$	distances that are intermediate values in the rounded diffraction calculations, eqs. (53) (54) (km)
d_5	intermediate distance in LoS region, eq. (146) (km)
$D_{1,2}$	distances associated with $\theta_{1,2}$ respectively, eq. (103) (km)
e.i.r.p.	equivalent isotropically radiated power, eq. (6) (dBW)
f	frequency, input parameter (MHz)
f_c	counterpoise factor for R_{Tc}, eq. (294)
$f_{c1,2}$	intermediate parameter used to calculate the residual weighted height function, eq. (75)
f_g	counterpoise factor for R_{Tg}, eq. (294)
$f_{m,\infty}$	factors used in long term variability discussed after eq. (226)
$f_{v,5}$	knife-edge diffraction factors, eqs. (87) (152)
f_2	factor used in long term variability, eq. (225)
$f_{\theta h}$	factor used in long term variability, eq. (229)
F	fade margin, eq. (245)
F_{AY}	specular reflection reduction factor, eq. (240)
$F_{d\sigma h}$	surface roughness factor for diffuse reflections, eq. (122)
F_{fs}	LoS attenuation factor, eq. (158)
F_r	ray length factor, eq. (117)
$F_{x1,2}$	intermediate parameters for rounded earth diffraction calculations, eq. (67)
$F_{1,2}$	intermediate parameters for rounded earth diffraction calculations, eq. (66)
$F_{\Delta r}$	reflection reduction factor, eq. (241)
$F_{\sigma h}$	surface roughness factor for specular reflections, eq. (121)
$g(0.1,f)$	frequency gain factor, eq. (223)
$g(0.9,f)$	frequency gain factor, eq. (224)
$g_{D,R}$	voltage gain factors, eqs. (125) (126)

$g_{D1,2}$	voltage gain factors Table 3
$g_{hD1,2}$	voltage gain factors, direct ray, horizontal polarization discussed after eq. (126)
$g_{hR1,2}$	voltage gain factors, reflected ray, horizontal polarization discussed after eq. (126)
g_{Rh}	gain factor, reflected ray, horizontal polarization, eq. (128)
$g_{R1,2}$	voltage gain relative to boresight discussed in § 6.2.3
$g_{vD1,2}$	voltage gain factors, direct ray, vertical polarization discussed after eq. (126)
$g_{vR1,2}$	voltage gain factors, reflected ray, horizontal polarization discussed after eq. (126)
$G_{ET,R}$	free space antenna gains for transmitting (T) and receiving (R) antennas, eq. (4) (dBi)
$G_{NT,R}$	relative gain of a elevation angle for transmitting (T) and receiving (R) antennas discussed after eq. (4) (dBi)
$G_{R1,2}$	antenna gains, eq. (124) (dBi)
$G_{T,R}$	main beam free space antenna gains for transmitting (T) and receiving (R) antennas discussed after eq. (4) (dBi)
$G_{W1,2}$	weighting factor for height gain function, eq. (76) (dBi)
$G_{1,2,3,4}$	intermediate parameters for rounded earth diffraction calculations, eq. (63) (dB)
$G_{fi1,2}$	values for the residual height gain function, eq. (77) (dB)
$G_{fiF1,2}$	residual height gain factor for F-O-ML path, eq. (79) (dB)
$G_{fiA1,2}$	residual height gain factor for O-A path, eq. (80) (dB)
$G_{fip1,2}$	residual height gain factor for a defined path, eq. (78) (dB)
h	height above mean sea level, eq. (15) (dB)
h_c	height of the counterpoise or ground plane above the facility height (h_{sml}), input parameter (km)
h_e	effective antenna height discussed before eq. (31) (km)
$h_{e1,2}$	effective heights for the lower (1) and higher (2) antennas, eq. (21) (km)
h_{em2}	effective aircraft altitude, eq. (144) (km)
$h_{ep1,2}$	effective heights for lower (1) and higher (2) antennas for paths defined for diffraction, eq. (47) (km)
h_{fc}	height of the lower antenna above the counterpoise or ground plane, eq. (19) (km)
$h_{L1,2}$	horizon elevations above mean sea level for the lower (1) and higher (2) antennas (36), eq. (45) (km)
$h_{LE1,2}$	horizon elevation for lower (1) and higher (2) antennas (29) (km)
$h_{Lr1,2}$	horizon elevations above effective reflecting surface for the lower (1) and higher (2) antennas, eqs. (37) (44) (km)
h_r	reflecting surface height, input parameter (km)
$h_{r1,2}$	heights above the effective reflection surface for the lower (1) and higher (2) antennas, eq. (18) (km)
h_{sl}	height of lower antenna above the facility height, input parameter (km)
h_{sml}	height of the facility above mean sea level, input parameter (km)
h_v	height of the scattering volume, eq. (186) (km)
$h_{1,2}$	heights above mean sea level for lower (1) and higher (2) antennas, eq. (18) (km)
$\hslash_{1,2}$	intermediate values for smooth earth diffraction calculations for lower (1) and higher (2) antennas, eq. (74)

$H_{c,q,t,z}$	heights defined for atmospheric absorption calculations in Fig. 12 (km)
$H_{1,2}$	antenna heights above and perpendicular to the reflective surface, eqs. (100 a&b) (km)
$H_{1/3}$	values for significant wave height in Table 2 used in eq. (119) (m)
$H_{\Upsilon 1,2}$	antenna heights above and perpendicular to the surface of the earth in Fig. 12 (km)
$H'_{1,2}$	antenna heights used in determining the two ray path, eq. (104) (km)
k_a	adjusted earth radius factor in the two ray method in LoS region, eq. (97)
K	ratio between steady component of received power and the Rayleigh fading component used to determine correct Nakagami-Rice phase interference fading distribution value for tropospheric multipath calculations from Table 13 (dB)
$K_{d1,2,3,4}$	intermediate parameters for rounded earth diffraction calculations, eq. (57)
$K_{F1,2}$	intermediate parameters for rounded earth diffraction calculations, eq. (59)
K_{LoS}	parameter for tropospheric multipath calculations, eq. (246)
K_{ML}	K_{LoS} value at $d = d_{ML}$, eq. (246)
K_T	parameter for tropospheric multipath calculations, eq. (246)
$K_{1,2,3,4}$	intermediate parameters for rounded earth diffraction calculations, eq. (58)
l	total ray length for the tropospheric scattering attenuation, eq. (189) (km)
$l_{1,2}$	ray lengths for the tropospheric scattering attenuation, eq. (188) (km)
$L(q)$	transmission loss not exceeded during time period q, eq. (1) (dB)
$L_b(0.5)$	median basic transmission loss, eq. (2) (dB)
L_{bf}	free space basic transmission loss, eq. (206) (dB)
L_{br}	reference level for the basic transmission loss, eq. (3) (dB)
L_{gp}	antenna gain path loss, eq. (1) (dB)
LoS	Line of Sight
msl	mean sea level
M	number of transmission loss levels used in mixing distributions, § 11.5
M_A	attenuation path slope for diffraction for O-A path defined in § 5.1 (dB/km)
M_d	attenuation path slope for combined diffraction of beyond-the-horizon paths, eq. (93) (dB/km)
M_F	slope of K value defined in § 5.1 (dB/km)
M_L	slope of the diffraction attenuation line just inside the radio horizon, eq. (161) (dB/km)
M_p	attenuation path slope for diffraction, eq. (69) (dB/km)
M_S	slope of successive scatter attenuation points discussed after eq. (205) (dB/km)
n	index used in ionospheric scintillation calculations, eq. (260)
$n_{1,2,3}$	values from Table 6 used in long term fading calculations, eq. (226)
N	refractivity for height h in an exponential atmosphere, eq.(15) (N-units)
N	number of distributions to be mixed, § 11.5
N_0	monthly mean surface refractivity, eq. (13) (N-units)
N_S	surface refractivity relative to the reflecting surface height, eq. (13) (N-units)
$P_a(q)$	power available for at least time period q, eq. (5) (dBW)
P_{TR}	total power radiated by the transmitting antenna, eq. (6) (dBW)
q	fraction of time availability

$q_{1,2}$	intermediate parameters used in tropospheric scattering calculations, eq. (201)
$Q_{a1,2}$	intermediate parameters used in tropospheric scattering calculations, eq. (174)
$Q_{A1,2}$	intermediate parameters used in tropospheric scattering calculations, eq. (178)
$Q_{b1,2}$	intermediate parameters used in tropospheric scattering calculations, eq. (175)
$Q_{B1,2}$	intermediate parameters used in tropospheric scattering calculations, eq. (179)
$Q_{O1,2}$	intermediate parameters used in tropospheric scattering calculations, eq. (173)
r	ray length used in the free space loss calculation, eq. (208) (km)
r_{BH}	ray length for beyond the horizon paths, eq. (210) (km)
r_c	distance in a counterpoise calculation, eq. (286) (km)
$r_{L1,2}$	ray length from antenna 1 or antenna 2 to horizon, eq. (209) (km)
r_0	the length of the direct ray from antenna 1 to antenna 2 in the two ray model, eq. (106) (km)
r_s	in-storm ray length, eq. (257) (km)
r_{WH}	ray length for within the horizon paths, eq. (209) (km)
$r_{1,2}$	the length of the direct ray from antenna 1or antenna 2 to the ground in the two ray model Fig. 9 (km)
r_{12}	the length of the reflected ray from antenna 1 to antenna 2 in the two ray model, eq. (107) (km)
R_c	counterpoise reflection coefficient magnitude discussed after eq. (140)
R_d	diffuse reflection coefficient, eqs. (123) (243)
$R_{e,h,v}$	reflection coefficient magnitudes for elliptical, horizontal, or vertical polarisation, eq. (138)
$R_{eo,s,w}$	partial effective ray lengths inside oxygen layer, rain storm layer, or water vapour layer, eqs. (217) (219) § 11.3 (km)
R_g	plane earth reflection coefficient magnitude, eq. (140)
R_r	reflected ray length ratio, eq. (115)
R_s	specular component of surface reflection multipath, eq. (242)
R_{Tc}	effective reflection coefficient associated with counterpoise reflection, eq. (284)
R_{Tg}	effective reflection coefficient associated with ground reflection, eq. (113)
S	modulus of symmetry for tropospheric scattering, eq. (194)
S_e	scattering efficiency term for the tropospheric scattering attenuation, eq. (193)
$S_R(q)$	power density at receiving antenna for at least time period q, eq. (7) (dBW/sq. m)
$S_{v,g,c,5}$	Fresnel integrals, eqs. (86) (293) (153)
S_V	scattering volume for tropospheric scatter calculations, eq. (204) (dB)
T	intermediate parameter for $G_{fi1,2}$, eq. (77)
T	relaxation time used in the calculation of water surface constants from Table 4
$T_{eo,s,w}$	storm height or layer thickness for oxygen layer, rain storm layer, or water vapour layer discussed in § 10.1.1 and § 11.3 (km)
V	variability levels used in mixing distributions, § 11.5
$V(0.5)$	parameter from eqs. (226) (237)
V_c	variability for specific climate or time block, eq. (262)

$V_e(0.5)$ variability adjustment term, eq. (231)

$V_{eI}(q)$ initial value of variability adjustment term, eq. (230)

W weighting factor between rounded earth and knife-edge diffraction, eq. (89)

W weighting factors used in mixing distributions, § 11.5

W_A relative power level for the Rayleigh fading component associated with tropospheric multipath, eq. (248)

W_R relative power level for the Rayleigh fading component associated with tropospheric multipath, eq. (244)

W_{RO} relative power level for the Rayleigh fading component associated with surface reflection multipath, eq. (159)

$W_{1,2}$ intermediate parameters for rounded earth diffraction calculations, eq. (64)

X_a parameter used in tropospheric scatter calculations, eq. (183)

$X_{A1,2}$ parameter used in tropospheric scatter calculations, eq. (187)

$X_{v1,2}$ parameter used in tropospheric scatter calculations, eqs. (199) (200)

$X_{1,2,3,4}$ intermediate parameters for rounded earth diffraction calculations, eqs. (61) (62)

$y_{1,2}$ intermediate parameters for rounded earth diffraction calculations, eq. (65)

$Y(q)$ variability of hourly median received power about the median, eq. (228) (dB)

$Y(0.1)$ reference variability level of hourly received power of the channel used to calculate other percentiles, eq. (227) (dB)

$Y(0.9)$ reference variability level of hourly received power of the channel used to calculate other percentiles, eq. (227) (dB)

Y_C complex parameter used in the calculation of the plane earth reflection coefficient, eq. (262)

$Y_{DU}(q)$ total variability of desired to undesired signal ratios $Y_{DU}(0.5) = 0$, eq. (12)

$Y_e(q)$ effective variability of hourly median received power about the median, eqs.(235) (236) (dB)

$Y_{eI}(q)$ initial value of the effective variability of hourly median received power about the median, eq.(230) (dB)

$Y_I(q)$ variability associated with ionospheric scintillation, eq. (261) (dB)

$Y_0(0.1)$ reference variability level used to calculate $Y(0.1)$, eqs. (226) (237) (dB)

$Y_0(0.9)$ reference variability level used to calculate $Y(0.9)$, eq. (226) (237) (dB)

$Y_r(q)$ variability associated with rain attenuation, eq. (258) (dB)

$Y_T(q)$ top limiting level in the lobing mode in the LoS region, eq. (232)

Y_v intermediate parameter to calculate v_g, eq. (288)

$Y_{136}(q)$ variability that is associated with ionospheric scintillation at 136 MHz, § 11.4

$Y_\pi(q)$ short term variability associated with multipath, Fig. 4 (dB)

$Y(q)$ total variability, eq. (220) (dB)

z intermediate parameter for the two ray model in the LoS region, eq. (96)

$z_{a1,2}$ intermediate parameters used in tropospheric scatter calculations, eq. (171) (km)

$z_{b1,2}$ intermediate parameters used in tropospheric scatter calculations, eq. (172) (km)

$z_{1,2}$ heights of antennas including the effective earth radius, eq. (101) (km)

$Z_{a1,2}$ intermediate parameters used in tropospheric scatter calculations, eq. (176) (km)

$Z_{b1,2}$ intermediate parameters used in tropospheric scatter calculations, eq. (177) (km)

$Z_{A1,2}$ intermediate parameters used in tropospheric scatter calculations, eq. (182) (km)

α angle from Fig. 9, eq. (109) (rad)

β angle used in atmospheric absorption calculations defined in § 10.1

γ index for parameters used in atmospheric absorption calculations in § 10.1

γ_e intermediate parameter used in tropospheric scatter calculations, eq. (170)

$\gamma_{oo,w}$ surface absorption rates for oxygen, water vapor, Fig. 13

δ parameter used in surface roughness factor calculation, eq. (120)

Δh terrain height, input parameter (km)

$\Delta h_{a1,2}$ effective altitude correction factors of the lower (1) and higher (2) antennas, eq. (99) (km)

Δh_d interdecile range of terrain heights, eq. (118) (m)

$\Delta h_{e1,2}$ difference between the actual and effective heights of the lower (1) and higher (2) antennas, eq. (22) (km)

Δh_m Δh expressed in metres in eq. (118)

ΔN differential refractivity for ray tracing, eq. (16) (N-units)

Δr difference between the lengths of the direct ray and the reflected ray in the two ray model, eq. (95) (km)

ε dielectric constant, input parameter

ε_c complex dielectric constant, eq. (136)

ε_o dielectric constant representing the sum of electronic and atomic polarisations, § 6.2.4

ε_s static dielectric constant for water, Table 4

$\varepsilon_{1,2}$ parameters used in tropospheric scatter calculations, eqs. (190) (191)

η parameter used in tropospheric scatter calculations, eq. (195)

ϑ angle in tropospheric scatter calculations, eq. (192) (rad)

λ_m wavelength of defined frequency in metres, eq. (9) (m)

θ scattering angle for the tropospheric scattering attenuation, A_s, eq. (181) (rad)

$\theta_{a1,2}$ angles used in calculating the scattering angle, eq. (164) (rad)

$\theta_{A1,2}$ angles used in tropospheric scatter calculations, eq.(180) (rad)

θ_{ce} counterpoise angle defined in Fig. 17, eq. (285) (rad)

$\theta_{e1,2}$ horizon elevation angles for lower (1) and higher (2) antennas, eqs. (38) (46) (rad)

θ_{eE1} horizon elevation angle for intermediate calculations, eq. (33) (rad)

$\theta_{esR1,2}$ ray elevation and central angles for lower (1) and higher (2) antennas from ray tracing, § 4.1 (rad)

$\theta_{es1,2}$ effective ray elevation and central angles for lower (1) and higher (2) antennas, eq. (27) (rad)

θ_{e5} angle used in the LoS transition region calculations, eq. (147) (rad)

$\theta_{g1,2}$ elevation angles of the ground reflected rays, eq. (133) (rad)

$\theta_{h1,2}$ parameters to calculate $\theta_{H1,2}$, eq. (109) (rad)

θ_{h5} angle in eq. (142) (rad)

$\theta_{H1,2}$ direct ray elevation angles, eq. (132) (rad)

θ_{FL} magnitude of earth facility latitude, input parameter (deg)

$\theta_{kg,c}$	angles associated with a counterpoise defined in Figs 17, 18, eqs. (287) (289) (rad)
θ_L	elevation angle of horizon to higher antenna ray from lower antenna horizon, eq. (39) (rad)
$\theta_{L1,2}$	horizon elevation angle adjustment terms, eq. (131) (rad)
$\theta_{r1,2}$	angles used in two ray geometry calculations, eq. (110) (rad)
θ_s	angle used in scattering region calculations, eq. (166) (rad)
$\theta_{sR1,2}$	ray elevation angles for lower (1) and higher (2) antennas from Fig. 4, eq. (20) (rad)
$\theta_{s1,2}$	smooth earth ray elevation and central angles for lower (1) and higher (2) antennas, eq. (26) (rad)
θ_v	diffraction angle for the O-A path, eq. (83) (rad)
θ_0	central angle used in two ray geometry calculations, eq. (111) (rad)
$\theta_{1,2}$	angles associated with effective earth radius from Fig. 9, eq. (102) (rad)
$\theta_{3,4}$	angles that are intermediate values for rounded earth diffraction calculations, eqs. (50) (51) (rad)
θ_5	angle used in the LoS transition region calculations, eq. (143) (rad)
θ_6	angle used in the LoS transition region calculations, eq. (148) (rad)
κ	wave number, eq. (196) (km^{-1})
σ	surface conductivity, input parameter (mho/m)
σ_h	root mean square deviation of terrain and terrain clutter within the limits of the first Fresnel zone, eq. (119) (m)
σ_i	ionic conductivity for water from Table 4 (mho/m)
φ	phase advance associated with complex earth reflection coefficient (rad)
$\varphi_{g,c}$	phase shift of effective reflection coefficient for ground or counterpoise reflection, eqs. (113) (284) (rad)
$\varphi_{kg,c}$	phase shift for knife-edge diffraction for ground or counterpoise, eq. (295) (rad)
$\varphi_{Tg,c}$	total phase shift of effective reflection coefficient for ground or counterpoise reflection, eq. (141) (rad)
$\hbar_{1,2}$	intermediate parameters in diffraction calculations, eq. (74)
δ	parameter in Fresnel zone calculations, eq. (120)
ψ	grazing angle from Fig. 9 discussed in § 6.1 (rad)
ν	Fresnel parameter for knife edge diffraction calculations, eq. (84) (rad)
$\nu_{g,c,5}$	knife-edge diffraction parameters, eqs. (290) (291) (149)

Attachment 3

Data sets from Figs 13 and 16

Gaseous absorption data from Fig. 13:

Frequency (GHz)	Oxygen absorption	Water vapour absorption
0.1	0.00019	0
0.15	0.00042	0
0.205	0.0007	0
0.3	0.00096	0
0.325	0.0013	0
0.35	0.0015	0
0.4	0.0018	0
0.55	0.0024	0
0.7	0.003	0
1	0.0042	0
1.52	0.005	0
2	0.007	0
3	0.0088	0
3.4	0.0092	0.0001
4	0.01	0.00017
4.9	0.011	0.00034
8.3	0.014	0.0021
10.2	0.015	0.009
15	0.017	0.025
17	0.018	0.045
20	0.02	0.1
22	0.021	0.22
23	0.022	0.2
25	0.024	0.16
26	0.027	0.15
30	0.03	0.11
32	0.032	0.14
33	0.035	0.1
35	0.04	0.099
37	0.044	0.098
38	0.05	0.0963
40	0.06	0.0967
42	0.07	0.0981
43	0.09	0.0987
44	0.1	0.099

Frequency (GHz)	Oxygen absorption	Water vapour absorption
47	0.15	0.1
48	0.23	0.101
51	0.5	0.103
54	1.8	0.109
58	4	0.118
59	7	0.12
60	15	0.122
61	8	0.127
62	5	0.13
63	3	0.132
64	1.7	0.138
68	1.2	0.154
70	0.9	0.161
72	0.5	0.175
76	0.35	0.2
84	0.2	0.25
90	0.14	0.34
100	0.1	0.56

Scintillation Data from Fig. 16:

	Variability about median signal level (dB)					
Scintillation index group	0	1	2	3	4	5
Time %						
0.001	0	4.4	5.8	10.8	13.7	14.5
0.002	0	4.2	5.5	10.2	13	13.8
0.005	0	3.9	5	9.2	12	13
0.01	0	3.6	4.7	8.2	11.1	12.4
0.02	0	3.4	4.4	7.6	10.3	11.7
0.05	0	3.05	3.95	6.5	9.2	10.7
0.1	0	2.8	3.65	5.8	8.4	10
0.2	0	2.55	3.35	5.2	7.5	9.5
0.5	0	2.15	2.9	4.35	6.35	8.2
1	0	1.85	2.55	3.8	5.45	7.5
2	0	1.55	2.2	3.25	4.55	6.55
5	0	1.1	1.65	2.5	3.4	5.2
10	0	0.8	1.2	1.8	2.55	4
15	0	0.6	0.95	1.4	2	3.2
20	0	0.4	0.75	1.1	1.6	2.6
30	0	0.2	0.45	0.7	0.98	1.6

Scintillation index group	Variability about median signal level (dB)					
	0	1	2	3	4	5
Time %						
40	0	0.05	0.2	0.3	0.5	0.75
50	0	0	0	0	0	0
60	0	–0.15	–0.3	–0.35	–0.5	–0.8
70	0	–0.35	–0.55	–0.7	–1	–1.7
80	0	–0.6	–0.9	–1.2	–1.8	–2.95
85	0	–0.7	–1.1	–1.5	–2.4	–3.8
90	0	–0.9	–1.4	–1.9	–3.1	–5
95	0	–1.3	–2	–2.6	–4.4	–7.05
98	0	–1.8	–2.6	–3.5	–6	–9.8
99	0	–2.15	–3.1	–4.2	–7.2	–12.2
99.5	0	–2.55	–3.65	–4.95	–8.5	–15
99.8	0	–3.05	–4.4	–6.05	–10	–19.1
99.9	0	–3.5	–5	–7	–11.1	–22.2
99.95	0	–4	–5.6	–7.9	–12.2	–25.8
99.98	0	–4.6	–6.5	–9.1	–14	–30.2
99.99	0	–5	–7.2	–10	–15.4	–34
99.995	0	–5.5	–8	–11	–16.7	–37.2
99.998	0	–6.2	–9.2	–12.4	–18.4	–42.5
99.999	0	–6.6	–10.1	–13.4	–19.5	–46

Bibliography

1   Gierhart, G.D. and M.E. Johnson (1983), The Electromagnetic Wave Propagation Model, DOT Report FAA-ES-83-3.

2   Gierhart, G.D. and M.E. Johnson (1978), Propagation Model (0.1 to 20 GHz) Extensions for 1977 Computer Programs, DOT Report FAA-RD-77-129.

3   Gierhart, G.D. and M.E. Johnson (1973), Computer Programs for Air/Ground Propagation and Interference Analysis, 0.1 to 20 GHz, DOT Report FAA-RD-73-103.

4   Johnson, M.E. and G.D. Geirhart (1978), Applications Guide for Propagation and Interference analysis Computer Programs (0.1 to 20 GHz), DOT Report FAA-RD-77-60.

5   Rice, P.L., A.G. Longley, K.A. Norton and A.P. Barsis (1967), Transmission Loss Predictions for Tropospheric Communications Circuits, NBS Tech. Note 101, I and II revised.

6   Bean, B.R., and G.D. Thayer (1959), CRPL Exponential Reference Atmosphere, NBS Monograph 4.

_____